(NASA-CR-169755) AN ON-BOARD NEAR-OPTIMAL CLIMB-DASH ENERGY MANAGEMENT Interim Report (Virginia Polytechnic Inst. and State Univ.) 122 p HC A06/MF A01 CSCL 01C

N83-16329

Unclas G3/05 02481

ON-BOARD NEAR-OPTIMAL CLIMB-DASH ENERGY MANAGEMENT

Alan R. Weston

Eugene M. Cliff

Henry J. Kelley

December 1982

Interim Report

NASA Grant NAG-1-203

NASA Langley Research Center

Aerospace and Ocean Engineering Department

Virginia Polytechnic Institute and State University

Blacksburg, Virginia

ACKNOWLEDGMENTS

Thanks are extended to thank Dr. Klaus Well, and Mr. Eugene Berger of DFVLR, Oberpfaffenhofen, West Germany, for their extensive help in the use of the multiple-shooting program, which they kindly supplied, and Dr. C. Gracey and Dr. D. Price of NASA Langley, for their help with the numerical work performed on the NASA Langley computer. This research was supported by NASA Grant NAG-1-203.

LIST OF FIGURES

SYMBOLS

The dimensional quantities referred to in this paper are given in U.S. Customary Units, in which the numerical calculations were made. The units are in brackets following the quantities. In the case of non-dimensional coefficients and parameters, the brackets are not included.

C_d.....Drag Coefficient

C_{do}.....Zero-Lift Drag Coefficient

C_l.....Lift Coefficient

D.....Drag (lb_f)

E.....Specific Energy (ft)

E_d.....Dash Energy (ft)

E_f.....Final Energy (ft)

E_{max}.....Maximum Sustainable Energy (ft)

g.....Acceleration Due to Gravity (ft/sec^2)

h.....Altitude (ft)

H.....Hamiltonian (ft/sec)

K.....Induced Drag Coefficient

L.....Lift (lb_f)

M.....Mach Number

m.....Mass (sl)

n.....Load Factor

Q.....Fuel Flow Rate (sl/sec)

q.....Dynamic-Pressure (lb_f/ft^2)

S.....Wing Surface Area (ft^2)

T.....Thrust (lb_f)

V.....Velocity (ft/sec)

V_d.....Dash Velocity (ft/sec)

W.....Weight (lb_f)

x.....Downrange (ft)

y.....Crossrange (ft)

The specific energy is defined as:

$$E = h + V^2/2g$$

GREEK SYMBOLS

γ.....Flight-path Angle

ε^1.....Fast Interpolation Parameter

ε^2.....Intermediate Interpolation Parameter

η.....Throttle Coefficient

λ_E.....Energy Multiplier

λ_h.....Altitude Multiplier

λ_m.....Mass Multiplier (ft/sl)

λ_x.....Down Range Multiplier

λ_y.....Lateral Range Multiplier

λ_γ.....Path-Angle Multiplier (ft)

λ_χ.....Heading Multiplier (ft)

ρ.....Density (sl/ft^3)

ϕ.....Bank Angle

χ.....Heading Angle

TABLE OF CONTENTS

Chapter I

INTRODUCTION

On-board flight control and guidance is a subject which has had varying reception in different fields of Aerospace Engineering. In the area of unmanned missiles there has been extensive research, with many resulting applications, in developing on-board guidance systems, as reported in the survey papers, Refs 1 and 2. These studies have encompassed many new optimal control and even differential gaming ideas (Ref 3): in this field the on-board flight computer is an accepted and usually necessary part of the guidance system. While conventional homing and proportional navigation guidance laws are simple, and require minimal computation, more complex guidance schemes may be implemented on-board by the use of singular perturbation methodology, as in Ref 4.

The willingness to apply state-of-the-art theoretical developments to manned aircraft is not as evident. This may be the result of a more conservative approach in applying new technology to machines which are responsible for peoples' lives, machines which are also extremely expensive, generally larger and more complex than many missiles. However one of the greatest obstacles may be the threatened removal of authority from the pilot: despite the existence

of sophisticated autopilots on many expensive aircraft, there is an aversion to total automation, particularly on the part of the pilot. As a result there is a significant gap between the flight-path optimization and differential gaming results which have been achieved in the last twenty years, and the their applications in on-board use. A part of this is due to the limited computational resources available, particularly on fighter and small general aviation aircraft, where weight and space are at a premium. Some of the latest developments relating to the latter case are given in Ref 5. On the other hand in the area of large transport aircraft the cost, weight and complexity of a small main frame computer is justified, but this has yet to be implemented. In civil aviation much research has been done in the area of trajectory optimization, with particular emphasis on efficient fuel usage and minimizing the direct operating cost. Attention has focused on the calculation of sub-optimal flight paths, using order-reduction to simplify the problem, as in Refs 6-9. Burrows (Ref.6) used singular perturbations and order reduction to derive sub-optimal short and long haul trajectories, with on-board corrections to speed and energy errors based on expanding the performance index to second order, which he found to be more effective than simple linear feedback. Sorenson and Waters

(Ref. 7) used an assumed constant energy cruise (as did Erzberger and Lee, Ref. 8), and pointed out that the on-board flight control needs to be coordinated with the ATC system, so that fuel saved during the flight is not wasted due to traffic congestion at the terminal area. Chakravarty and Vagners (Ref. 9) attempted to provide justification for their state variable-selection through the use of non-dimensionalization. Transitions onto fuel-optimal climbs and descents are studied in Ref. 10, where they are used to derive a near-optimal feedback control law. Sub-optimal terminal guidance is examined by Erzberger, Ref. 11, for a fixed-wing aircraft, and by Beser, Ref. 12, for a tilt-rotor aircraft. Optimal shipboard terminal guidance is studied in Refs 13-15. Despite the active interest and work, as described above, in this area the applications have lagged behind. A description, for example, is given in Ref. 16 of the DC-9-80 Digital Flight Guidance System; here the emphasis is on establishing reliability and safety criteria for the engine and flight control systems. It seems safe to say that in this area applications efforts have focused on feasibility and reliability rather than optimality. As mentioned earlier, the computational resources on a fighter aircraft are even more limited than on a transport, for obvious reasons of space and weight constraints. In contrast

with large transports there is a much greater range of applications for on-board optimal control for fighter aircraft. This is because a fighter can and often has to perform a much wider range of maneuvers (in terms of flight path angles and back angles for instance) as studied in Refs 17-19. In many missions there is less, if any a priori knowledge of the flight path. Also it is often desirable for security to minimize the communication with the ground, which eliminates the possibility of solving flight-control problems on the ground and relaying commands to the air.

With this background it is the objective of this study to investigate on-board real-time flight control, with the intention of developing algorithms which are simple enough to be used in practice, for a variety of missions involving three-dimensional (3-D) flight. Initially an approach is developed which is restricted to the intercept mission in symmetric flight, based on Ref. 20. Extensive computation is required on the ground prior to the mission but the ensuing on-board exploitation is extremely simple. The scheme takes advantage of the boundary-layer structure common in singular perturbations, studied in Ref. 21, arising with the multiple time scales appropriate to aircraft dynamics. Energy modelling of aircraft, as first examined in Refs. 22-24 and extensively developed in Refs 25-27 is used as the

starting point for the analysis. In the symmetric case, a nominal path is generated which fairs into the dash or cruise state. Feedback coefficients are found as functions of the remaining energy-to-go (dash energy less current energy), along the nominal path. These serve to generate transitions towards the nominal path, closed loop and to counter disturbances. In this situation the guidance method is similar to the neighbouring-optimal guidance methods of Refs 28-32; these have been applied space shuttle re-entry problems, Refs. 33-35, and orbital transfer guidance, Refs. 36-37. However there are two significant differences between this study and these references. In the present work the gain indexing is done in terms of the current energy; this avoids the problems encountered in estimating the index time, as in the time-to-go or min-distance methods. Also, for the extension to 3-d flight, families of reference paths are used instead of a single trajectory , with heading-to-go as the additional running variable.

1.1 PROBLEM FORMULATION

The overall problem is to develop an on-board, real-time flight control system, which is near-optimal, for an aircraft flying an intercept mission, with arbitrary initial conditions. The equations of motion for a point-mass model of an aircraft can be written:

$$\dot{E} = V(\eta T - D)/W$$

$$\dot{h} = V\sin\gamma$$

$$\dot{\gamma} = (L\cos\phi - W\cos\gamma)/mV$$

$$\dot{\chi} = L\sin\phi/mV\cos\gamma$$

$$\dot{x} = V\cos\gamma\cos\chi$$

$$\dot{y} = V\cos\gamma\sin\chi$$

$$\dot{m} = -\eta Q$$

These equations embody the assumptions of thrust along the path, zero side-force, and flight over a flat earth with constant gravity. Also winds aloft are assumed to be zero, and the atmosheric properties standard.

1.2 SYMMETRIC FLIGHT

The first approach was to restrict the problem and simplify the model considerably, to reduce the analytical and computational burden, during the initial research and development of the guidance scheme. The restrictions in the problem are the following: to consider only symmetric flight, with fuel open, i.e. fuel optimization is not examined, which leads to maximum thrust in most maneuvers of practical interest. The target is assumed to be at a sufficient distance from the interceptor that a climb-dash is required: in other words a range-optimal climb to the dash point on the level flight envelope, blending into a steady-state dash. This sequence ends with a terminal transient, which is considered briefly in the next chapter. The time spent during the climb is assumed to be much smaller than the time spent at the dash state. The restriction in the aircraft model is that the variation in mass due to the fuel expenditure is ignored. Under these limitations, the equations of motion are reduced to:

$$\dot{E} = V(\eta T - D)/W$$

$$\dot{h} = V\sin\gamma$$

$$\dot{\gamma} = (L - W\cos\gamma)/mV$$

$$\dot{x} = V\cos\gamma$$

1.3 AERODYNAMIC MODELLING

The aircraft which is used as an example to perform numerical calculations is a high-performance interceptor. The drag is modelled as a parabolic function of the control:

$$C_d = C_{do} + K C_l^2$$

The coefficients C_{do} and K are functions of Mach Number:

$$C_{do} = C_{do}(M)$$

and

$$K = K(M)$$

The thrust is a function of Mach Number and altitude:

$$T = T(M,h)$$

The way in which these three functions are represented is important in the computational work undertaken in this study. The reasons for this are discussed, and the different methods which were used are described in Chapter 5 and Chapter 6.

Chapter II

OPTIMAL CONTROL: REDUCED-ORDER MODELLING

Reduced order modelling, based on time-scale separations observed in vehicle dynamics, is particularly attractive to the analyst in solving problems for lifting atmospheric flight. Numerical computations are simplified by the reduction in the system order and as a result the number of initial conditions which may have to be guessed or iterated upon is also reduced. Further, an improvement in the conditioning of the differential equations results from the confinement of the more unstable dynamics to boundary-layer corrections, which are relatively short in time. It has been appreciated since Kaiser's early work (Ref.22) that the h and γ variables can be changed much more rapidly than the specific energy, E, which explains the introduction of this new variable. Also the energy can be thought of as a 'fast' variable in comparison to the range, at least in cases where the climb is a transient which fairs into a steady-state cruise or dash condition, i.e. when the time spent in the steady state is much greater than that spent on the climb, as assumed here. This leads to the reformulating the equations of motion, following the development of Ref. 25, with the inclusion of the interpolation parameters, ε^1 on

the left hand sides of the differential equations for h and γ, and ε^2 on the left hand side of the differential equation for E:

$$\varepsilon^2 \dot{h} = V \text{ SIN } \gamma$$

$$\varepsilon^2 \dot{\gamma} = (L - W \text{ COS } \gamma) / M V$$

$$\varepsilon^1 \dot{E} = V (\eta T - D) / W$$

$$\dot{x} = V \text{ COS } \gamma$$

To solve the problems of time-optimal control the variational Hamiltonian is formed:

$$H = \lambda_E \dot{E} + \lambda_h \dot{h} + \lambda_\gamma \dot{\gamma} + \lambda_x \dot{x}$$

and the Maximum Principle (Refs.38 and 39) is applied. The resulting Euler differential equations are:

$$\varepsilon^2 \dot{\lambda}_h = -\frac{\partial H}{\partial h}$$

$$\varepsilon^2 \dot{\lambda}_\gamma = -\frac{\partial H}{\partial \gamma}$$

$$\varepsilon^1 \dot{\lambda}_E = -\frac{\partial H}{\partial E}$$

$$\dot{\lambda}_x = -\frac{\partial H}{\partial x}$$

The introduction of three separate time scales in the state system must conform to the requirement of the Tihonov theory (Ref. 40) that the ratio $(\varepsilon^2/\varepsilon^1) \to 0$ as $\varepsilon^1 \to 0$, as shown in Ref. 25. When both ε^2 and ε^1 are equal to 1 the original point-mass model is recovered.

2.1 RECTILINEAR-MOTION MODEL

The simplest model possible is obtained when both ε^1 and ε^2 are taken 0. By examination of the differential equations, the following consequences of these assumptions may be noted:

$$\varepsilon^1 = 0 \longrightarrow \begin{bmatrix} \dot{h} = 0 \\ \dot{\gamma} = 0 \end{bmatrix} \longrightarrow \begin{bmatrix} \gamma = 0 \\ L = W \end{bmatrix}$$

$$\varepsilon^2 = 0 \longrightarrow \dot{E} = 0 \longrightarrow \eta\, T = D$$

These equations embody the assumptions that the altitude, h, the path angle, γ, and the energy, E, can all be varied instantaneously in a control-like fashion subject to the constraints. In this slow rectilinear-motion model the path-angle is, however, fixed at a value of zero, and the lift coefficient is chosen at any energy/altitude combination so that the lift equals the weight. Further, the throttle is constrained so that the horizontal forces are balanced. The energy and altitude are chosen to minimize the Hamiltonian. This consists only of the range rate and the associated multiplier, which is constant because the Hamiltonian is not an explicit function of range in this, or any other modelling in this study. As a result the min-H operation leads to the high speed point on the level flight envelope. In the language of singular perturbation theory

this is the zeroth-order 'outer solution', which the solutions from the other time scales must fair into assymptotically. The matching of different solutions and the composite generation are discused in a later section. The next time-scale is now examined.

2.2 ENERGY-STATE MODELS

The next level of order reduction is generally referred to in the literature as energy modelling. In this case ε^1 is set to 1, and ε^2 to zero. Again the altitude and path-angle are assumed to be 'fast' and and 'control-like', but the energy change is analyzed and E assumes the role of a 'slow' variable. Again the path-angle is fixed at zero, and the lift coefficient chosen so that the lift equals the weight; but the only remaining 'control-like' variable (apart from the throttle, η) is the altitude: at any energy the altitude must be picked so as to minimize the Hamiltonian, which is now defined as:

$$H = \lambda_x \dot{x} + \lambda_E \dot{E} = \lambda_x V + \lambda_E \dot{E}$$

where the differential equation for E is given by:

$$\dot{E} = V (\eta T - D) / W$$

$$\dot{\lambda}_E = -\frac{\partial H}{\partial E}$$

The altitude which minimizes the Hamiltonian is therefore going to be determined, at any energy, by the relative values of λ_E and λ_x and their signs: their ratio determines the relative importance of range rate and energy rate, and their signs determine the sense of the optimization. For example, if λ_E is small enough the altitude picked will correspond to the maximum possible instantaneous range rate possible at that energy, if λ_x is negative. This is the lowest altitude (and highest speed) which is allowed by the terrain limit, dynamic-pressure limit or Mach limit, whichever is greatest. On the other hand if the range multiplier is set to zero the altitude chosen will maximize the instantaneous excess power or energy rate, if λ_E is negative. This special case is the so-called 'energy-climb', and is discussed in the following subsection. Note that if either multiplier is positive the rate of change of the associated state will tend to be minimized.

2.3 ENERGY CLIMBS

Of the possible energy-state results the energy-climb is the simplest to calculate: as the Hamiltonian only contains one term, only one differential equation needs to be integrated assuming that λ_E remains negative. The initial value of the

multiplier does not in general have to be determined: so long as it is negative the same path will result. Indeed if time histories are not required none of the differential equations need to be integrated at all: the altitude-energy path may be found simply by maximizing the level-flight energy rate at any energy. The energy climb for the aircraft studied is shown on Fig.1. It is interesting to note that this schedule shows multiple jumps in altitude, arising from realistic variations in the thrust data. This is somewhat different to other examples which have been examined, for example the F-4, where the altitude discontinuities in the energy-climb are primarily due to the transonic drag-rise (Ref 41).

2.4 ENERGY-RANGE CLIMBS

When the range multiplier, λ_x, is not assumed to be zero, i.e. 'energy-range climbs' are examined, the analysis and resulting computations are slightly more complex than the 'energy-climb' discussed above. First of all the λ_E equation must be integrated, as the relative magnitude of λ_E to λ_x at any time or energy is important in choosing the altitude. Secondly, as a result of this, the initial ratio of λ_E to λ_x, r^0, must be carefully picked: different values of r^0

will result in different paths with different terminal states. As the value of r^0 is increased from zero the resulting trajectories move downward in the flight envelope, with the terminal energy moving from the maximum energy, E_{max}, towards the dash energy, E_d. At a certain value of $r^0 = R^0$ a path results which fairs gracefully into the dash-point. This is the range-optimal 'energy-range climb' which is desired and is shown in comparison to the energy climb found earlier in Fig. 2, with the level flight envelope also shown. Determining the correct value of r^0 is an initial-value problem, but limited to only one dimension, and the usual one-dimensional search techniques, (i.e. golden-section, cubic and parabolic fits) may be employed. For values of r^0 which are greater than R^0 the resulting trajectories are range-optimal for terminal energies which are lower than E_d, over different time spans. These paths are characterized by a climb which approaches the dash point, a dash, and finally a terminal transient which takes the energy down to the desired level. This transient begins with an instantaneous dive to the maximum range rate (speed) at E_d, as allowed by the terrain, dynamic-pressure, or Mach limit, whichever is the most severe restriction at the current energy level. In the case studied, no Mach limit and dynamic-pressure limits were applied; rather the thrust

data was faired off to limit the level-flight envelope from exceeding such limits, as explained in Chapter 6. As a result the terminal manoever takes the aircraft down to the terrain limit, (outside the flight envelope), where it remains, losing energy. This situation is unchanged until the energy is reached corresponding to the dash speed at the terrain limit. At this point the engine is switched off (λ_E changes sign) and were speed brakes included in the model they would be applied: the instantaneous energy rate is made most negative. This sequence is shown in Fig. 3 for the aircraft being studied. For the case were Mach and dynamic-pressure limits are applied the equivalent maneuver is shown in Fig. 4.

This process needs some explanation: when the E_f is less than E_d, the aircraft must perform some terminal transient which loses energy in the most range-optimal way. There are two choices, or ways in which it can lose energy: at speeds below or speeds above the dash speed. Obviously the range-optimal strategy is to spend as much time in the latter region and as little in the former as is possible. This is done by switching off the engine when the speed drops below the dash speed, and if possible extending the drag brakes. The problem of the terminal-maneuver transient is not pursued here; it is of research interest.

2.5 METHOD OF MATCHED ASYMPTOTIC EXPANSIONS

By the use of singular-perturbation theory, boundary-layer type corrections can be used to overcome the energy-modelling weaknesses, i.e. initial and final jumps in altitude, as in Refs. 25 and 42, and transonic or internal jumps, as in Ref. 41. While the altitude discontinuities are eliminated by expansion to the zeroth order, realistic path-angle values are obtained, in the Ref. 25 approach, only by continuing the expansion to the first order or higher. This is a nontrivial problem in the case where the altitude transitions occur at the beginning or the end of a trajectory, and is even more complex in the case of the internal jump. As a result, even the corrected energy model loses its attraction when realistic path-angles are required for onboard use as commands. A scheme for providing more realistic path-angle results in the zeroth order is explored in Ref 43.

2.6 CONCLUSIONS

To conclude this chapter, some of the results of the reduced-order modelling are summarized below.

First of all energy-state modelling, while attractive in its simplicity, is inappropriate and unsuitable for on-board

guidance use on its own, i.e. uncorrected, for the intercept mission contemplated. This is because it generates significant initial and terminal discontinuities in altitude and path-angle, which the aircraft is supposed to follow instantaneously. Secondly, multiple instantaneous jumps are also possible along along the optimal path, and lastly the path-angle is obtained as zero, in the usual approximation, which is a again a big disadvantage as the actual path-angles can be quite large.

Corrections to the energy-state model which overcome these weaknesses are possible and have been demonstrated in the literature (Refs 41,42). However this additional complexity is extremely unwelcome for on-board calculations due to limited storage and, more importantly, execution time available on-board; indeed solutions are not guaranteed due to the instabilities of the state-Euler system which need to be suppressed. In this context it is questionable whether this approach is in fact easier or quicker than solving the optimal control problem for the full system.

However, certain ideas from the energy-state model are undeniably attractive. The solutions suggest a hierarchical structure of states in optimal control solutions. This is exhibited in the following way: altitude and path-angle 'command' values are determined by the current energy, and

in this sense the energy is the dominant state. If the current values h and $\dot{\gamma}$ do not coincide with these predetermined values a rapid transition can be made which brings them to their 'correct' values. These ideas form the basis of the guidance scheme which is presented in the next chapter.

Chapter III

ON-BOARD GUIDANCE

An alternative to using order reduction, suggested in Ref. 20, which is simple enough to lend itself to onboard implemention is now developed, for the case of symmetric flight. The scheme has roots in the hiearchical structure of optimal-control solutions of the energy model, in which the specific energy is a relatively 'slow' variable and its value determines the control-like 'fast' variables, h and γ.

3.1 NOMINAL PATH

The phenomenon described above suggests that trajectories of the point-mass model funnel rapidly, (rather than instantaneously as in the energy model), into the vicinity of a single path, which leads to the dash-point. The idea pursued in this thesis, and Ref 44, based upon Ref 20., is to determine this 'skeletal path' for the point-mass model, for as wide a range of energies as possible. This is the nominal, or reference trajectory and the altitude and path-angle histories are recorded as functions of the energy or energy-to-go, rather than time or time-to-go, as is common in other neighboring optimal guidance schemes (Refs 28-37). The advantage of this approach in an on-board context is

that approximations to the final time are not necessary, and implementation of the scheme is greatly simplified as a result.

3.2 FEEDBACK LAW

The next step is to generate a neighboring-optimal feedback guidance law which will control the aircraft so as to follow a neighbor of the nominal optimal path. There are two basic reasons for doing this. First of all the reference path is of little use open loop: even if the aircraft is at any time on the reference path, the control commands which are stored along this trajectory will be insufficient to keep the aircraft close to it. This is because disturbances and errors inevitably arise both in the actual flight (i.e. variable winds etc) and in representing the control history using a cubic spline (Ref 45) Secondly, even if this first problem could be ignored, the reference path is of little, if any, use when the aircraft has initial conditions which are far removed from the nominal: for instance if the aircraft is initially loitering at high altitudes and subsonic speeds, on combat patrol, for example. Linear-feedback coefficients are proposed to generate the necessary transients to bring the aircraft to the neighborhood of the nominal optimal and stabilize the subsequent path. The

guidance law is a linear feedback control based on the difference between the nominal and actual altitude and path-angle values.

3.3 FEEDBACK COEFFICIENTS

The feedback coefficients, which correspond to minimizing the second-variational approximation to the performance index, as in Refs. 28-37, are found by perturbing the altitude and path-angle separately from their nominal values along the reference trajectory. The optimal-control problem is re-solved and the partial derivative of the control with respect to the states (at fixed energy) is estimated by difference quotient approximation. The partial derivatives which are mentioned here are the variations in the parameters of an initial value problem; they should not be confused with the variations of the control along the trajectory. They are defined for an arbitrary value of energy = E^1 in the following way:

let $C_1^*(t)$ be the control which takes the aircraft from an initial point at low energy, E^0, (altitude and path-angle zero), along the nominal path up to the dash point on the level flight envelope, while optimizing range; the resultant state time histories are given by

$$h^*(t),\ \gamma^*(t),\ \text{and}\ E^*(t)$$

let the energy of the aircraft reach the value E^1, while travelling along the nominal path, at a time t^1:

$$E^1 = E^*(t^1)$$

Then at E^1 the 'correct' altitude and path-angle are given by $h^*(t^1)$ and $\gamma^*(t^1)$. To find the altitude feedback coefficient at this energy level the procedure is as follows:

find the range-optimal path which has the same terminal conditions, and terminal time as before but use the nominal state at t^1 as the initial conditions, with a perturbation, Δh, introduced in the initial altitude:

$$\gamma(0) = \gamma^*(t^1)$$

$$E(0) = E^1$$

$$h(0) = h^*(t^1) + \Delta h$$

The solution of this problem results in a new control time history, $C_{lnew}(t)$. The altitude feedback coefficient is found by the following secant approximation:

$$\frac{\partial C_l(E^1)}{\partial h} = \frac{C_{lnew}(0) - C_l^*(t^1)}{\Delta h}$$

3.4 ON-BOARD USE

The C_l commands to the autopilot are taken from the nominal path with linear corrections for the variation of the altitude and path-angle from their nominal values. On-board use requires only the storage of the states (h and γ), control (lift coefficient or load factor), and the two feedback coefficients, each as functions of energy, or energy-to-go. The feedback guidance law with the appropriate functional dependencies are shown below:

$$C_l = C_l^*(E) + \frac{\partial C_l}{\partial h}(E)\,(h - h^*(E)) + \frac{\partial C_l}{\partial \gamma}(E)\,(\gamma - \gamma^*(E))$$

To summarize the only variables required to be stored on-board in symmetric problem are :

$$C_l^*(E)$$

$$h^*(E)$$

$$\gamma^*(E)$$

$$\frac{\partial C_l}{\partial h}(E)$$

$$\frac{\partial C_l}{\partial \gamma}(E)$$

Chapter IV

OPTIMAL SOLUTIONS FOR THE POINT-MASS MODEL

A requirement of the proposed idea is a large number of optimal-control solutions to the point-mass-modelled problem. Optimal control solutions can be found in many different ways. They can be found by the use of direct methods, such as gradient methods, where the control history is parameterized in sectionally-linear or spline approximation and the terminal conditions are met by either penalty or projection techniques. Alternatively, the problem can be resolved into a two-point boundary value problem, with split boundary conditions. Half are known at the initial time and the other half at the final time. This can be solved by the use of indirect methos such as simple or multiple shooting (Refs. 22,23). To solve the problem of time-optimal control the variational Hamiltonian is formed:

$$H = \lambda_E \dot{E} + \lambda_h \dot{h} + \lambda_\gamma \dot{\gamma} + \lambda_x \dot{x}$$

and the Maximum Principle (Refs 38,39) is applied.

The rsulting Euler differential equations are :

$$\dot{\lambda}_E = -\frac{\partial H}{\partial E}$$

$$\dot{\lambda}_h = -\frac{\partial H}{\partial h}$$

$$\dot{\lambda}_\gamma = -\frac{\partial H}{\partial \gamma}$$

$$\dot{\lambda}_x = -\frac{\partial H}{\partial x}$$

The lift and the throttle setting must be chosen to minimize the Hamiltonian, which requires that:

$$\frac{\partial H}{\partial C_l} = 0$$

and

$$\eta = 1$$

$$(\lambda_E < 0)$$

4.1 METHOD OF SOLUTION

Euler solutions were found in the present work by the method of multiple shooting, using the algorithm and computer program of Refs. 33,48 kindly supplied by DFVLR, Oberpfaffenhofen, West Germany. In this method, the interval of integration is broken up into many subintervals. This is preferable to 'simple shooting', where the initial-value problem is attempted directly, as optimization

problems of lifting atmospheric flight are ill-conditioned, the state-Euler system being violently unstable. Partitioning the time interval has the effect of suppressing error growth. This method was used primarily for reasons of accuracy. This need arises, for example, in the calculation of the feedback gains, found by the difference of the control at the beginning of two optimal solutions. Typically to find the gains to 5 figures the control must be known to about 8 figures. The multiple-shooting method has greater accuracy than the other methods available, and although it is often difficult to generate the initial reference trajectory, the subsequent calculation of the feedback gains is relatively easy as the method has good convergence properties in the vicinity of a solution. Further discussion on these topics is found in Chapter 8.

Chapter V

INITIAL EXPOSURE TO OPTSOL

The first use of the multiple shooting program OPTSOL obtained from DFVLR was to solve a very simple optimal control problem. This, taken from Bryson and Ho (Ref. 49) page 121, is similar to the brachistochrone, and was solved numerically both with and without a constrained arc, to test the user-supplied software required for the program.

5.1 AIRCRAFT DATA MANIPULATION

The program OPTSOL had been brought to VPI&SU with subroutines already created to enable the solution of aircraft flight mechanics problems and, rather than try to start from the beginning, attempts were made to use the existing computational tools, at least until familiarity had been gained with the program. In particular, the data which was used to model the aircraft under study was extensively modified so that the integration subroutine in OPTSOL, known as DIFSYS, was able to function. This proved to be a problem, as DIFSYS, as received, was extremely sensitive to the degree of smoothness of the right hand sides of the differential equations. In fact if discontinuities are

encountered in any derivative up to the eighth, the stepsize of integration shrinks to zero. As all data of the point-mass model had been represented by cubic splines and spline lattices to facilitate interpolation, considerable effort was spent on the generation of an analytical representation which would reproduce both the values and the shapes of the data with consistency. This had been done at DFVLR by using polynomial expressions, and this method was examined for the aircraft data on hand and abandoned.While a polynomial of sufficiently high order will fit any number of consistent data points exactly, there is an increasing distortion of shape with increasing order of polynomial. In fact even low order polynomils did not match the data at all well. The approach taken was to use a combination of polynomials, exponentials and arctangent functions to accomplish this. In the case of the single valued functions, i.e. $C_{do}(M)$, $K(M)$, this was not too difficult. The arctangent functions can be used as'soft'switches, separating different portions of the data, which can be represented by a simple function locally (i.e. by a straight line or a parabola). However in the case of multivariable functions such as thrust and fuel flow this is definitely a nontrivial problem (however only thrust was attempted). In the case of thrust, the representation was achieved by fitting against Mach number, using coefficients

which were functions of altitude. 19 variables were optimized using a conjugate gradient process which minimized the sum of the square of the errors at the grid points. The functions developed for Thrust, C_{do}, K, are shown in Appendix A, and the aerodynamic data are shown graphically in Figs. 5 and 6.

After construction of the smooth data, the flight envelope was calculated and drawn (Fig 7). As in the case of some high-performance jet-fighter aircraft the envelope turns out not to be performance limited, i.e. the level flight maximum sustainable speed is much higher than the Mach limit. In this case M=2.4 is the Mach limit and the high speed point occurred at roughly M=3.0. It should be mentioned that aerodynamic and thrust data are not actually available for M= 2.4 and the flight envelope found by extrapolation is essentially a conjecture. The important thing is that the excess power at level flight is greater than zero for a range of altitudes along the Mach limit, for which both thrust and aerodynamic data are reliable. This problem, which in general requires treatment of state-inequality constraints, was dealt with in the following way: the Thrust was faired off sharply against Mach Number, near the Mach limit so that the flight envelope no longer exceeded it. This was done by multiplying the thrust by a

switching arctangent function which rapidly (but smoothly) brought the thrust to zero while leaving it unaffected elsewhere. The dynamic-pressure limit was treated in the same way. The analytical formulation for these two limits are included in Appendix A. The flight envelope with the Mach-number limit is shown in Fig. 8; the effect of both of the limits is shown in Fig. 9.

5.2 INITIAL FLIGHT-MECHANICS PROBLEM

Once the dataset had been finalized, OPTSOL was used to generate some optimal trajectories for a simple atmospheric flight problem: maximize final speed, from a given initial state, with final path angle zero and final altitude free. This was was solved for several different time intervals, using simple shooting (initially), and also multiple shooting, to gain familiarity with the use of multiple shooting and to investigate the methods of finding families of trajectories , for instance by time stretching. The time-histories for a family of four different trajectories are shown in Fig. 10-12. These are, respectively, speed, path-angle, and altitude plots.

5.3 FIRST TRAJECTORIES TO THE DASH POINT

The next step was to attempt to find paths which went to the high speed point, over a fixed time interval and to try to decrease the initial energy while lengthening the overall flight time. This was done by starting at an altitude and speed combination ,(path-angle zero), just below the dash point, guessing the values of the costates. A total integration time of 5 seconds was used, and as can be imagined, the first guess was far from the targeted final conditions; however by requiring OPTSOL to satisfy boundary conditions by successive proximity rather than in one jump, a trajectory which reached the specified altitude and path angle combination was found. However, it was not possible to to get the final speed to the desired value in the 5 second interval, because the time was not long enough to reach it. To achieve the desired final speed and to observe the manner in which the system approaches the equilibrium point (the possibility of an oscillatory solution near the high speed point , analogous to oscillatory cruise solutions was considered a possibility), attempts were made to lengthen the time of integration, by stretching the sub-intervals in the multiple-shooting scheme. Initially it was found to be very difficult to extend the trajectory at all - OPTSOL would not converge for even extremely small increases in the

final time. Eventually the interval was increased to 6 seconds. The final speed also increased but still did not reach the value at the dash point. It became virtually impossible to increase the final time any further due to numerical integration difficulties. For this reason and computational expense, the approach was reassessed at this point.

5.4 EIGENVALUE ANALYSIS

The system was linearized about the high speed point to examine the dynamics of the system in the vicinity of the equilibrium point . The analysis revealed that the stablility eigenvalues were all placed along the real axis. At first the absence of complex roots akin to phugoid oscillation suggested that the linearization had been incorrect. After this had been checked and rechecked, the analysis was repeated at a point removed from the vicinity of the sharp arctangent functions which had been used to limit the flight envelope, as it was conjectured that the switching functions may have introduced large gradients affecting the dynamics of the closed-loop system . The throttle coefficient was reduced to 0.68, reducing the speed of the dash point by about 100 ft/sec, well away from the

arctangent switch region, and the linearized analysis was repeated. The eigenvalues were found to have both real and imaginary parts, as expected, showing that the steps taken to limit the flight envelope had engendered significant effect on the dynamics of the state-Euler sytem. The s-plane positions of the two cases are shown in Fig. 13 and 14.

5.5 BACKWARDS INTEGRATION OF STABLE EIGENVECTORS

It was thought that a useful starting trajectory could be found by using the stable eigenvectors of the linearized sytem. If the equilibrium state is disturbed in proportion to a stable eigenvector the disturbance will die out in the linear case and should fair in towards the equilibrium point, for some finite time at least,in the nonlinear case, if the disturbance is small enough. So if such a trajectory is integrated backwards in time (using the full nonlinear system) a series of points will be generated which will fair in towards the dash point, at least for some time. Only one of the three eigenvectors approached the dash point from the desired direction, i.e. from points lower in altitude and slower in speed. This was integrated for 22 seconds and used as an initial guess for OPTSOL. The path-angle at the

initial time was non-zero and attempts were made to reduce it to zero. Again convergence troubles were encountered: OPTSOL could not tolerate large changes in the initial values and the effort was finally abandoned. Apart from the cost of computing and poor convergence behaviour, the system also displayed an alarming instablity to small changes: on occasions the speed in the final seconds dropped from its maximum value (about 2300 ft/sec) to 1 ft/sec.

5.6 CONCLUSIONS

It was concluded that the thrust-tailoring approach taken to make the problem easier had instead probably made it worse. The integration subroutine DIFSYS is very sensitive to small changes in derivatives of the right hand sides. By using a multiplicity of sharp arctangent functions the computational burden became large, as every time DIFSYS encountered an arctangent transition the stepsize of integration automatically became very small , increasing the computer time required. Further it was evident the system was overly sensitive to small changes in initial values. As a result it was decided to use a simpler integration subroutine and to return to splined data.

Chapter VI

MODIFICATIONS TO OPTSOL

The first step to modify the operation of the program OPTSOL was to change the integration routine. The variable step, eighth order Runge-Kutta package DIFSYS seemed to be a primary scource of the numerical difficulties and computational expense experienced in the early use of OPTSOL. It was removed in favor of a much simpler fixed step-size fourth order Runge-Kutta-Gill subroutine.

6.1 SPLINED AIRCRAFT DATA

This substitution enabled the use of cubic splines and spline lattices of Ref (45) for representation. of the aircraft thrust and aerodynamic data. The problem of the Mach-limit violation was handled by fairing off the thrust data gently over four tenths of a Mach Number and increasing the drag by adding more missiles. The aerodynamic and thrust data are included in tables 1-4. The new flight envelope was calculated and is shown in Fig. 15. The coordinates of the dash point were found by a Newton iteration applied to the usual necessary conditions.

6.2 FAMILY OF TRAJECTORIES TO THE DASH POINT

The new data were used to calculate an 'energy-climb' schedule(Ref.25); this was used as a guide for guesses of initial altitude, energy and trajectory time combinations. A thirty-panel division of the trajectory was employed to find trajectories starting at lower altitudes, over longer times. This procedure was successful in finding optimal-range histories starting from an initial energy of 30,000 ft. After this point it became difficult and expensive to progress any further down in altitude and energy. It was thought that a smaller stepsize might be necessary to evaluate partials with sufficient accuracy for the method to converge. However this did not improve matters significantly. But when the program was brought to Langley Research Center the situation improved. The CDC computer has a word-length which is approximately double that of the IBM 370, so with double precision at Langley about 28 decimal digits were obtainable compared to 14 or 15 digits at VPI. This had a signifi ant effect on the program's operation. Much smaller stepsizes were used to evaluate the Jacobian without a penalty in round-off error, and it is conjectured that the resulting improvement in the accuracy of the Jacobian helped the convergence of OPTSOL. The trajectory extension continued until zero altitude was reached over a trajectory of 282 seconds.

Chapter VII

OPTIMAL-REFERENCE-PATH CALCULATIONS

The first objective is to generate a reference optimal path using point-mass-model dynamics, over the widest possible energy range. In the climb-dash problem, the highest energy of interest corresponds to that of the high-speed point on the aircraft envelope, the dash 'outer' solution. The lowest energy corresponds to the trajectory which just kisses the terrain limit, i.e. below this energy, optimal solutions which start at zero altitude would dive below the terrain limit if it were absent. This lower energy is found by examining the initial load factor of a family starting from level flight at the terrain limit altitude: when the initial load factor is unity the lower energy is determined. This is shown in Fig. 16, where the initial load factor is plotted for several different initial energies.

7.1 FINAL LOAD FACTOR

Once the energy had been found which pulled off the ground with an initial load factor of 1, the effect of the flight time was investigated. To satisfy the final conditions in a finite time requires that the aircraft perform some

maneuvering near the terminal energy: the longer the time allowed to approach the equilibrium point, the more gradual the approach should be. The effect of flight time on the final load factor was studied (for the same inital and final conditions) and results are shown in Fig. 17 . This clearly demonstrates how the optimal path tends to fair in asymptotically as the flight time is increased. The load factor dropped to 1.001 after the flight time had been increased to 360 seconds. This time was chosen for the nominal path adopted in guidance-scheme development, and the altitude and path-angle (state variables) as well as the lift-coefficient (control variable) have been splined as a function of the energy. The load factor is shown in Fig. 18 , drawn against energy, showing the grid points used in the spline. Fig. 19 - 22 show the energy histories for path-angle, altitude, load factor and lift coefficient respectively for t_{max} = 360 secs. The other paths from the same initial energy, but over longer times, showed identical state and control energy histories over almost all the energy range. However at the terminal energies the effect of different flight times is most evident. Comparisons of the trajectories which result for different flight times are shown in Fig. 23 - 26 for path-angle, altitude, load factor and lift coefficient respectively. These variables are

plotted versus energy for the last 2000 ft of energy, for t_{max} = 300 and t_{max} = 360 seconds. The dramatic effect that the flight time has on the final state and control behaviour is obvious from these pictures.

7.2 ONE PANEL INTEGRATION

After each converged solution was obtained a trajectory was performed for the entire time, from the initial conditions. At higher energies and over shorter times this would ordinarily generate final states which were close to those specified in OPTSOL, but owing to the error propagation of the mismatched paths at each grid point, there is a difference between a one-panel integration and a 30-panel integration. However at energies with zero initial altitude the error propagation was such the final conditions were not nearly met. After about 150 to 200 seconds the instabilities in the state-Euler system would produce extreme results. This raised the question as to whether the solution generated by OPTSOL is optimal or even near optimal. To this end the number of panels was reduced first to 10, then to 6. Attempts to drive the number smaller than this were not succesful as it appeared that the computer was 'running out of digits', despite the fact that 28 were being used. However the difference between the solution for 6

panels and for 30 panels lies beyond the 9th digit and so it was assumed that no benefit would be gained by trying to reduce the number of panels.

7.3 ENERGY-MODEL / POINT-MASS-MODEL COMPARISONS

Having established the nominal optimal path which takes the aircraft up to the dash point, it is of interest to stop and consider the two different models which have been used to study the problem, in particular it is of interest to compare the two different paths which climb up to the high-speed point. These are shown in the h-v plane in Fig 27, surrounded by the level-flight envelope. The energy-range-climb model is indeed close to the point-mass model particularly at higher energies.

Chapter VIII

FEEDBACK COEFFICIENTS - CALCULATIONS

This chapter describes the numerical work done to evaluate and represent the feedback coefficients used in the guidance law for the case of symmetric flight. In this case the coefficients are the partials of the lift coefficient with respect to the altitude and path-angle, at a fixed energy.

8.1 METHOD OF EVALUATION

The calculation of the variation in the control due to errors in the altitude and path-angle is treated as an initial-value problem, and has been extensively discussed in Chapter3 To improve the accuracy of the feedback coefficients, each one was evaluated twice, by introducing positive and negative perturbations, and taking the average of the two difference-quotient values. This method also allowed the determination of the optimal size of disturbance (in terms of the resulting accuracy) by varying the size of the disturbance ,examining the degree of agreement between the two values untill the 'best' stepsize has been found for both altitude and path-angle. While it is true that the optimal stepsize will in general vary along the reference path, it was found that this change was negligible and one

value was effective in evaluating the entire range for either coefficient. As the stepsize is reduced the errrors due to nonlinearities shrink, but those due to a finite word-length grow: hence a compromise defines the optimal disturbance. It has been noted that a multiple shooting method such as OPTSOL is well suited to these kinds of calculations: although it was an arduous task to establish the nominal path, once this had been achieved, the neighboring solutions were found rapidly (within 3 or 4 iterations) and with highaccuracy. This last point is important, as the use of numerical differentiation of the initial control to find the feedback gains required high precision the control. Typically it was found that 8-9 decimal digits of information were required for 4-6 figure accuracy in the gains.

8.2 PILOT SCHEME

Feedback coefficients were initially found over a small range of energies, to evaluate the usefulness of the scheme before committing the computational resources needed for the full-scale operation. The last fifth of the energy range was chosen for this purpose as the integration times are the shortest and this minimises the cpu time rquired to find optimal control solutions. The energies and corresponding

times were taken from the reference trajectory (of 360 seconds) in the following manner: the total energy change was divided into twenty. The reference path was then integrated again and whenever the energy at the end of an integration step exceeded an integer number of divisions of the total energy change, the time and energy were recorded. The times and energies for the pilot run are shown in table7. The disturbance sizes were varied so as to maximize the agreement in between the two values obtained for each coefficient. The optimal perturbation in altitude was found to be 0.05 feet; in path-angle it was found to be 0.0000001 radians. Agreement between the values of both of the coefficients was found to vary in between 4 and 6 figures.

In addition to the energy levels already chosen for feedback coefficient evaluation, it was necessary to find values close to the final energy as well. This is because spline representations are very unreliable when used to extrapolate data. The energy at the beginning of the last panel in the multiple-shooting method, i.e. at 348 seconds, was chosen as the upper limit for this purpose. The gains at this energy, which is just 0.11 feet below the maximum value, turn out to be an order of magnitude larger than the gains at lower energies. This sensitivity of neighboring-optimal-guidance schemes close to the terminal state has been noted in the

literature (Refs.(28-37)). It is worth commenting , however, that the apparent unboundedness in the gains near the final state could have been a result of the method by which they were calculated; it is quite possible that a finite integration time, which is shorter as the terminal state is approached, was responsible. In other words if a longer time of integration had been allowed for the paths which were close the final state a different behaviour might have been observed. However this effect is highly local, and due to limitations of time and money this topic was not pursued. Any actual implementation of the scheme would of course have to take this into account, possibly by setting an upper limit on the magnitudes of the gains, to avoid control saturation with small errors. To examine the transition in the feedback coefficients near the terminal state, the analysis was repeated for 3 more energies close to the final time, at 336,324, and 300 seconds. This is an inexpensive set of calculations as the integration times are extremely short. Also the coefficients were evaluated at the energy corresponding to the trajectory time of 188.7 seconds, as it was felt that they were needed for accurate spline representation.

The next problem was to spline the coefficients as functions of the energy-to-go. Difficulties were encountered at first

when the splining was attempted. Cubic splines are not suited in general to represent functions where large variations in the gradient exist. In this case the gradient changes by six orders of magnitude in the vicinity of the end-point, resulting in large extraneous oscillations appearing throughout the spline representation, which render the interpolation useless. One way (not very satisfactory) is to ignore the spurious points which are causing the trouble. This was done in this case, and the plots of the coefficients are shown Figs 28,29.

To overcome these difficulties the splines-under-tension of Ref. 50 were used. These are similar in character to the cubic splines of Ref 45 which had been used so far; the additional feature of the splines-under-tension package is the ability to minimise spurious wiggles near regions of rapidly changing gradient by the use of a tension factor, σ. By increasing σ the anomalies can be reduced but not eliminated, at least in the vicinity of the end point. The problem is that as the tension factor is increased the oscillations near the end point die down but the rest of the representation becomes essentially polygonal, i.e. linear interpolation between the data points.

8.3 LOGARITHMIC SPLINING

It became apparent that the normal or ordinary method of splining was inadequate and a different approach was needed to continue. Essentially this is a boundary-layer type problem: there is a region where the coefficients vary rapidly. It seemed to be appropriate to separate the two regions and, using different methods, spline each one separately. The only requirement would be that the two representations fair into each other smoothly. One possibility is to use the normal splines in the 'outer' region, and spline the terminal coefficients in terms of the logarithm of the energy-to-go, matching the slopes at the junction between the two regions.(Another possibility is to use the inverse of energy-to-go in the terminal region, but this was not used for reasons as the large variations in the gradients, which are the roots of this problem, still exist). The logarithmic method was used to spline the coefficients for the range of energies considered in this pilot section. The results are shown in Figs 30 and 31. These show the gains using 10 gridpoints for interpolation. These show a dramatic improvement over the previous attempts to spline the data: these earlier efforts had been so bad that they would only be visible on the same graphs as a series of vertical lines passing through the gridpoints. It

was considered likely that with a few additional points the small remaining anomalies would be eliminated. An additional 16 points were evaluated in the vicinity of these outstanding 'wiggles' and finally a usable representation was generated, shown in Figs 32 and 33, as functions of energy. They are shown as functions of the logarithm of energy-to-go in Figs 34,35.

When the decision was made to carry on and evaluate the coefficients over the rest of the energy range, the same method was used to spline the data: the logarithm of the energy-to-go was used, and there was no need to go to a boundary layer type of approximation after all. The coefficients as they were represented over the entire energy range are shown as functions of the energy in Figs 36 and 37. The corresponding plots versus the logarithm of energy-to-go are shown in Figs 38 and 39.

Chapter IX

SIMULATION AND TESTING

Following the satisfactory splining of the nominal states, controls and feedback coefficients as functions of the energy-to-go, the guidance scheme was tested by running a simulation of the point-mass-model, using the feedback law, and comparing the resulting trajectory with an Euler solution which started from the same initial conditions. Before the entire range of feedback coefficients had been worked out a pilot scheme tested out the idea on a small range of energy near the dash-point. This test was performed with an initial disturbance of 1000 ft; the trajectory which resulted from the guidance law is compared with the Euler solution from the same initial conditions and the nominal path in Fig 40 where the altitude is plotted as a function of energy. The guidance law is so close to the optimal path from the same starting point that it is almost impossible to discern the difference between them on this Figure. The difference in altitude between the two is shown as a function of time in Fig 41 it can be seen that the difference is always less than 11 ft. With zero disturbance the autopilot was able to follow the nominal path more than satisfactorily, over the entire range of energies, despite

the inevitable errors which arise in the spline representations. Tests were perfc rmed with the initial altitude disturbed from that of the nominal path at different energies by 1000, 5000, 10000, and 15000 feet above and by 5000, 10000 feet below the nominal path. The resulting trajectories are shown in Figs. 42-46. These show that the feedback law follows the optimal solution closely, even when the initial disurbance is far outside of the range of linearity of the feedback gains. The cost was calculated for the situation with an initial altitude of 15000 ft above the nominal value, at the point where the two trajectories faired into the dash point. The difference between the ranges was less than 600 ft, an extremely small number considering that the dash speed is 2400 ft/sec.

Chapter X

EXTENSION TO 3-D FLIGHT

This chapter descibes the work done to extend the analysis to three dimensional flight, and suggests what direction future efforts might take.

10.1 CROSS RANGE CONSIDERATIONS

The problem of extending the analysis to 3-D flight is now considered. The state system is augmented to include y, the cross range, and χ, the heading angle. The addition of the corresponding multipliers to the full state-Euler system raises the order of the problem to twelve. For the intercept problem the final value of y must be zero; the value of the final heading, relative to the initial heading, must either be calculated on-board, or be supplied by the GCI. This will in general vary, for a maneuvering target, and the value stored on-board must be periodically or continuously updated.

The boundary condition on y leads to a dependance of the optimal solution on the cross range: for the same heading-to-go and energy-to-go there will exist many different possible values of y. As a result, if this formulation is used, cross range-to-go is an additional running variable:

this increases the order of the nominal paths required, which means a large increase in the computations on the ground, as well as an increase in the storage requirements on-board.

To get around this situation it is proposed to avoid using an additional running variable by letting the final value of y be free: this can accounted for in the computation of the final heading needed for intercept, as specified by the on-board flight computer or the GCI. The intercept paths which result from the two different methods are compared in Figs 47 and 48, for a target which is initially far away from the interceptor.

10.2 COMPUTATIONAL CONSIDERATIONS

The first approach considered to generate a family of paths to the dash point was to use the symmetric flight reference path as a starting point for the augmented system, and introduce a small heading-to-go at the initial time. The argument for doing this is that for very small headings the state-Euler system should not be changed very much: the paths are close to each other. However this method is only useful for a small number of combinations of heading-to-go and energy-to-go. This is because the turning rate at the energy at which the aircraft lifts off the ground is so high

that all the heading-to-go disappears in a short time, and over a very small energy range. In general a method must be found which generates the part of the family of reference paths which combines moderate and large headings-to-go and moderate to small energies to go. The difficulty lies in knowing what initial conditions to pick for the altitude and the path-angle: when the aircraft is lifting off the ground, these variables are specified, but in the general case, starting from an arbitrary energy-to-go and heading-to-go combination, the selection is a problem. Letting them be free is not acceptable as it can lead to an initial lift coefficient of zero (i.e. in the symmetric case): the optimization algorithm takes advantage of the freedom to choose the initial conditions in a way which maximizes the short term benefit. This does not fit in with the concept of a nominal refence path, where the altitude and path-angle are the same at the same combination of energy and heading-to-go.

The solution that is reccomended is to use the altitude that comes out of the energy-turn model, as in Ref 25. Here the heading is assumed to be a 'slow' variable, and has the same status as energy. However, instead of having to choose one variable, (such as the ratio of the initial energy multiplier to the range multiplier, as in Chapter 2), the

initial heading multiplier must also be iterated upon. This is done using a Davidon-Fletcher-Powell algorithm, to find the path which fairs into the dash point with zero heading. An example of such a path over a small range of energy and heading-to-go is shown in Fig 49, where the heading is shown against energy, and in Fig 50, where the heading vs time plot for the same initial conditions is shown.

10.3 SELECTION OF THE INITIAL PATH-ANGLE

The energy-State model produces altitude predictions which are fairly accurate as a function of the current energy, (away from altitude jumps), as can be seen Fig where the Euler solution to the climb-dash is compared to the energy-range solution. However the same can not be said for the path-angle, which is predicted to be zero along the path. As a result a modification is considered, (Ref 43), which produces realistic values along the path. The difference lies in the selection of the fast and slow variables: if altitude is chosen, zero path-angle results, if velocity is chosen, a value of the path-angle results which is to high. A new fast variable is examined in Ref 43 which picks path-angle values in between these two values, and which may be used as initial conditions for the problem at hand.

Chapter XI

IMPLEMENTATION AND CONCLUSIONS

11.1 IMPLEMENTATION

Before the scheme may be used on a real aircraft there are some important simplifications and restrictions which have been applied in the interest of reducing the initial work-load which must be accounted for.

First, the weight variation of the aircraft must be included in the modelling as a substantial percentage of the total weight may be used up during a mission. This is perhaps the easiest or at least the most straight-forward problem: the required action is to increase the order of the system, i.e. the mass is added as another variable and the resulting boundary conditions are simply that the initial mass is known, initial mass multiplier is unknown, and the final mass is unknown resulting in the mass multiplier being zero at the final time.

Fuel optimization is a problem which will no doubt be of interest, with different combinations of fuel and range being optmized. Problems can occur here with a non-convex hodograph, i.e. leading to the possibility of chattering controls, in this case the throttle.

Other problems of the real world which have not been addressed are variations in atmospheric conditions i.e. winds aloft and non-standard temperature distribution against altitude. Possibly these could be dealt with by anlaysing the effect of small perturbations, finding an approximation to the first order changes in the variables which are stored on-board and using simple linear corrections. Certainly this is the simplest way of tackling such difficulties and it would be interesting to examine how effective this approach would be.

Another problem of interest is that of variable configuration, i.e. the effect on the guidance scheme of changes in the aircrafts characteristics due to battle damage, releasing external stores, etc.

The biggest problem that must be looked at is the extension to 3-D, discussed in the last chapter.

11.2 CONCLUSIONS

The numerical results bear out the following conclusions: first, that all trajectories which fair into the high-speed point consist of a rapid transition onto a reference or skeletal path if they do not originate on it. Secondly, the linear-feedback scheme proposed is able to control the

aircraft so that it closely follows the appropriate neighbor of the nominal path for large perturbations of initial conditions.

11.3 FUTURE WORK

A 3-D extension of the computational scheme is of interest in which there are two dominant states, i.e. heading-to-go in addition to energy-to-go. As a result, families of optimal paths which fair into the dash-point will be needed, and the feedback coefficients will be functions of two variables (represented via a spline lattice) instead of one.

REFERENCES

1. Pastrick, H.L., Seltzer, S.M., Warren, M.E. Guidance Laws for Short-Range Tactical Missiles. Journal of Guidance and Control, 1981, Vol. 4 No. 2, pp 98-108.
2. Haeussermann, W. Developments in the Field of Automatic Guidance and Control of Rockets. Journal of Guidance and Control, 1981, Vol. 4, No. 2, pp 225-239.
3. Anderson, G.M. Comparison of Optimal Control and Differential Game Intercept Missile Guidance Laws. Journal of Guidance and Control, 1981, Vol. 4, No.2, pp 109-115
4. Sridhar, B., Gupta, N.K. Missile Guidance Laws based on Singular Perturbation Methodology. Journal of Guidance and Control, 1980, Vol. 3, No. 2, pp 158-165.
5. Stengel, R.F., Miller, G.E. Flight Tests of a Microprocessor Control System. Journal of Guidance and Control, 1980, Vol. 3, No.6, pp 494-500
6. Burrows, J.W. Fuel Optimal Trajectory Computation. Journal of Aircraft, 1982, Vol. 19 , No.4, pp 324-329.
7. Sorenson, J.A., Waters M.H. Generation of Optimal Vertical Profiles for an Advanced Flight Management System. NASA CR 165674, March 1981

8. Erzberger, H., Lee, H. Constrained Optimum Trajectories with Specified Range. Journal of Guidance and Control, 1980, Vol. 3, No. 1, pp 78-85.

9. Chakravarty, A., Vagners, J. Application of Singular Perturbation Theory to On-BoardAircraft Optimization. AIAA Paper 81-0019

10. Gracey, C., Price, D. Altitude/Path-Angle Transitions in Fuel Optimal Problems for Transport Aircraft. Paper submitted for the ACC Conference June 1983, San Fransisco.

11. Erzberger, H., Mclean, J.D. Fuel Conservative Guidance System for Powered Aircraft. Journal of Guidance and Control, 1981, Vol. 4, No.3, pp 253-261.

12. Beser, J. Approach Guidance Logicfor Tilt Rotor Aircraft. Journal of Guidance and Control, 1979, Vol. 2, No.6, pp 528-535.

13. Merrick, V. K., Gerdes, R.M. Design and Piloted Simmulation of a VTOL Flight Control System. Journal of Guidance and Control, 1978, Vol. 1, No. 3, pp 209-215.

14. Urnes, J.M., Hess, R.K., Moomaw, R.F., Huff, R.W. Hdot Automatic Carrier Landing System for Approach Control in Turbulence. Journal of Guidance and Control, 1981, Vol. 4, No.2, pp 177-183.

15. McGee, A.L., Paulk, C.H., Steck, S.M., Merz, A.W. Evaluation of the Navigation Performance of Shipboard VTOL Guidance Systems. Journal of Guidance and Control, 1981, Vol. 4, No. 4, pp 433-446.

16. Osder, S. DC-9-80 Digital Flight Guidance System Monitoring Techniques. Journal of Guidance and Control, 1981, Vol. 4, No. 1, pp 41-49.

17. Uhera, S., Stewart, M.J., Wood, L.J. Minimum Time Loop Maneuvers of Jet Aircraft. Journal of Aircraft, 1978, Vol. 15, pp 449-455.

18. Shinar, J., Merari, A., Blank, D., Medinah, E.M. Analysis of the Optimal Turning Maneuvers in the Vertical Vertical Plane. Journal of Guidance and Control, 1980, Vol. 3, No. 1, pp 69-77.

19. Well, K.H., Faber, B., Berger, E. Optimization of Tactical Aircraft Maneuvers Utilising High Angles of Attack. Journal of Guidance and Control, 1982, Vol. 5, No.2, pp 124-130.

20. Kelley, H.J. and Well, K. , ' An Approach to Intercept On-Board Calculations', Optimization Incorporated/DFVLR Memorandum, September 1980.

21. Wasow, W., 'Asymptotic Expansions for Ordinary Differential Equations', Wiley/Interscience, New York.

22. Kaiser, F. Der Steigflug mit Strahlflugzeugen-Teil I, Bahngeschweidigbeit besten Steigens. Versuchsbericht 262-02-L44, Messerschmitt A.G., Augsburg, 1944. Translated as British Ministry of Supply RTP/TIB, Translation GDC/15/148T.

23. Lush, K.J. A review of the problem of choosing a climb technique with proposals for a new climb technique for high performance aircraft. Aero. Res. Council Rept. Memo. 2557, 1951.

24. Rutowski, E.S. Energy approach to the general aircraft performance problem. J. Aero. Sci., 1954, (21), 187-189.

25. Kelley, H.J. Aircraft maneuver optimization by reducedorder approximation. In C.T. Leondes (Ed.), Control and Dynamic Systems, Vol. 10, 1973, Academic Press, New York.

26. Breakwell, J.V. Optimal flight-path-angle transitions in minimu-time airplane climbs. J. Aircraft, 1977, (14), 782-786.

27. Bryson, A.E., Desai, A., Hoffman, K. Energy State Approximation in Performance Optimization of Supersonic Aircraft. Journal of Aircraft, 1969, Vol. 6, pp 481-488.

28. Kelley, H.J. Guidance Theory and Extremal Fields. IRE Transactions on Automatic Control, 1962, Vol. 7, No. 5, pp 75-82.

29. Kelley, H.J. An Optimal Guidance Approximation Theory. IEEE Transactions on Automatic Control, 1964, Vol. 9, No. 4, pp 375-380.

30. Breakwell, J.V., Speyer, J.L., Bryson, A.E. Optimization and Control of Nonlinear Systems using the Second Variation. Journal of SIAM Control, 1963, Vol. 1, No. 2, pp 193-223.

31. Powers, W.F. A Method for Comparing Trajectories in Optimum Linear Perturbation Guidance Schemes. AIAA Journal, 1968, Vol. 6, No. 12, pp 2451-2452.

32. Powers, W.F. Techniques for Improved Convergence in Neighboring Optimum Guidance. AIAA Journal, 1970, Vol. 8, No. 12, pp 2235-2341.

33. Pesch, H.J. Numerische Berechnung Optimaler Flugbahn Koerrekturen in Echzeit-Rechnung. Dissertation, Technische Universitat Munchen, 1978.

34. Pesch, H.J. Neighboring Optimum Guidance of Space Shuttle Orbiter Type Vehicle. Journal of Guidance and Control, 1980, Vol. 3, No. 5, pp 386-392.

35. Speyer, J.L., Bryson, A.E. A Neighboring Optimum Feedback Law Based on Estimated Time-to-go with

Applicationto Re-entry Flight Paths. AIAA Journal, 1968, Vol. 6, No. 5, pp 769-776.

36. Wood, L.J. Petrurbation Guidance for Minimum Time Flight Paths of Spacecraft. AIAA Paper 72-915.
37. Hart, J.D. A Comparison of Low-Thrust Guidance Techniques. Phd Dissertation, University of Texas at Austin, 1971.
38. Pontryagin, L.S., Boltyanskii, V.G., Gamkrelidze, R.V., Mishchenko, E.F. 'The Mathematical Theory of Optimal Processes' John Wiley, New York, 1962
39. Leitmann,G., 'An Introduction to Optimal Control', McGraw-Hill, New York, 1966
40. Tihonov, A.N.,'Systems of Differential Equations containing Small Parameters in the Derivatives, Matematichiskii Sbornik 31, (1952)
41. Weston, A.R., Cliff, E.M., Kelley, H.J.,'Altitude Transitions in Ener Limbs', AUTOMATICA, Vol. 19, No. 2, 1983.
42. Ardema, M.D.;'Solution of the Minimum-Time-to-Climb by Matched Asymptotic Expansions,'AIAA Journal, 1976
43. Kelley, H.J., Cliff, E.M., Weston, A.R. Energy State Revisited. Paper to appear, 1983.
44. Kelley, H.J., Well, K.H. An Approach to Intercept Calculations, 1983. Paper submitted to the ACC Conference, June 1983, San Fransisco.

45. Mummolo, F. and Lefton, L.,'Cubic Splines and Cubic Spline Lattices for Digital Computation,'Analytical Mechanical Associates, Inc. ReportNo.72-28, July 1972, revision dated December 1974.

46. Bryson,A.E. and Ho,Y.-C., 'Applied Optimal Control', Juin/Blaisdell, Waltham, Mass., 1975

47. Keller, H.B., 'Numerical Methods for Two-Point Boundary Value Problems, Blaisdell, London, 1968

48. Keller, H.B., 'Numerical Solution of Two Point Boundary Value Problems!,SIAM, 1976

49. Bulirsh, R.; 'Die Mehrzielmethode zur numerischen Losung von Nichtlinearen Randwertproblemen und Aufgaben der optimalen Steuerung,' Vortrag im Lehrgang Flugbahnoptimierung der Carl-Cranz Gesellschaft. V. October, 1971.

50. Cline, A.K., 'Scalar- and Planar- Valued Curve Fitting Using Splines Under Tension', Communications of the ACM, April 1974

Appendix A

$$C_{do} = 0.0242 + \arctan(50(M-1.0))(1.0+0.35\exp(-4.5(M-1.8)^2)(0.012/\pi) + 0.08\exp(-55(M-1.1)^2] + 0.0096\exp(-20(M-1.35)^2) + 0.003\exp(-20(M-1.6)^2)$$

$$C_{dcl} = (0.5+0.2026\arctan(50(M-1.23))\arctan(50(2.25-M))(0.39M-0.475) + 0.075 + 0.05\exp(-150(M-0.985)^2) + 0.4(0.5+\arctan(50(M-2.25))$$

$$C_{lmax} = 0.82 + (0.72/\pi)\arctan(50(0.9-M))+ (1.23-0.6M)(0.5+0.2026\arctan(50(M-0.9))\arctan(50(2.05-M))$$

$$Thrust(M,h) = (0.5+(1/\pi)\arctan(40(M-XM2))(H2-H1) + H1 + (0.5+(2/\pi^2)\arctan(40(M-XM1))\arctan(40(XM2-M)))(H2-H1/XM2-XM1)(M-XM1)$$

XM1,XM2,H1,H2 are functions of altitude:

$XM1 = (3.84(\exp(0.165((h+1.74)))) - 4.82)$

$XM2 = 0.0156h^2 + 2.83h + 1.1$

$H1 = (f1.g1 + f2.g2)f3(41000)$

$H2 = (f11.g1+f22.g2)(0.5+(1/\pi)\arctan(40(0.91-h)))40405$

$f1 = -2.43h^2 - 1.59h + 0.974$

$f2 = 2.38h^2 - 3.24h + 1.24$

$g1 = (0.5 + (1/\pi)\arctan(40(0.3-h))$

$g2 = (0.5 + (1/\pi)\arctan(40(h-0.3))$

$f11 = 1.35h^2 - 1.53h + 1.56$

$f22 = 3.25h^2 - 6.25h + 2.98$

$f3 = (0.5 + (1/\pi)\arctan(40(0.75 - M))$

$h = \text{altitude}/10^5$

Mach Limit Fairing

The thrust is multiplied by the factor given by:

$f = (0.5 + (1/\pi)\arctan(150(2.4 - M)$

Dynamic Pressure Limit Fairing

The thrust is multiplied by the factor given by:

$f = (0.5 + (1/\pi)\arctan(150(M^* - M)$

$M^* = \sqrt{(4000/rho)} \ / \ ss$

rho = density

ss = speed of sound

Table 1 Cdo Data

Mach Number	Cdo
0.00	0.01950
0.50	0.01950
0.80	0.01950
0.88	0.02097
0.90	0.02134
1.00	0.03533
1.10	0.04095
1.20	0.04656
1.30	0.04570
1.40	0.04950
1.50	0.04934
1.60	0.04918
1.70	0.04744
1.80	0.04570
1.90	0.04450
2.00	0.04330
2.10	0.04166
2.20	0.04001
2.30	0.03801
2.50	0.03451

Table 2 Cdcl2 Data

Mach Number	CdCl2
0.00	0.07500
0.40	0.07500
0.60	0.07500
0.77	0.07500
0.80	0.07500
0.90	0.10000
1.00	0.12500
1.10	0.07500
1.20	0.10000
1.40	0.15000
1.60	0.22500
1.80	0.30000
2.00	0.38750
2.15	0.45000
2.20	0.47500
2.25	0.47500
2.40	0.47500

Table 3 Clmax Data

Mach Number	Clmax
0.00	1.180
0.40	1.180
0.60	1.180
0.80	1.160
1.00	1.080
1.20	0.930
1.40	0.810
1.60	0.700
1.80	0.630
2.00	0.570
2.20	0.500
2.40	0.460
2.50	0.460

Table 4 Thrust Data (lbs)

Alt (kft)	Mach Number														
	0	0.2	0.4	0.6	0.8	1.0	1.2	1.4	1.6	1.8	2.0	2.2	2.4	2.6	3.0
0	38580	41110	44270	39630	54390	62170	65600	65600	65600	65600	65600	65600	59040	29520	0
10	33070	33070	33070	37160	42370	49950	54230	59930	59930	59930	59930	59930	53940	29520	0
20	23240	23240	23240	26830	30900	37630	43520	48070	54770	54770	54770	54770	49290	24645	0
30	15540	15540	15540	17950	21210	26450	32120	38070	42600	48010	52430	55810	50230	25115	0
40	12000	12000	12000	12000	14400	18400	22400	26800	30200	34000	37200	40000	36000	18000	0
50	6648	6648	6648	6648	7978	10230	12800	15110	17220	20150	21960	24020	22580	11290	0
60	5660	5660	5660	5660	5660	5660	6540	8200	9800	11200	12760	14000	13320	6660	0
70	4400	4400	4400	4400	4400	4400	4400	4400	4400	5400	6400	7200	6930	3465	0
80	2200	2200	2200	2200	2200	2200	2200	2200	2200	2700	3200	3600	3460	1730	0
100	0	0	0	0	0	0	0	0	0	0	0	0	0	0	0

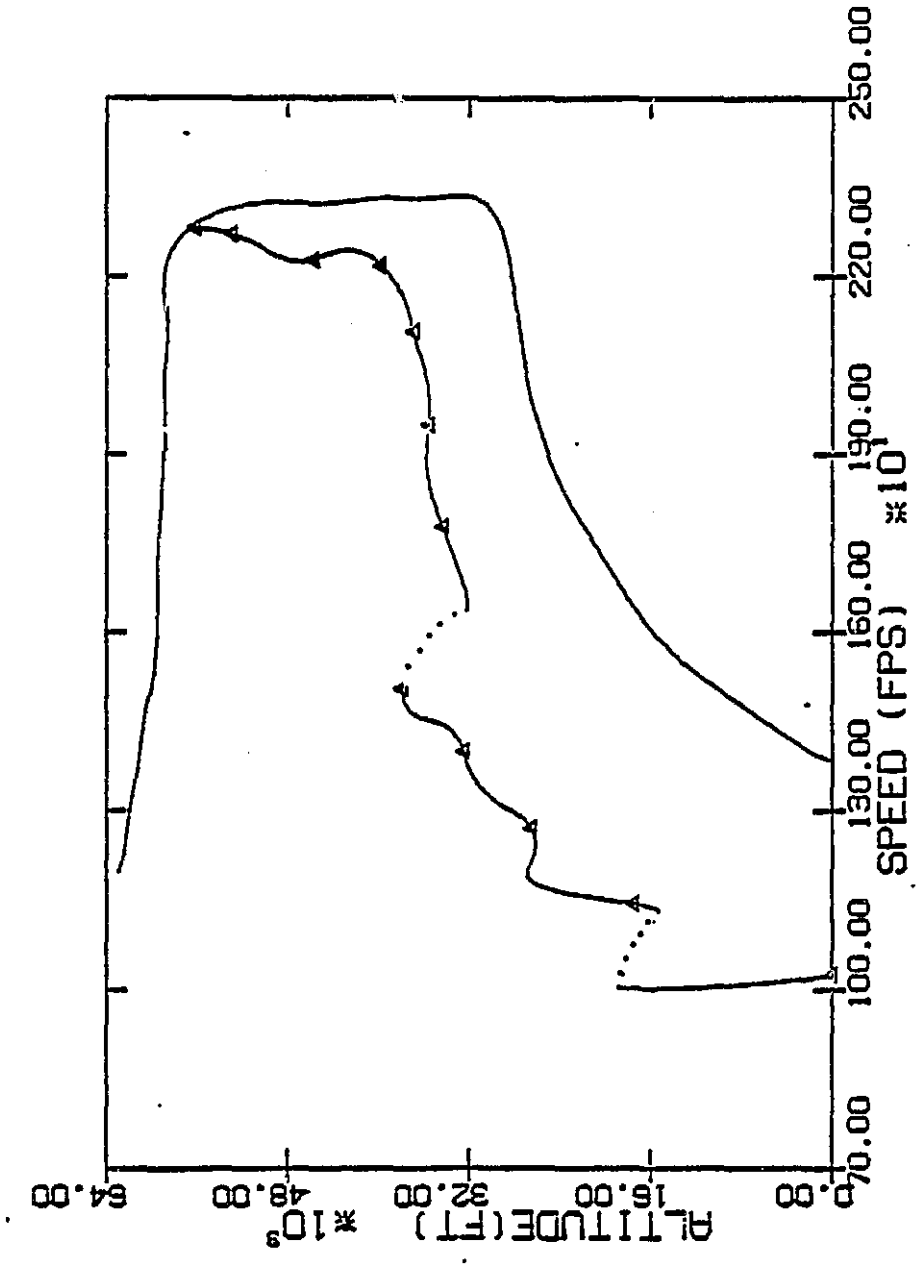

Fig 1.....Energy Climb Schedule on h-v plane

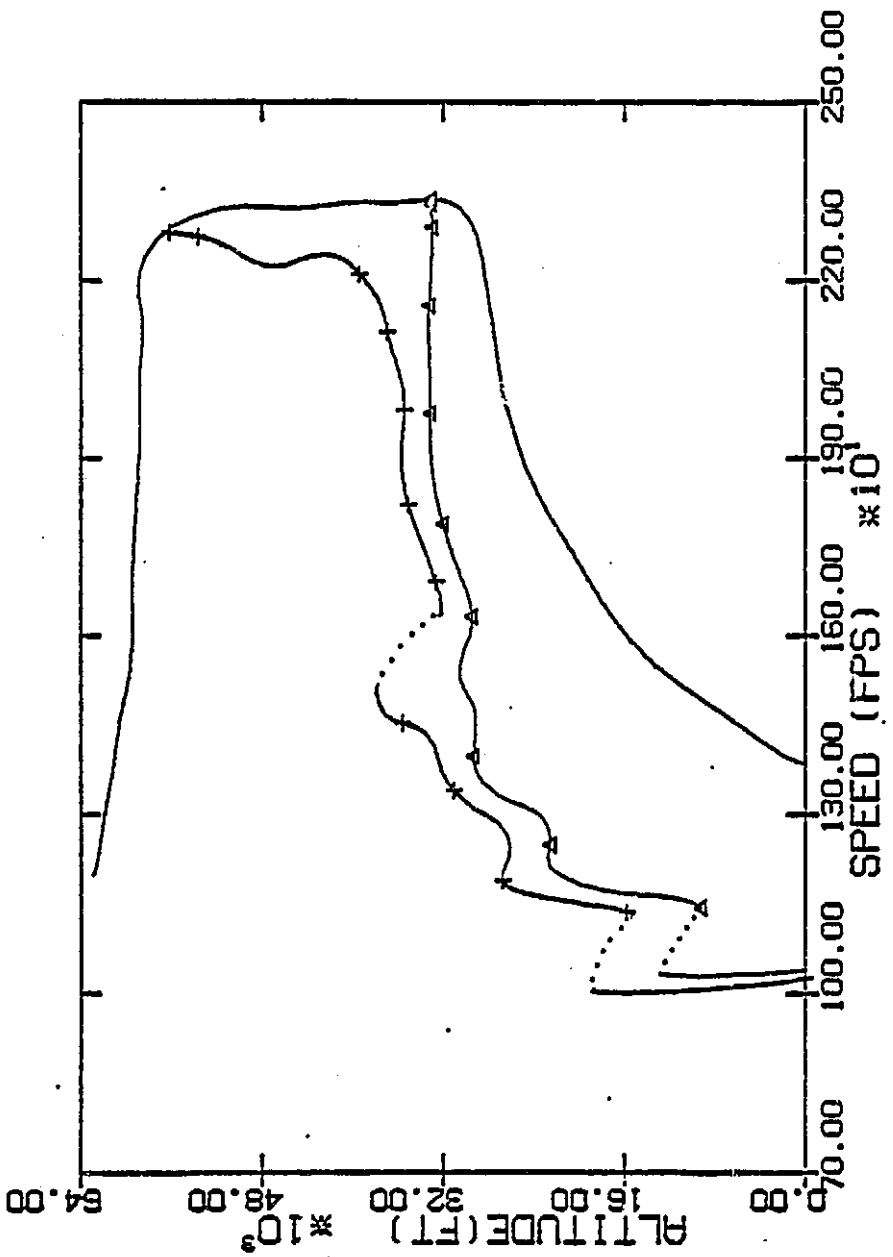

Fig 2.....Energy-Range-Climb to the Dash Point

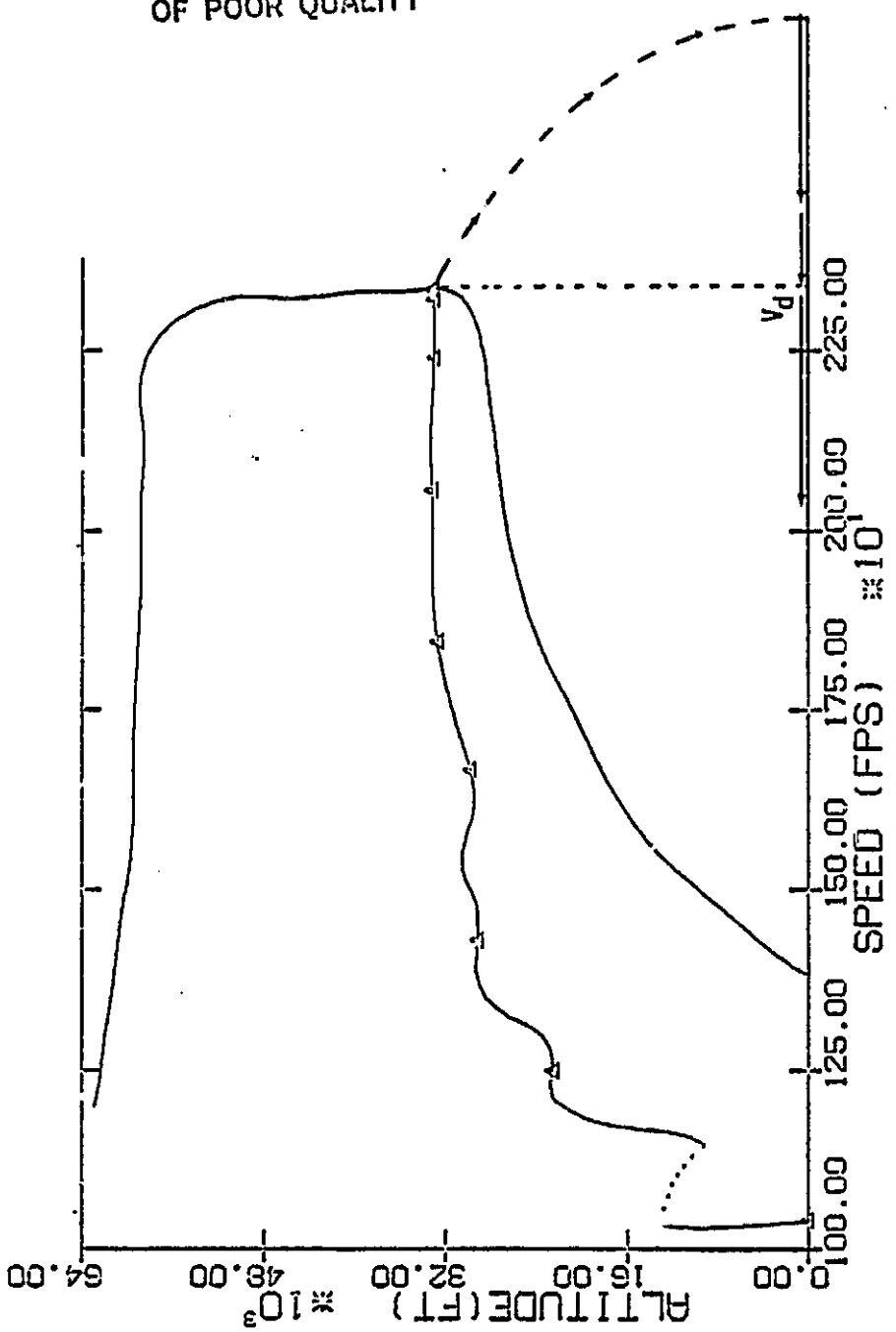

Fig 3.....Terminal Energy Transient

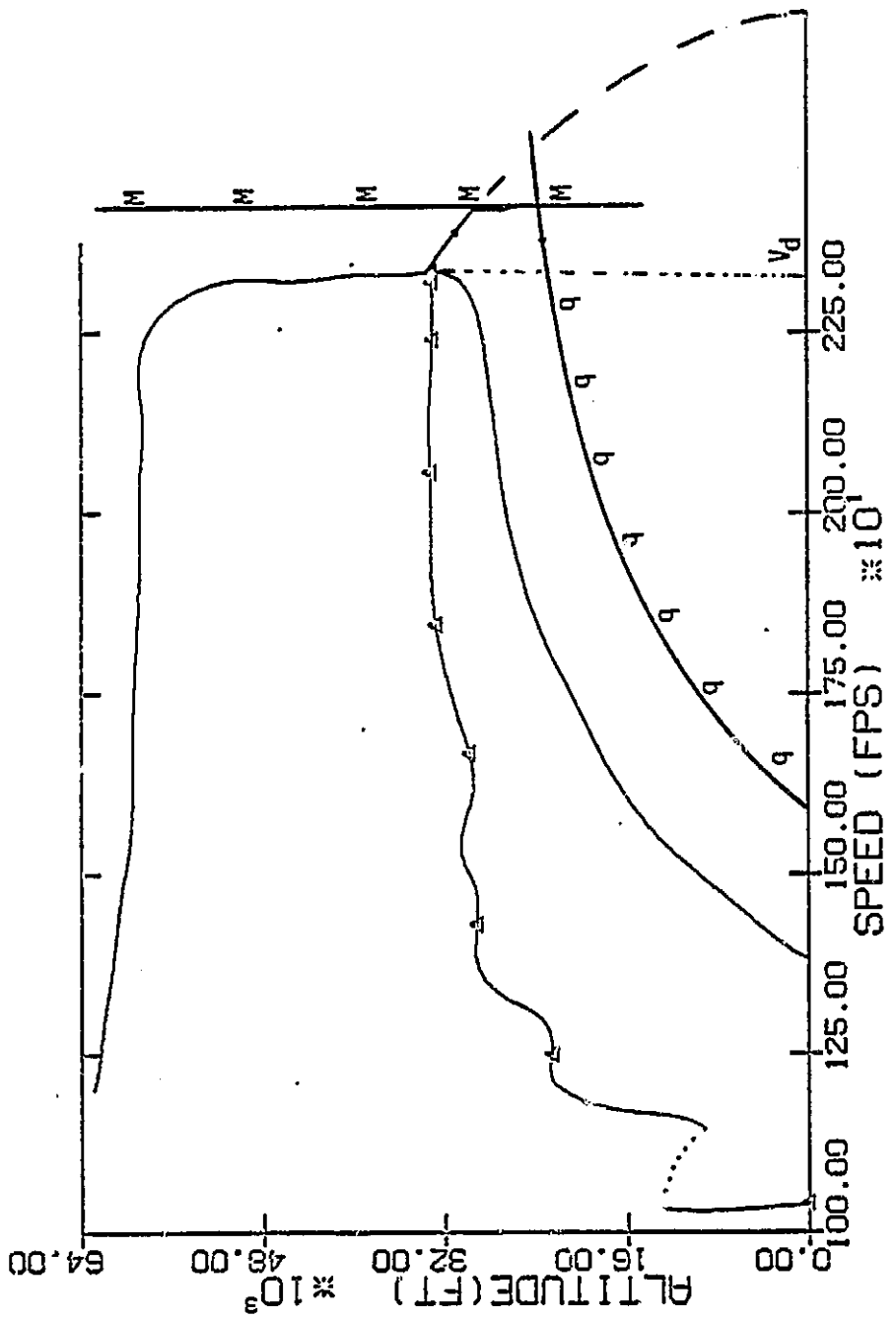

Fig 4.....Terminal Transient

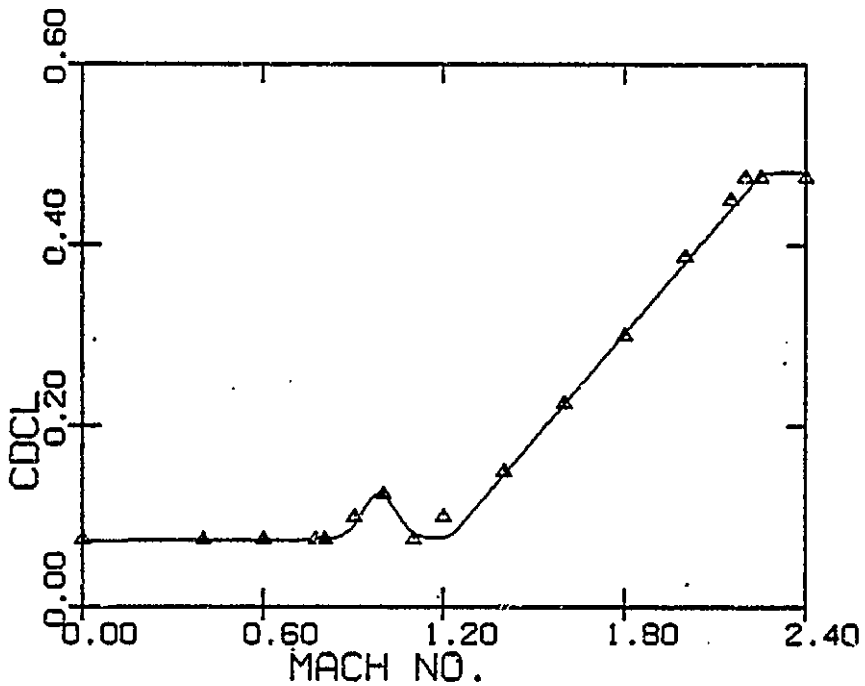

Fig 6.....K(M) Smoooth Data

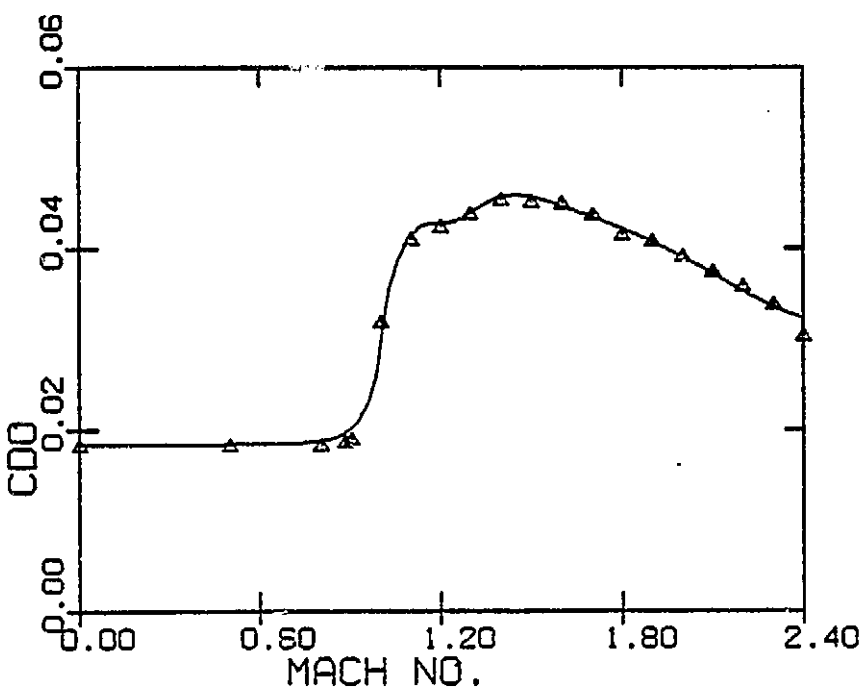

Fig 5.....C_{do}(M) Smooth Data

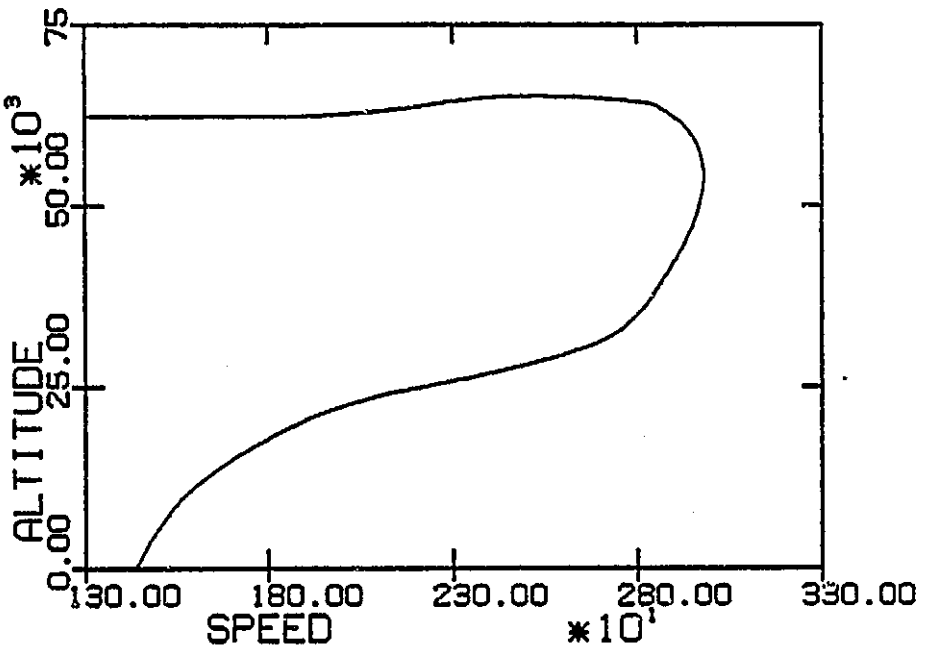

Fig 7.....Unlimited Flight Envelope, Smooth Data

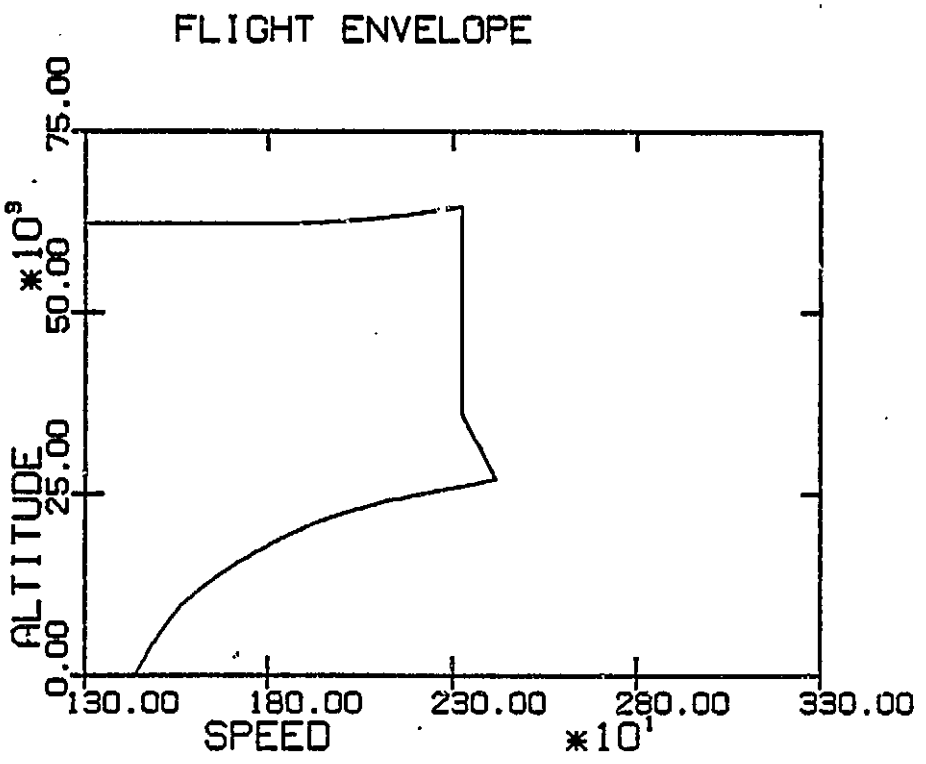

Fig 8.....Envelope with Mach Limit, Smooth Data

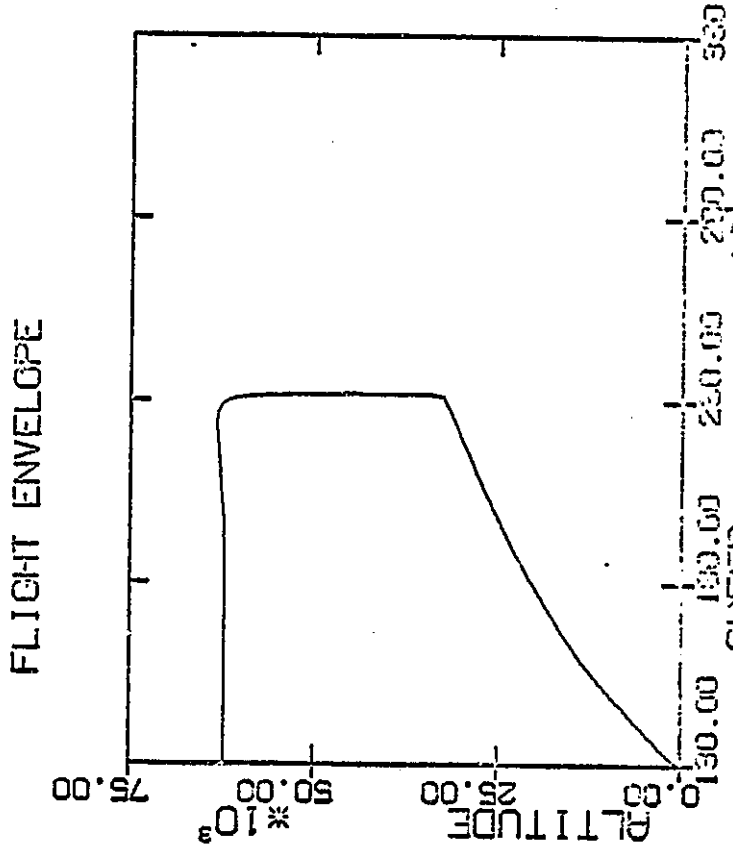

Fig 9.....Envelope with q and Mach Limits

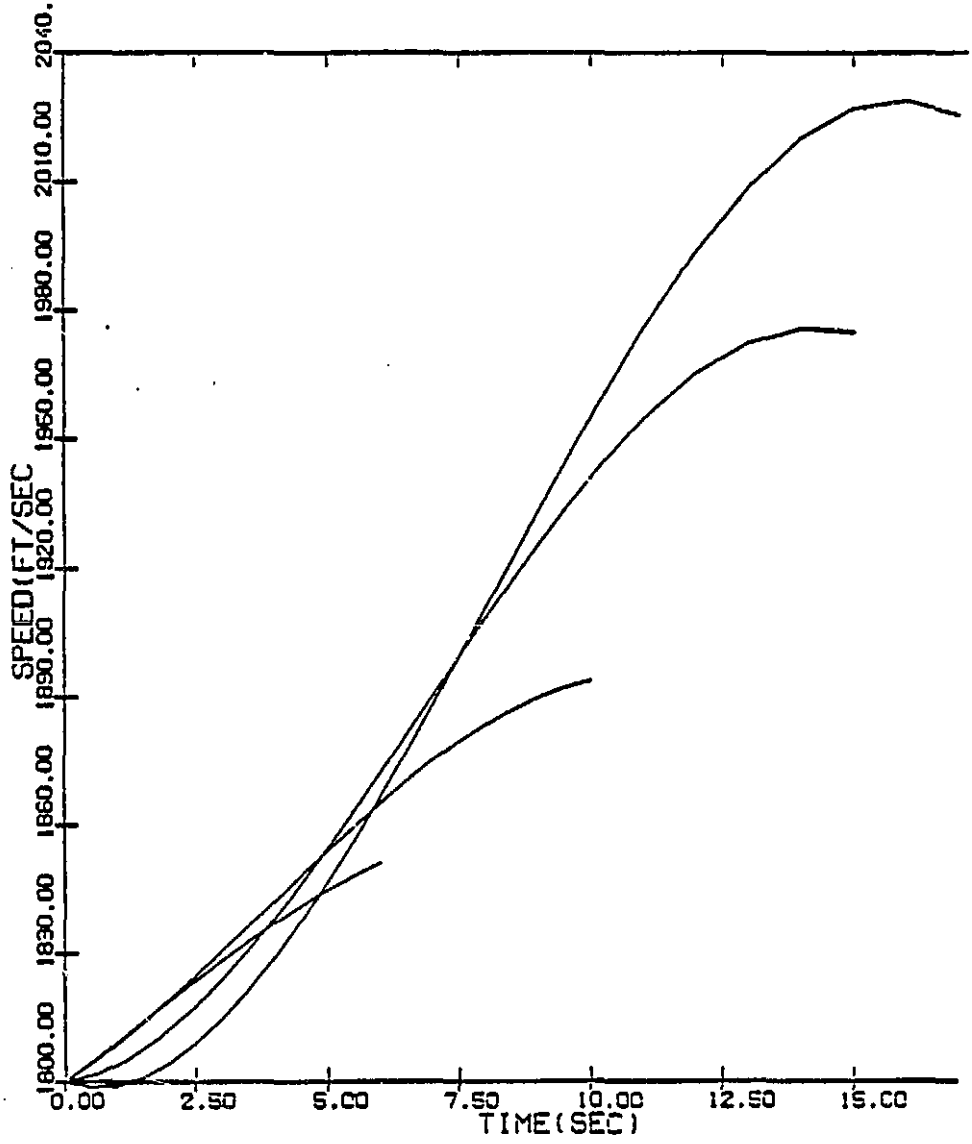

Fig 10.....Speed vs Time

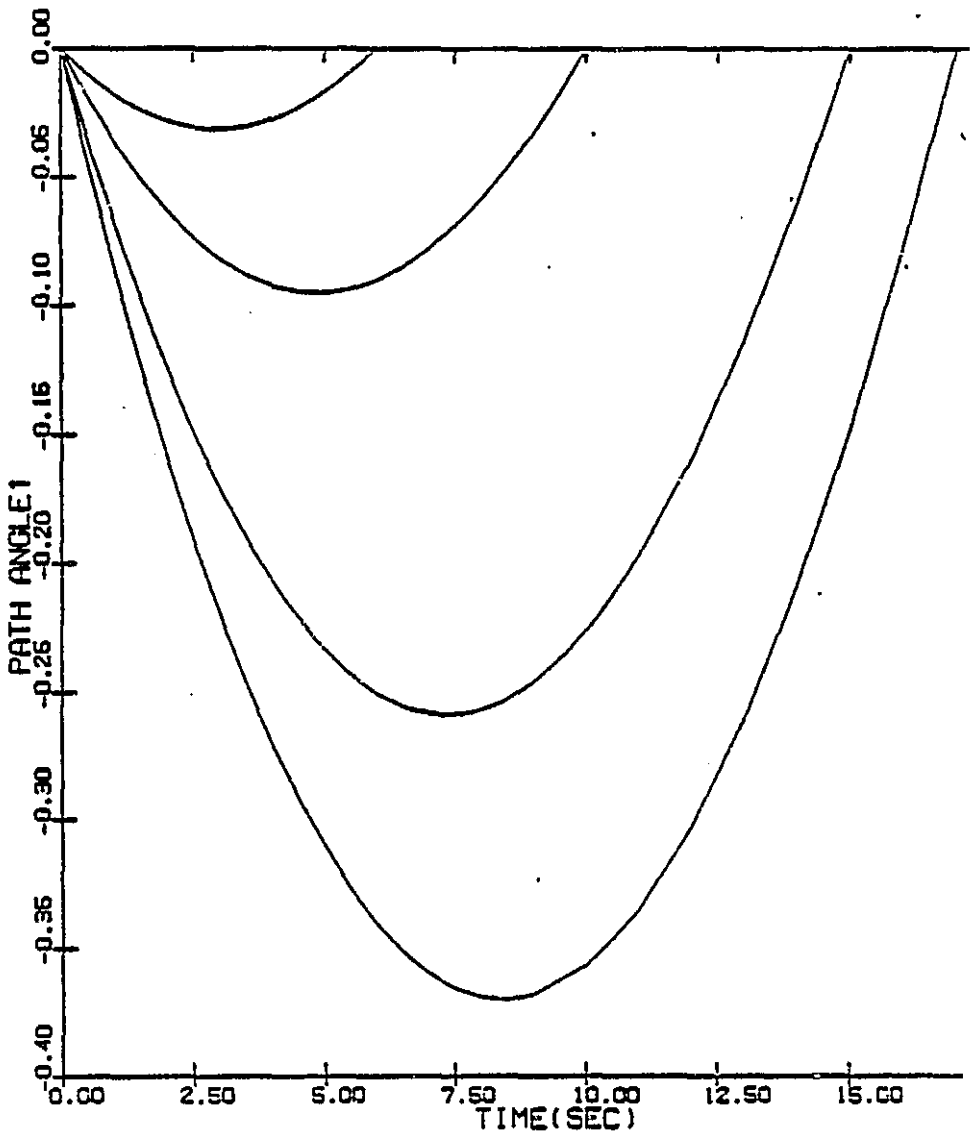

Fig 11.....Path-Angle vs Time

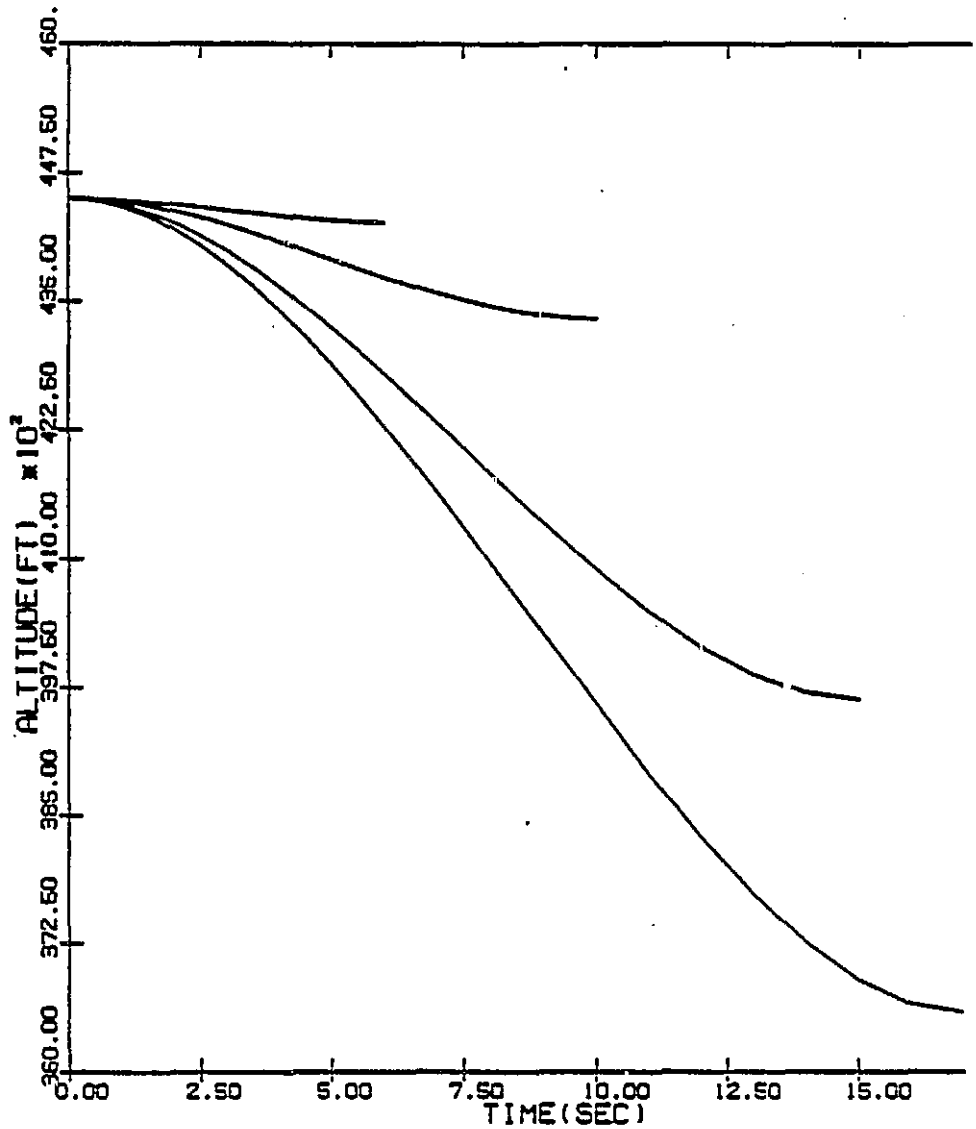

Fig 12.....Altitude vs Time

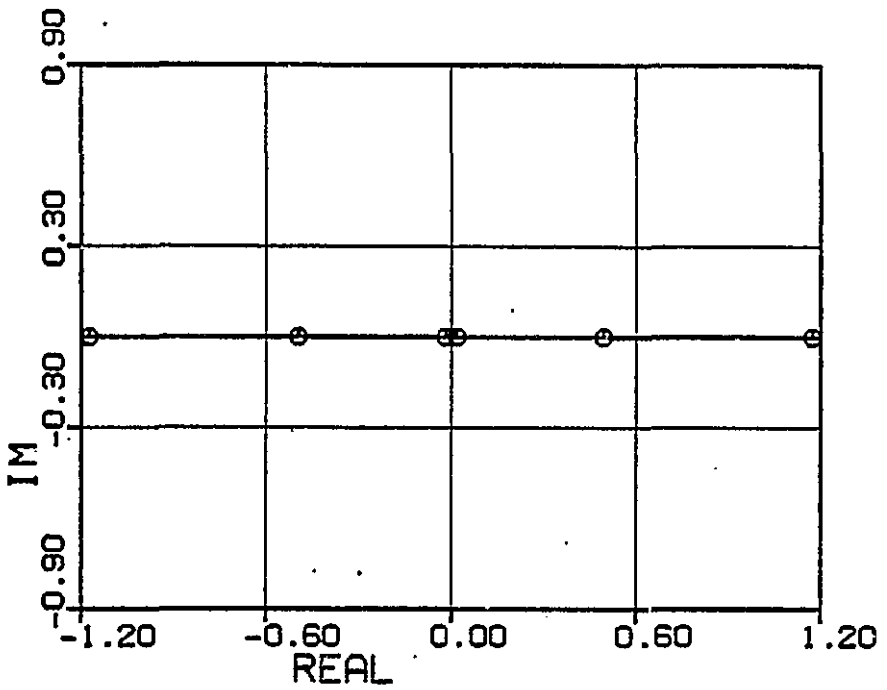

Fig 13.....Eigenvalues at the Dash Point

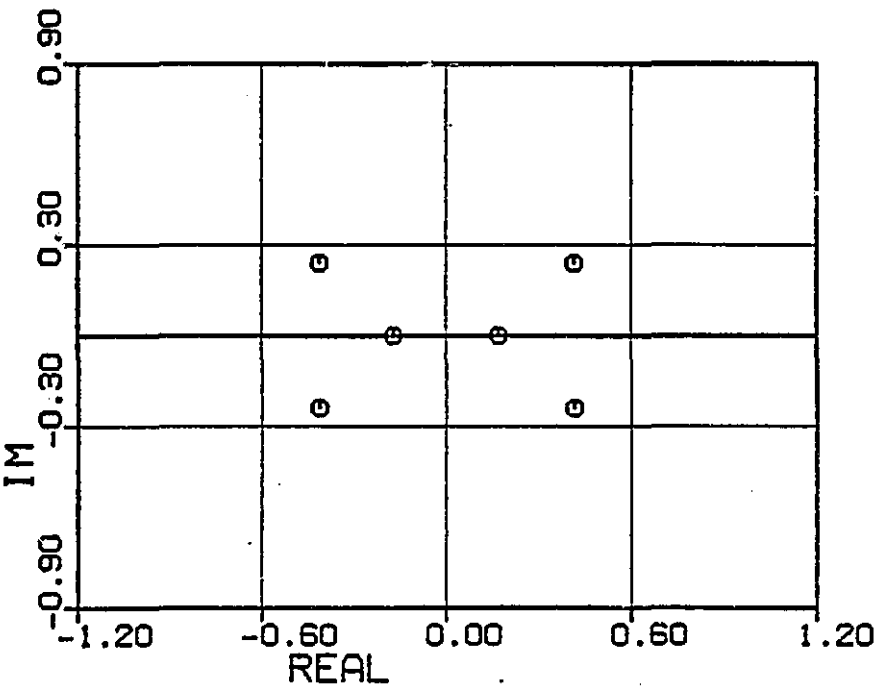

Fig 14.....Eigenvalues at Reduced Throttle

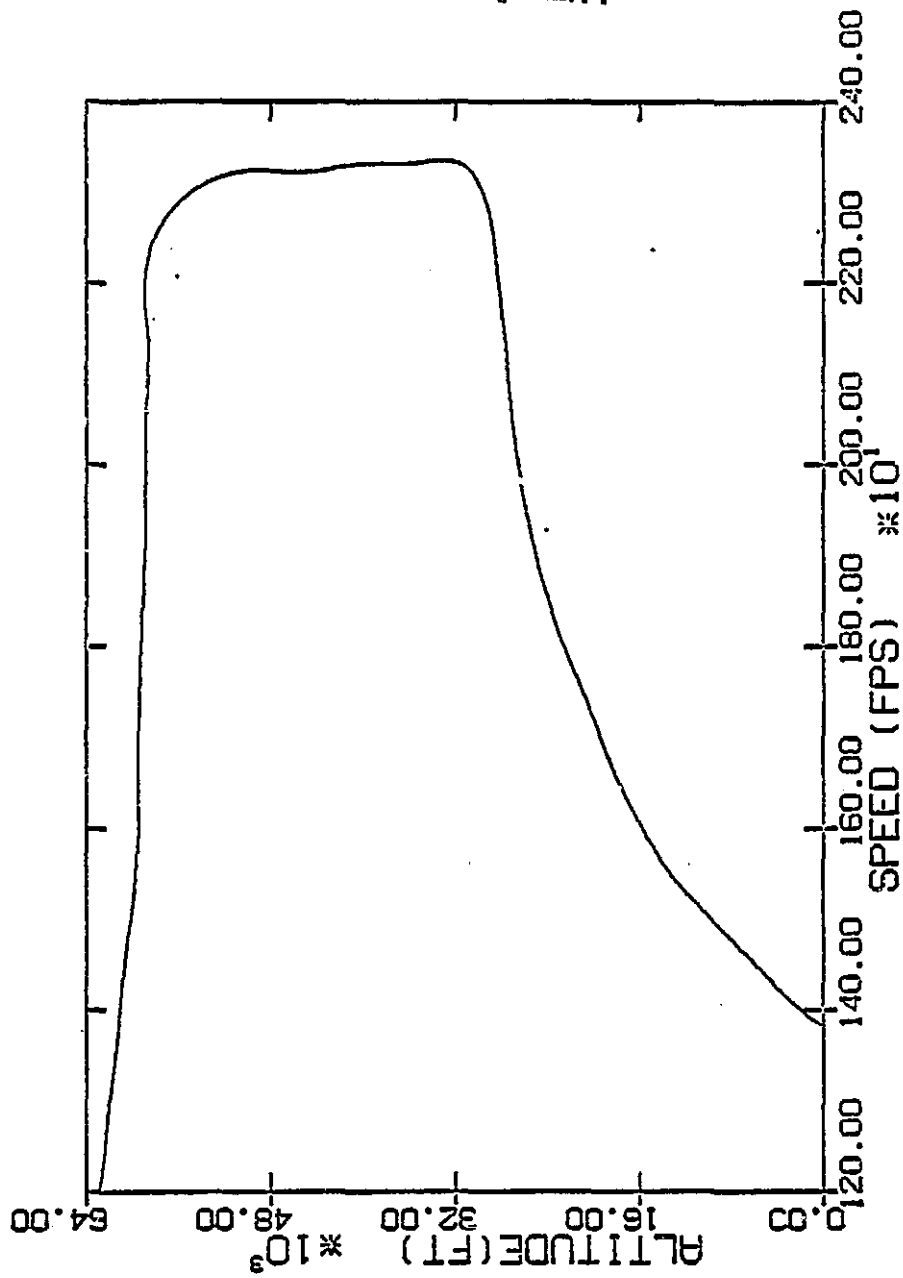

Fig 15.....Flight Envelope Spline Data

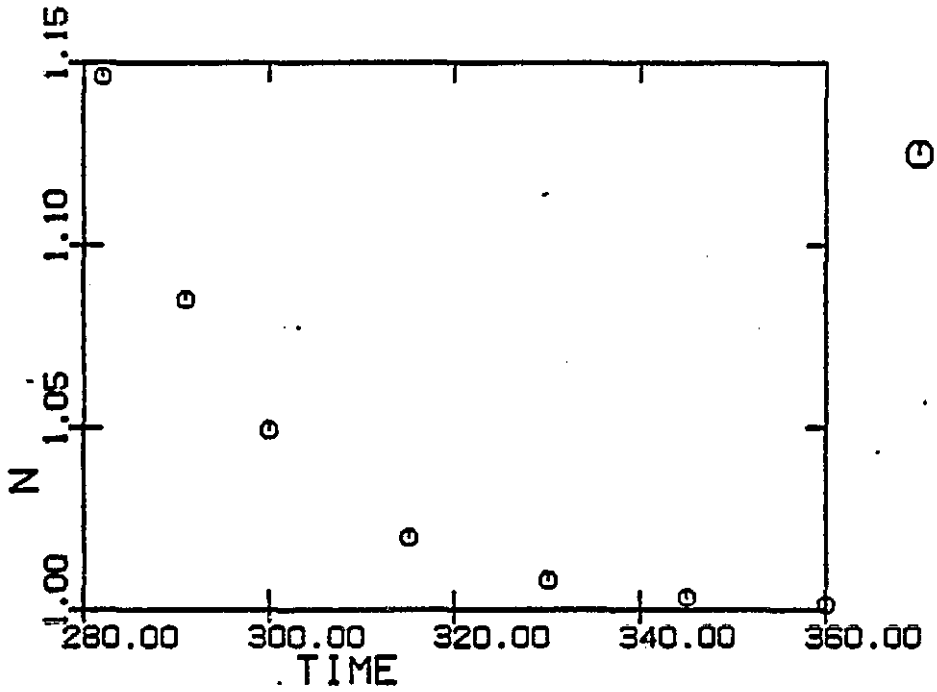

Fig 17.....Final Load Factor

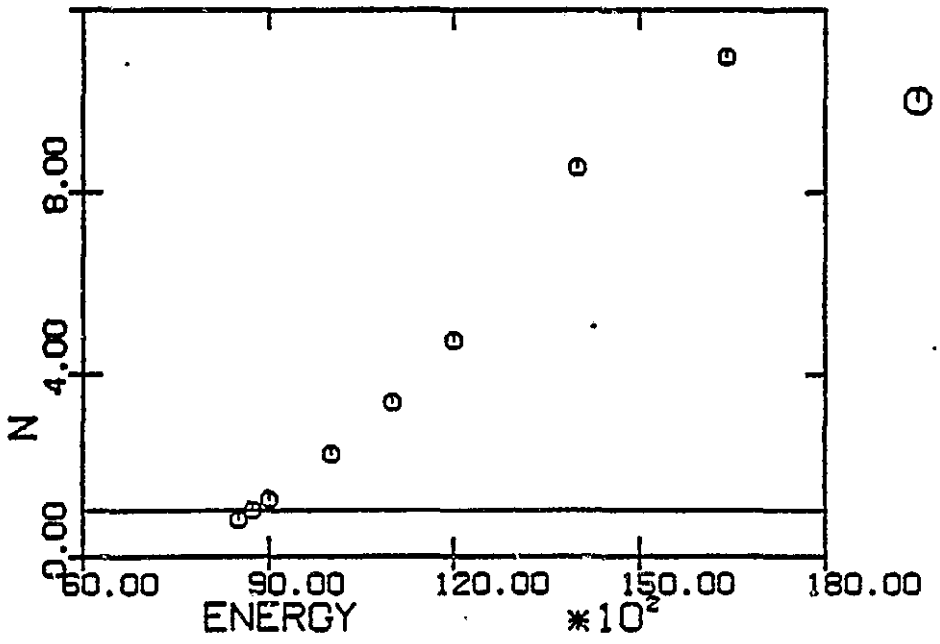

Fig 16.....Initial Load Factor

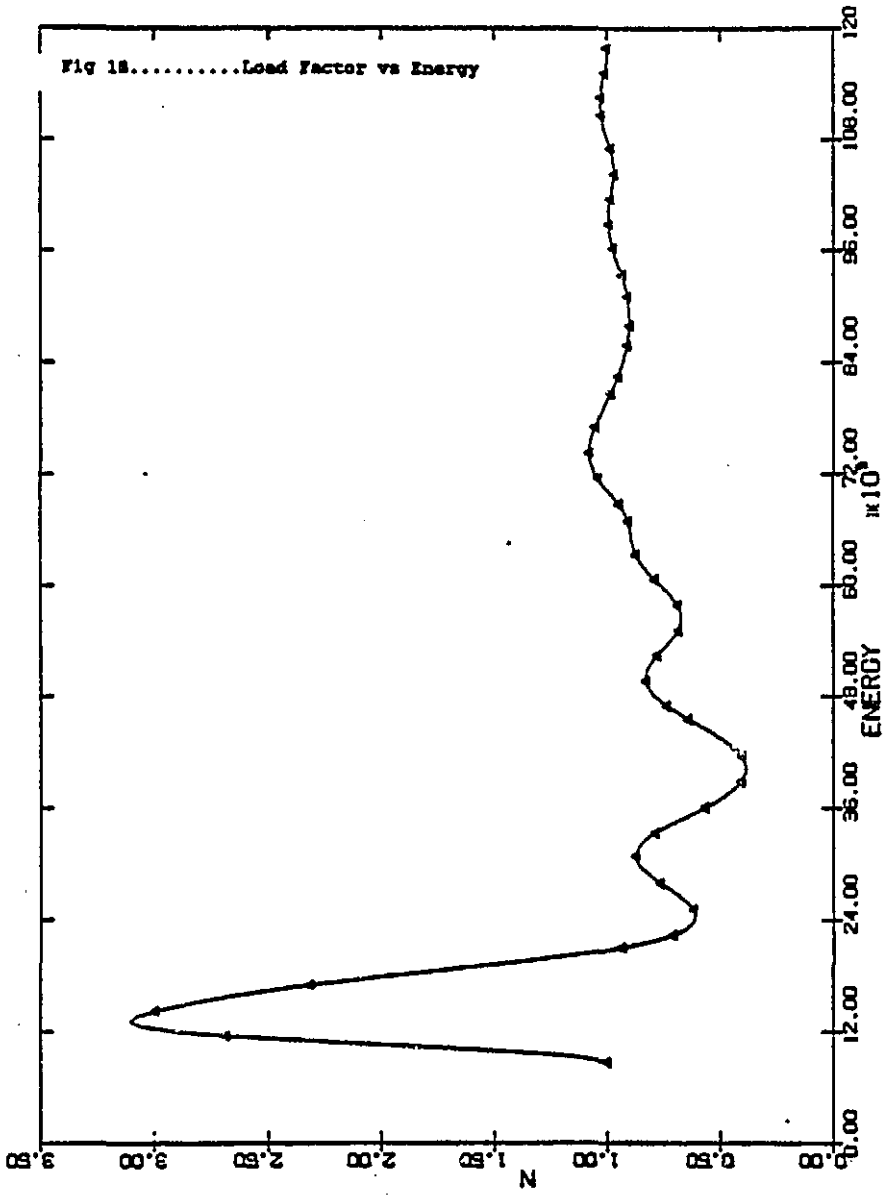

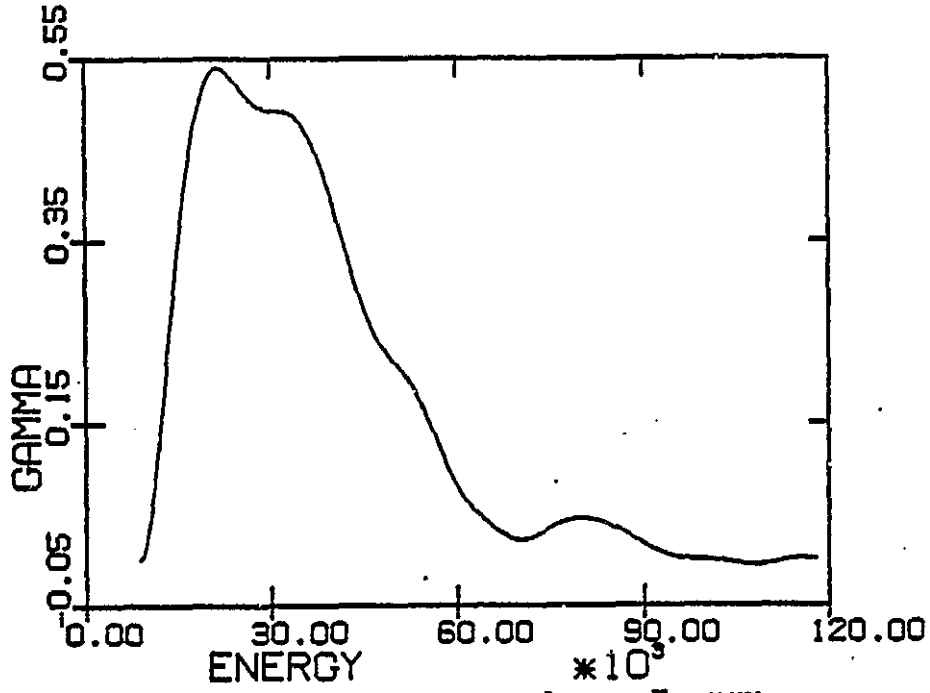

Fig 19.....Path-Angle vs Energy

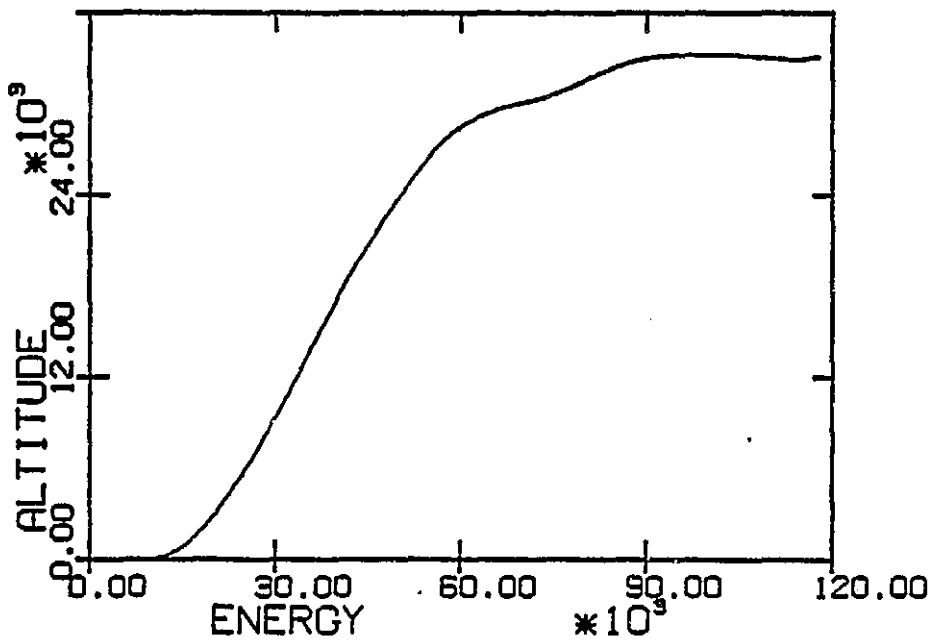

Fig 20.....Altitude vs Energy

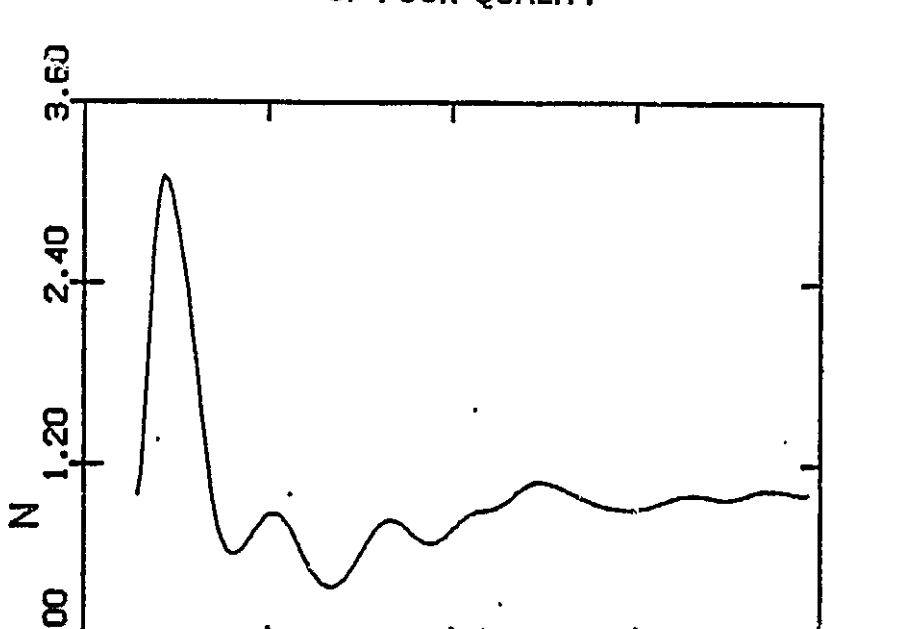

Fig 21.....Load Factor vs Energy

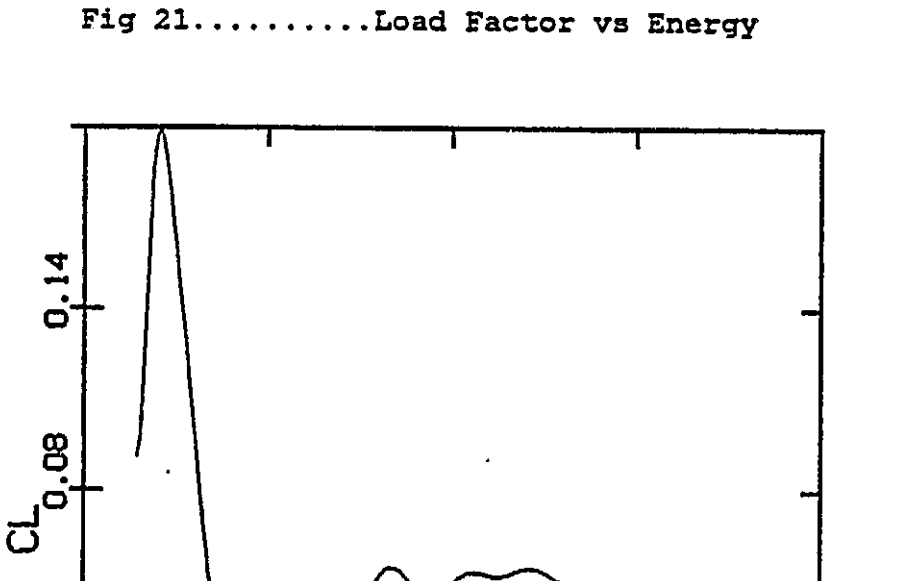

Fig 22.....Lift Coefficient vs Energy

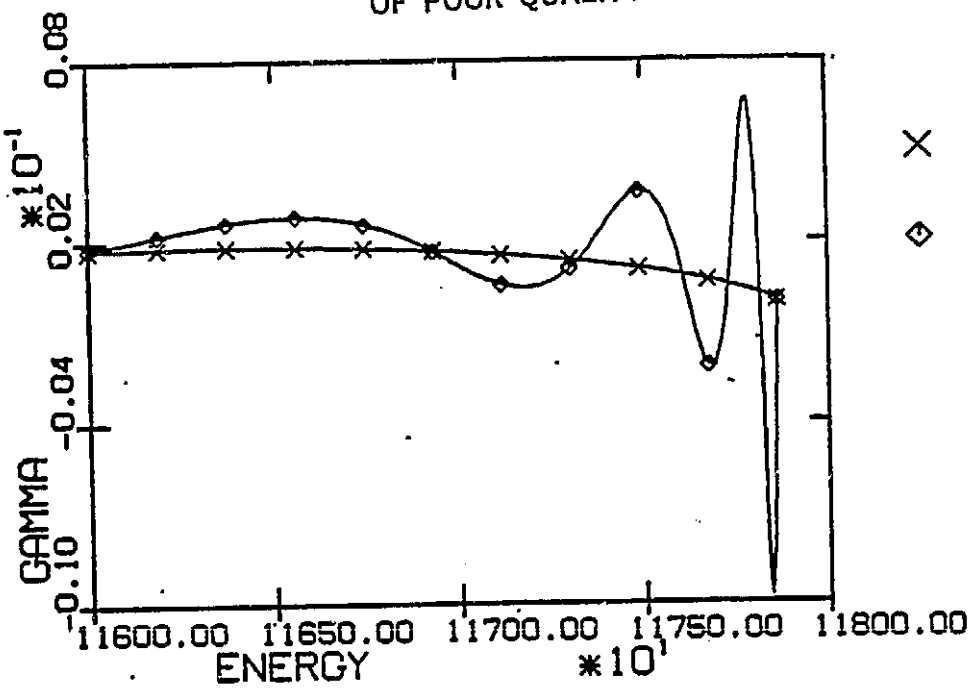

Fig 23.....Path-Angle vs Energy 300,360 seconds

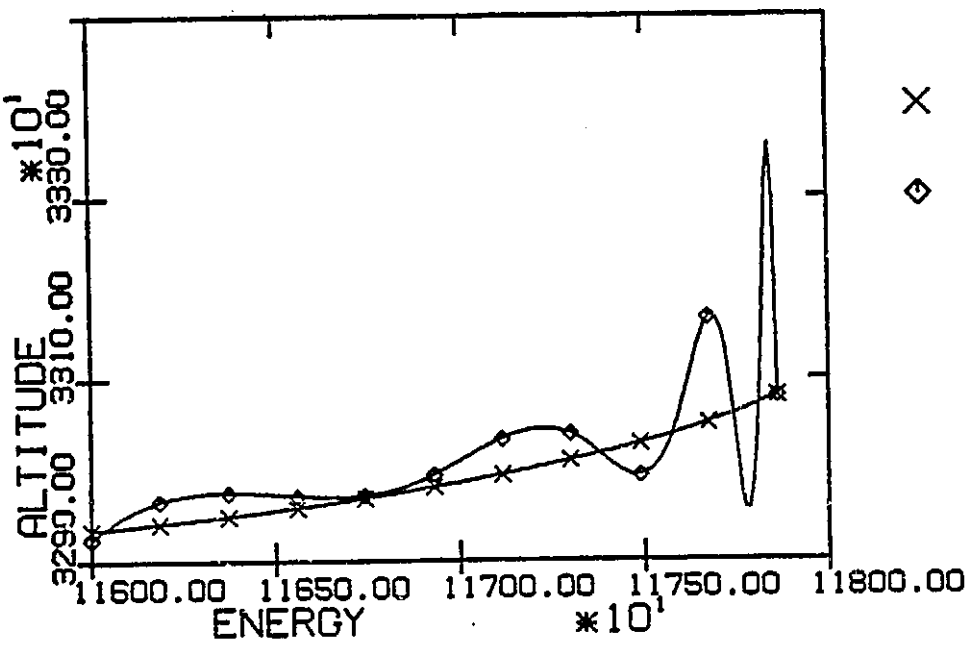

Fig 24.....Altitude vs Energy 300,360 seconds

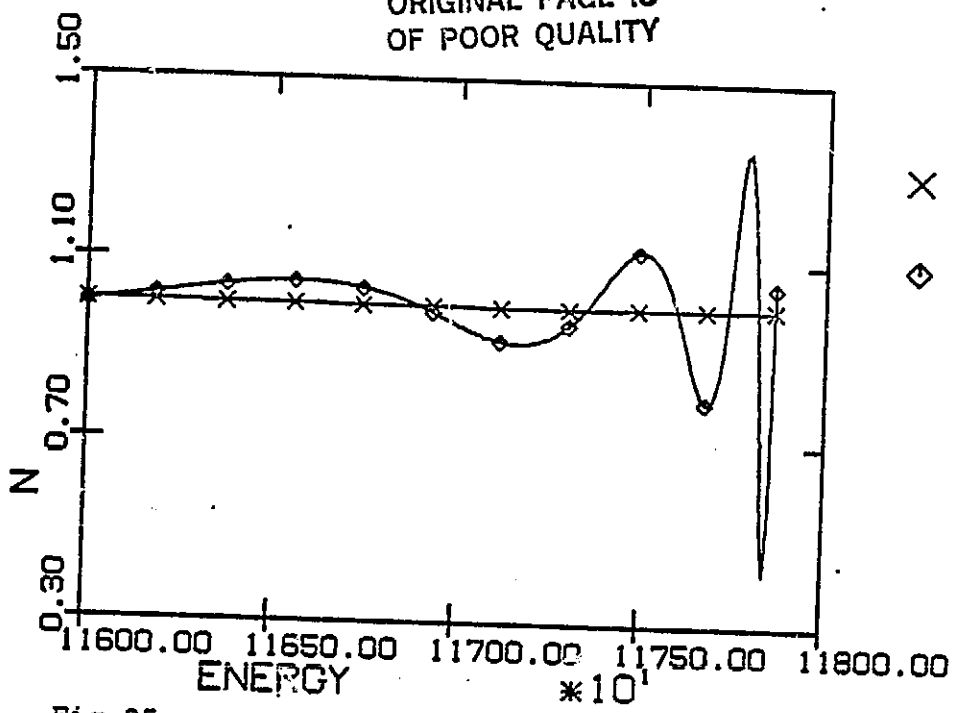

Fig 25.....Load Factor vs Energy 300,360 seconds

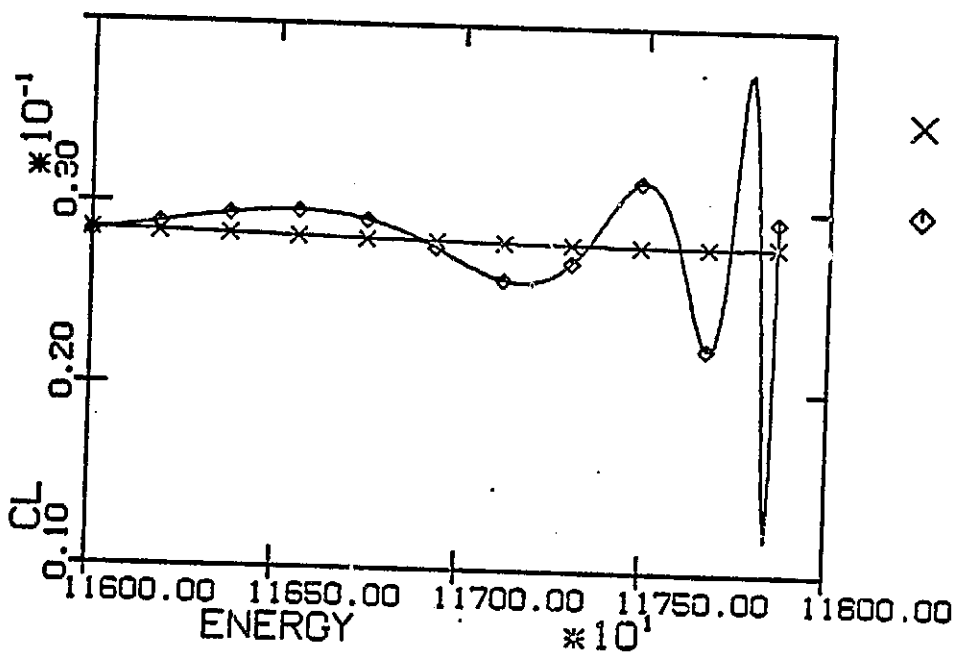

Fig 26.....Lift Coefficient vs Energy 300,360 seconds

C-2

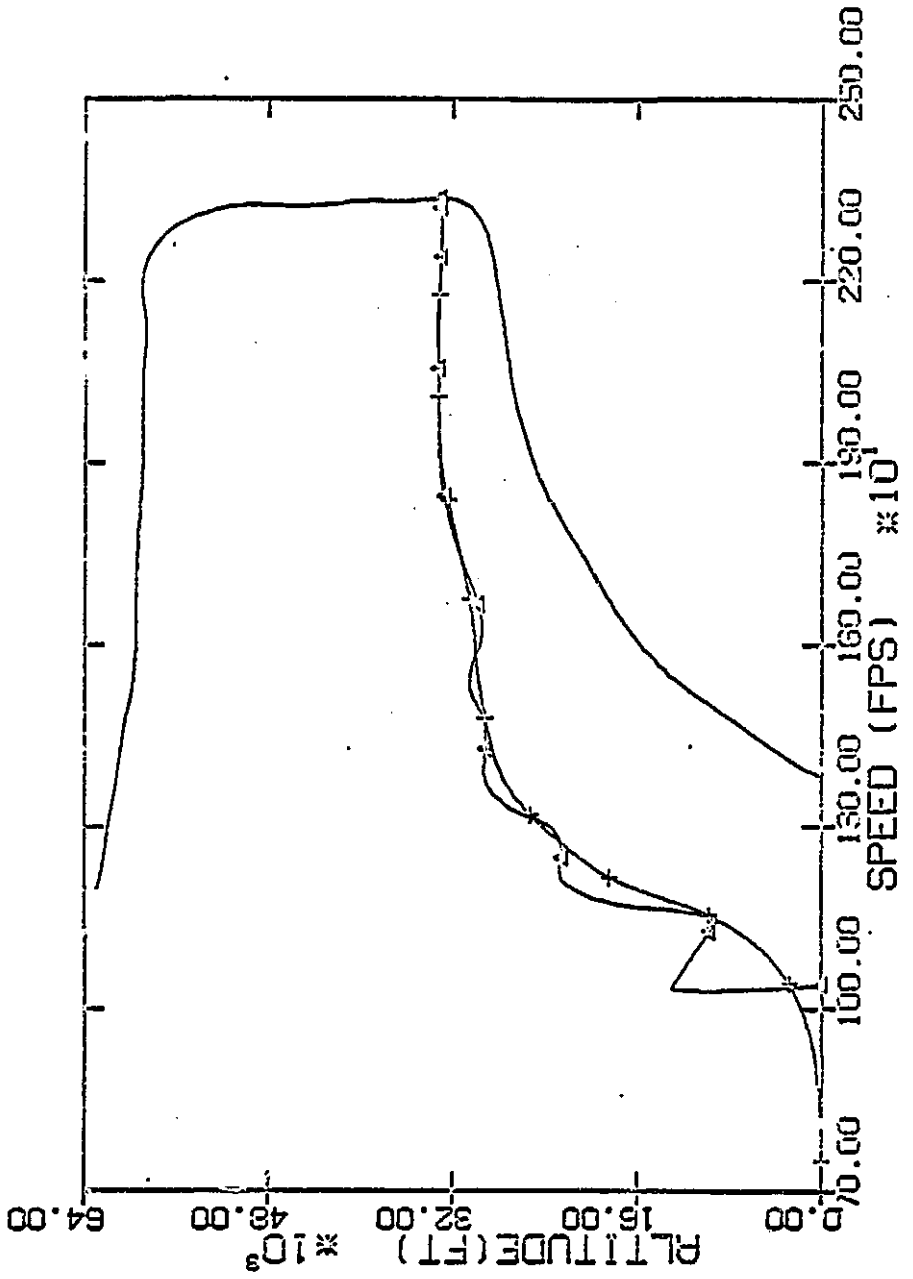

Fig 27.....Range-Energy-Climb and Point Mass Solution

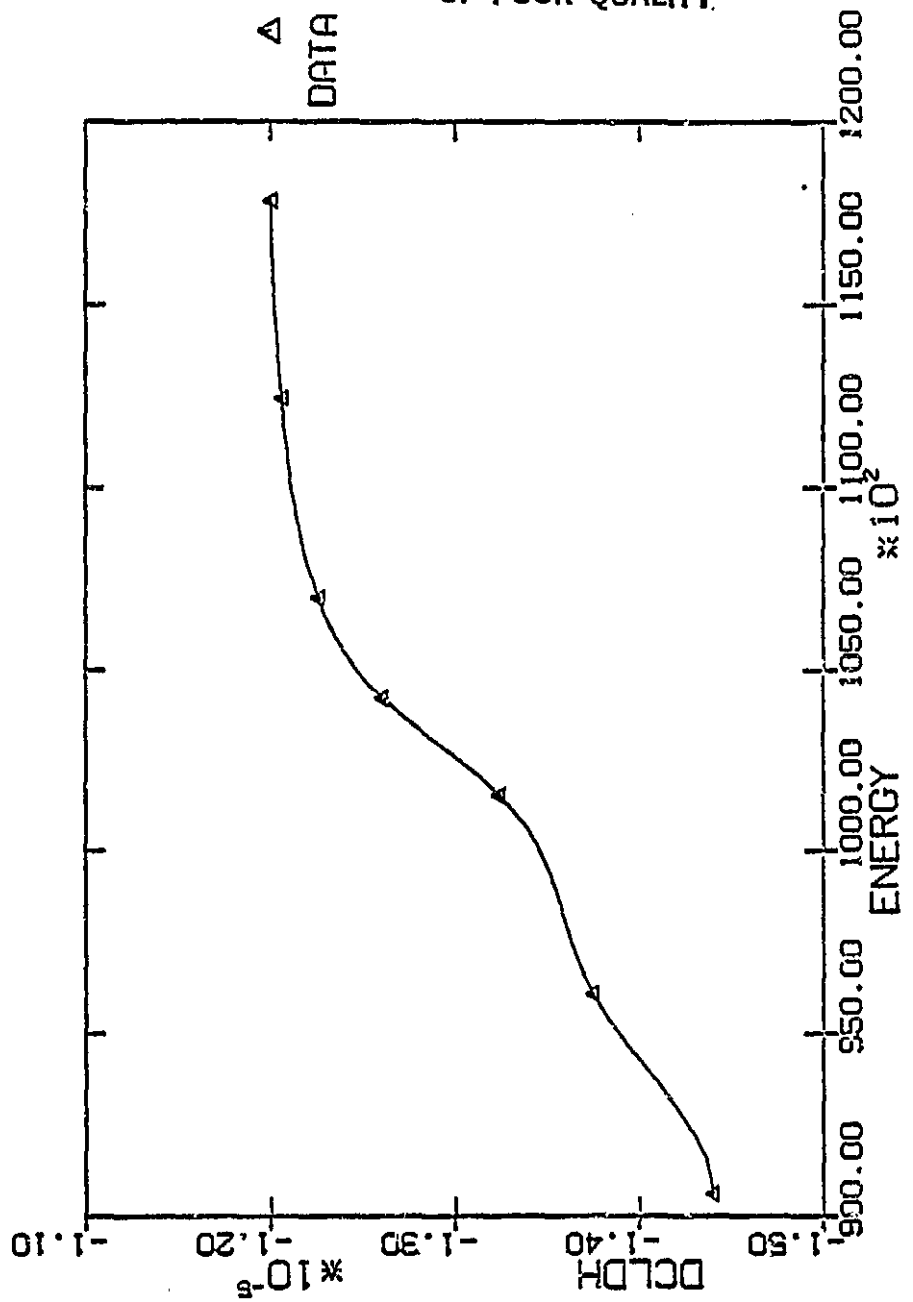

Fig 28.....Altitude Gain vs Energy

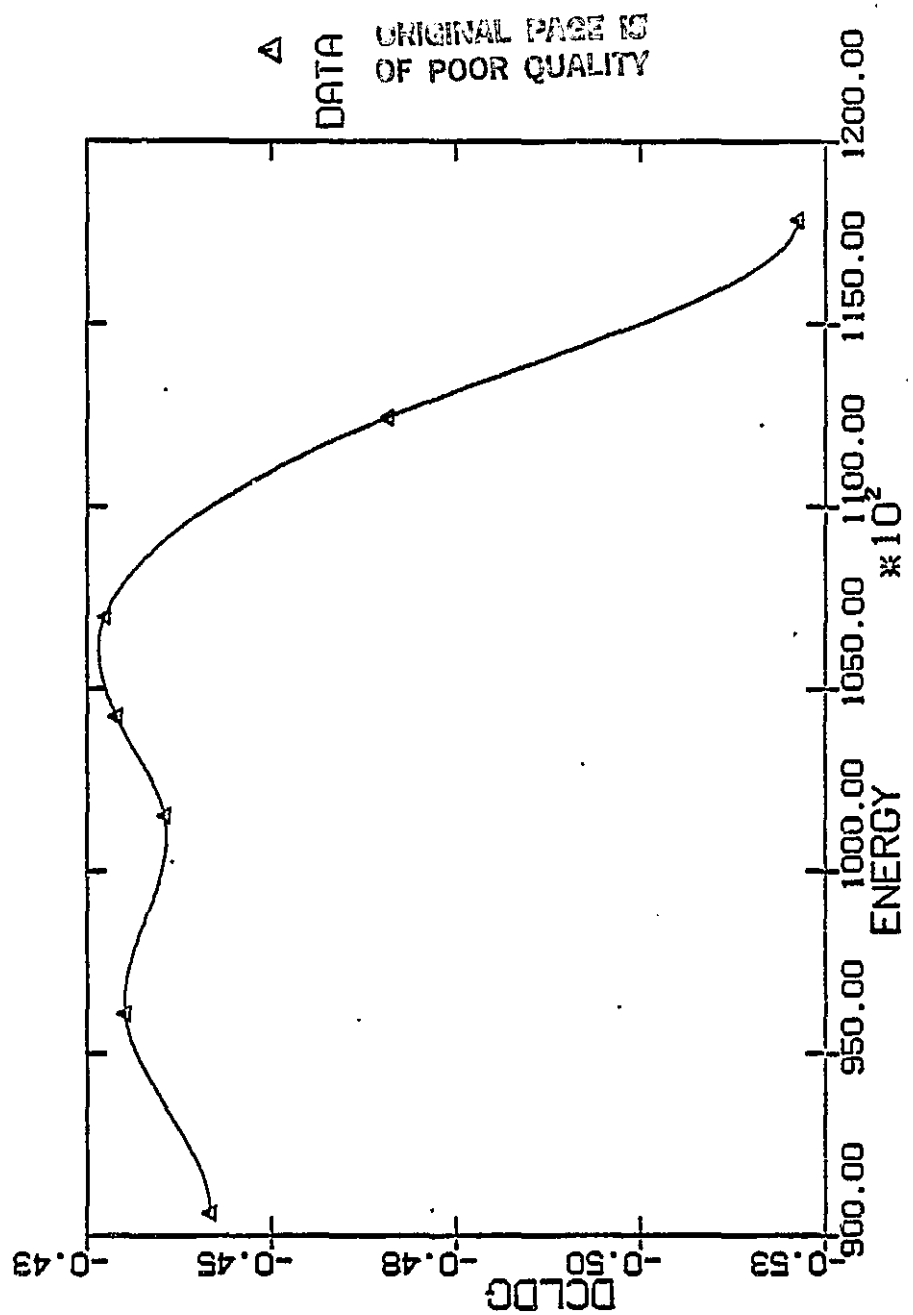

Fig 29.....Path-Angle Gain vs Energy

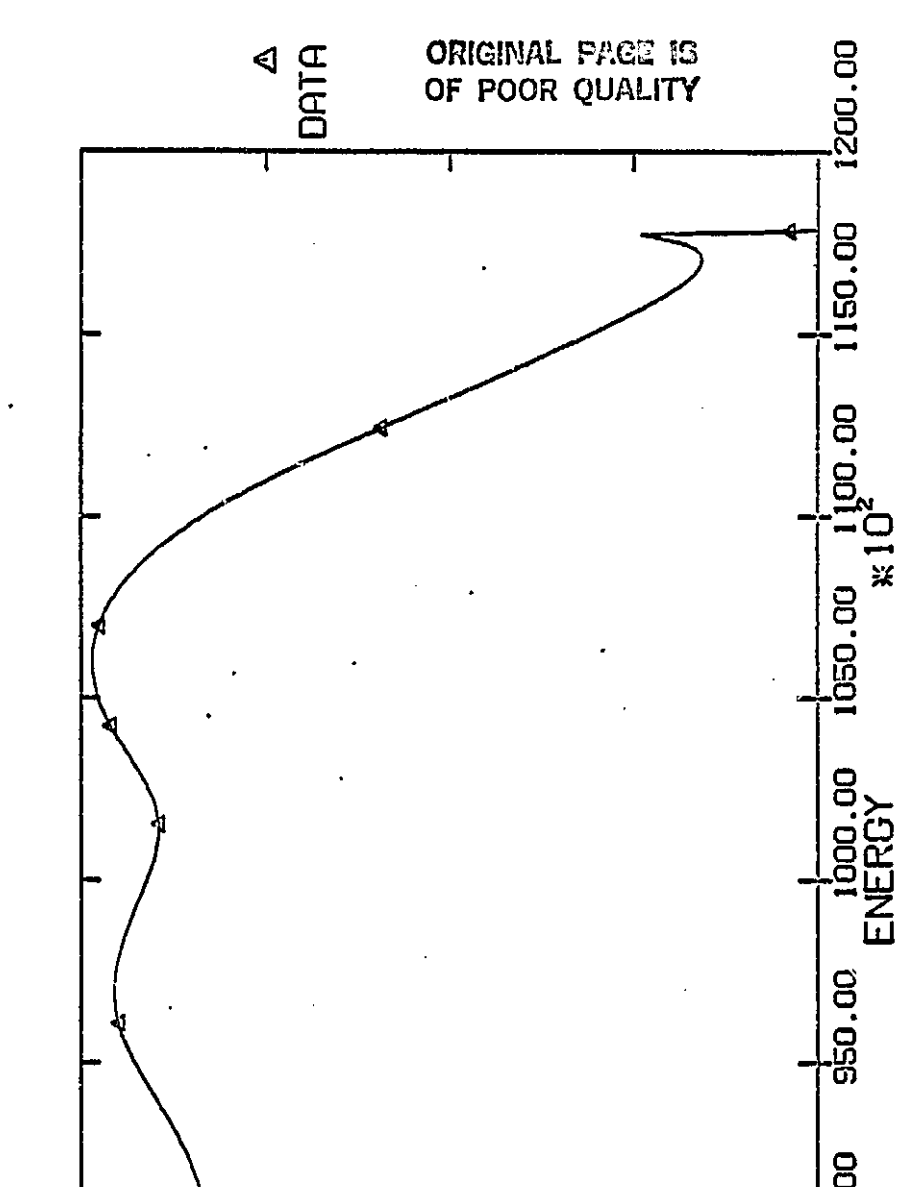

Fig 30.....Altitude Gain Energy

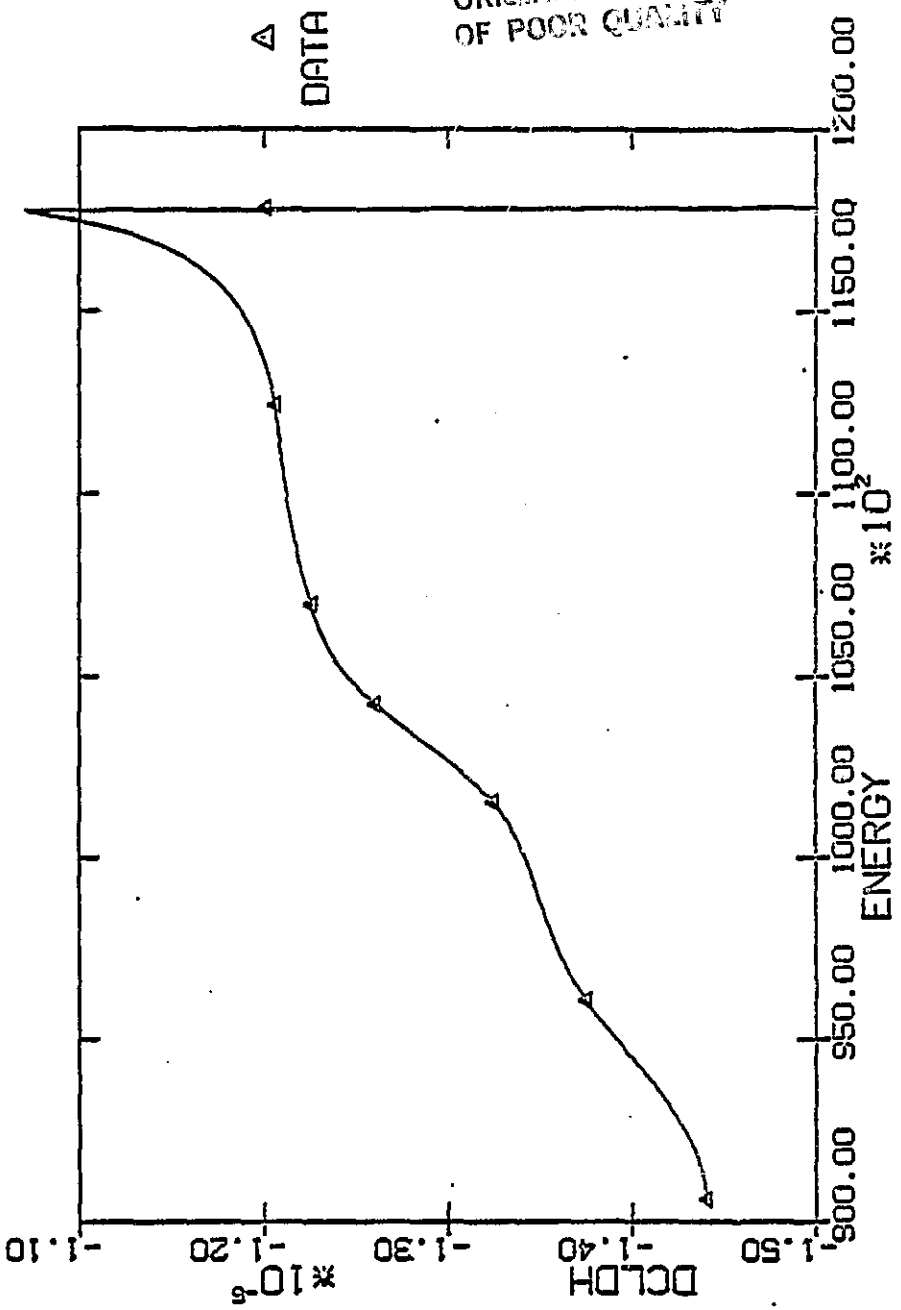

Fig 31.....Path-Angle Gain vs Energy

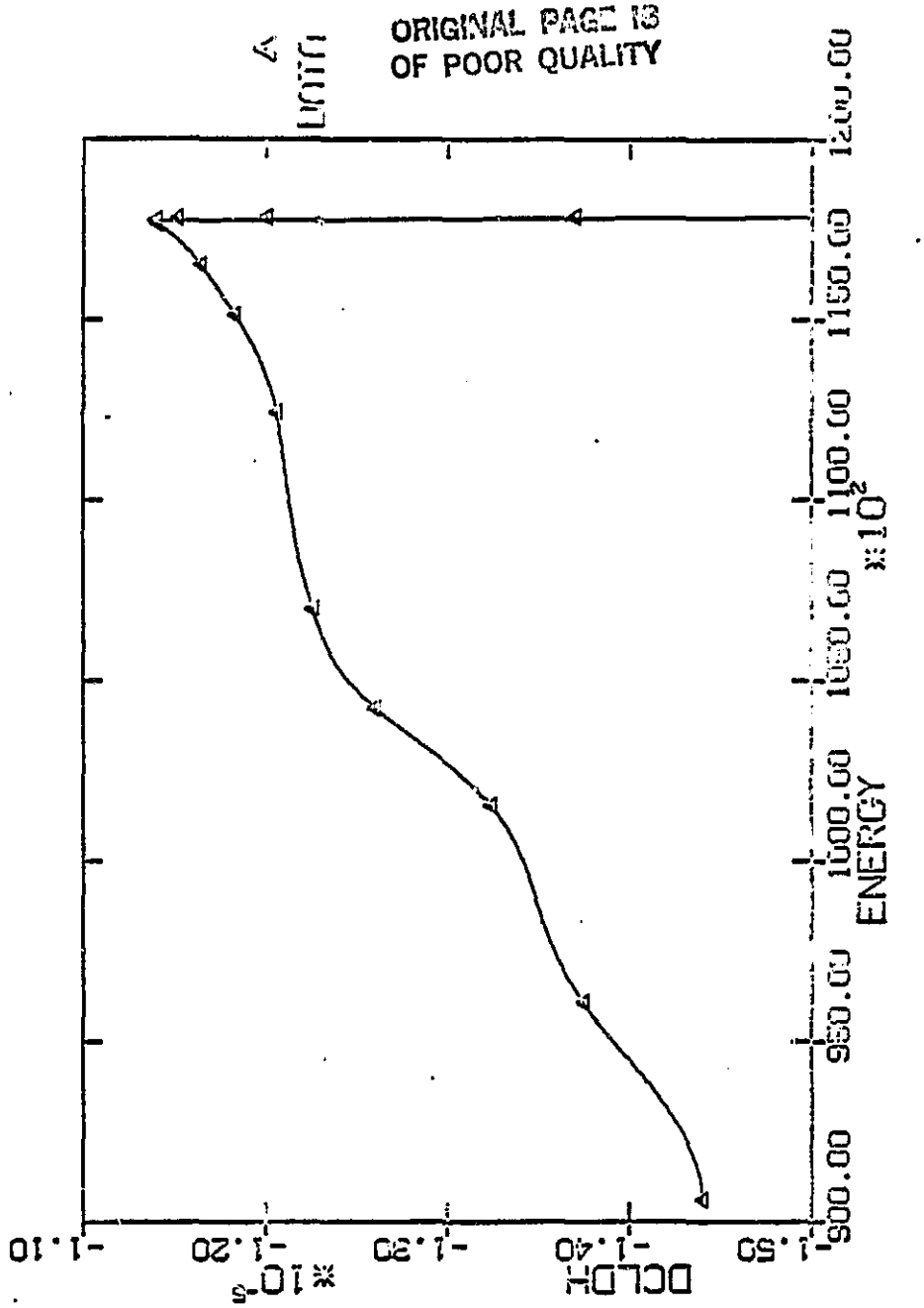

Fig 32.....Altitude Gain vs Energy

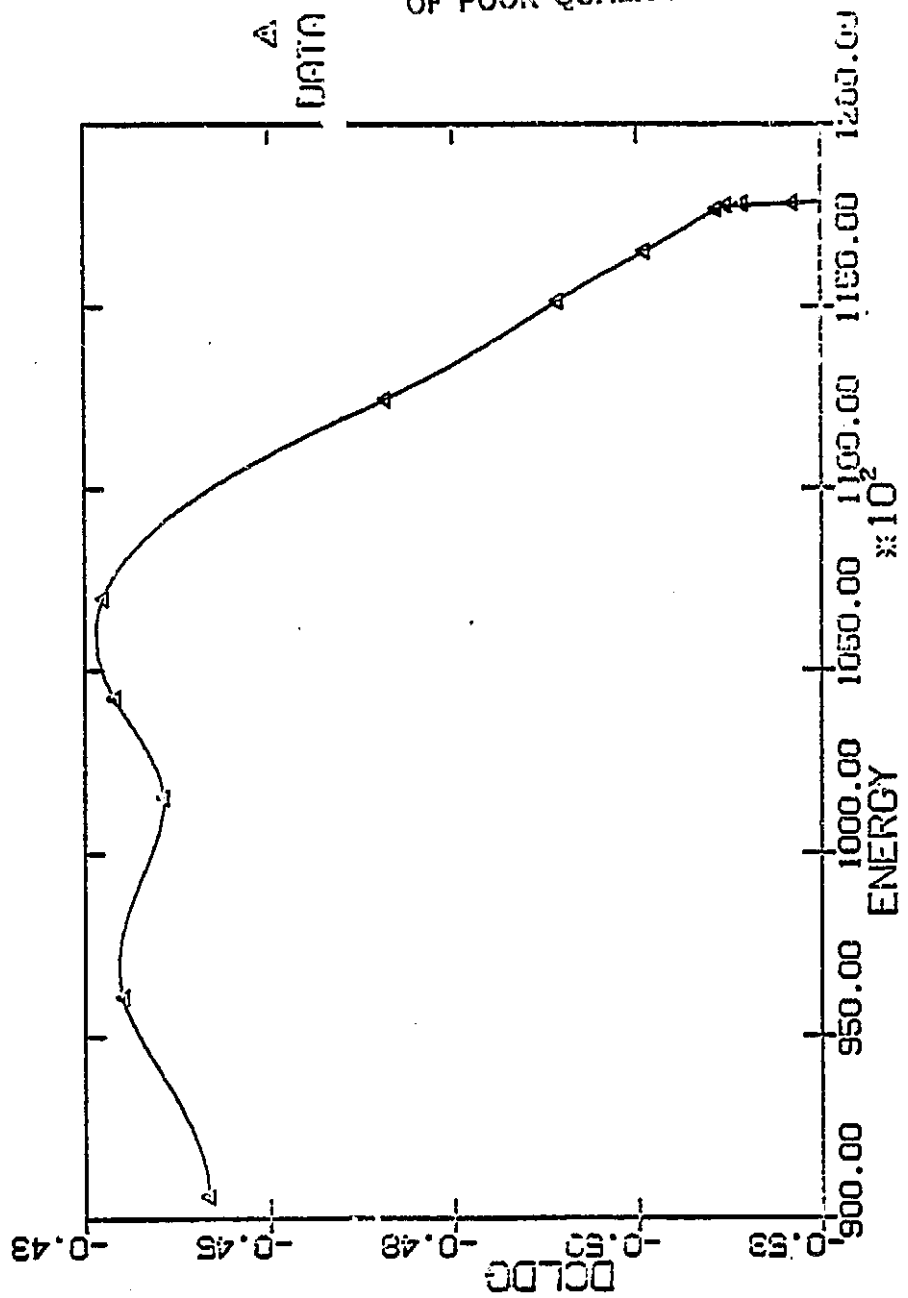

Fig 33.....Path-Angle Gain vs Energy

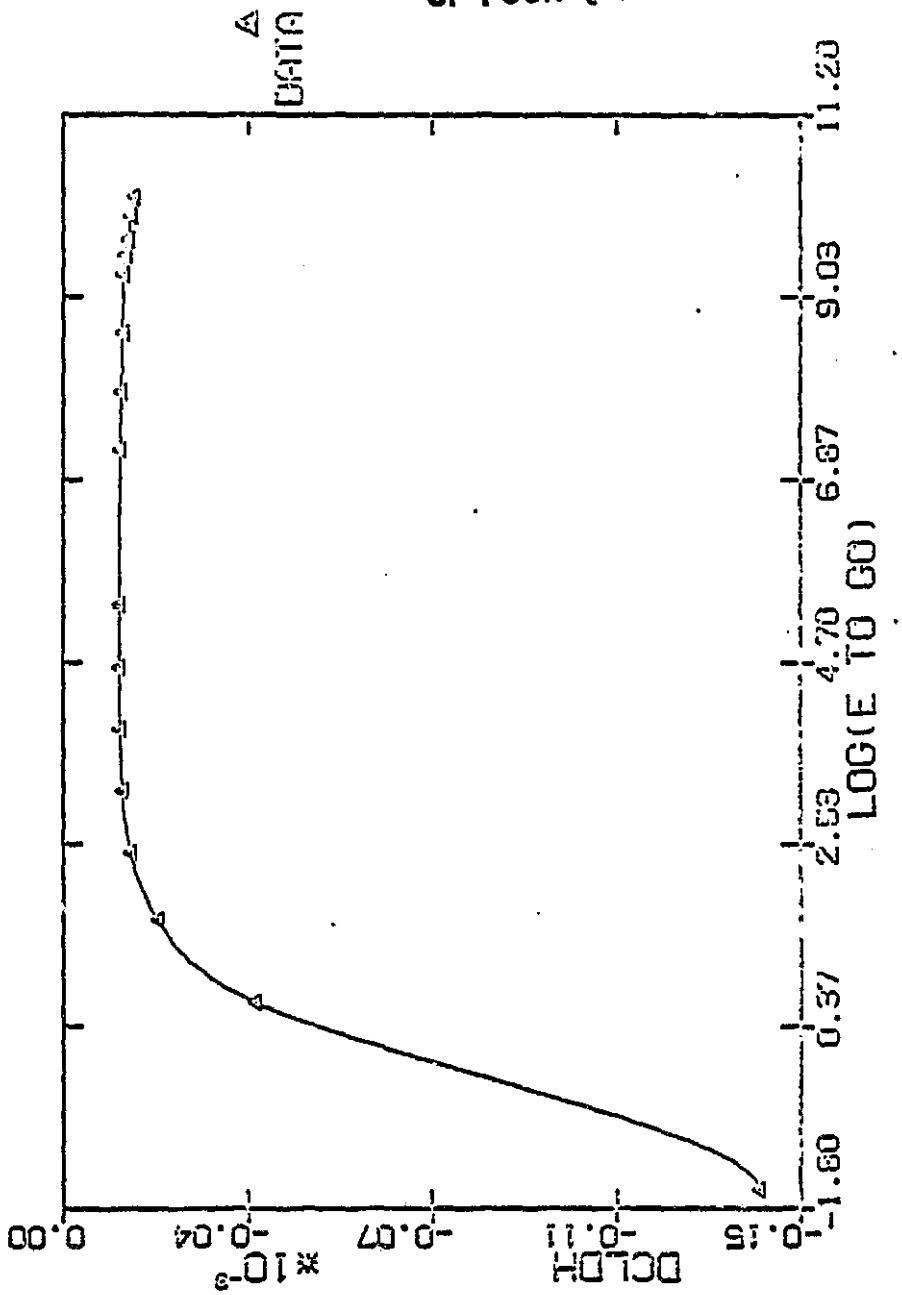

Fig 34.....Altitude Gain vs Log(E)

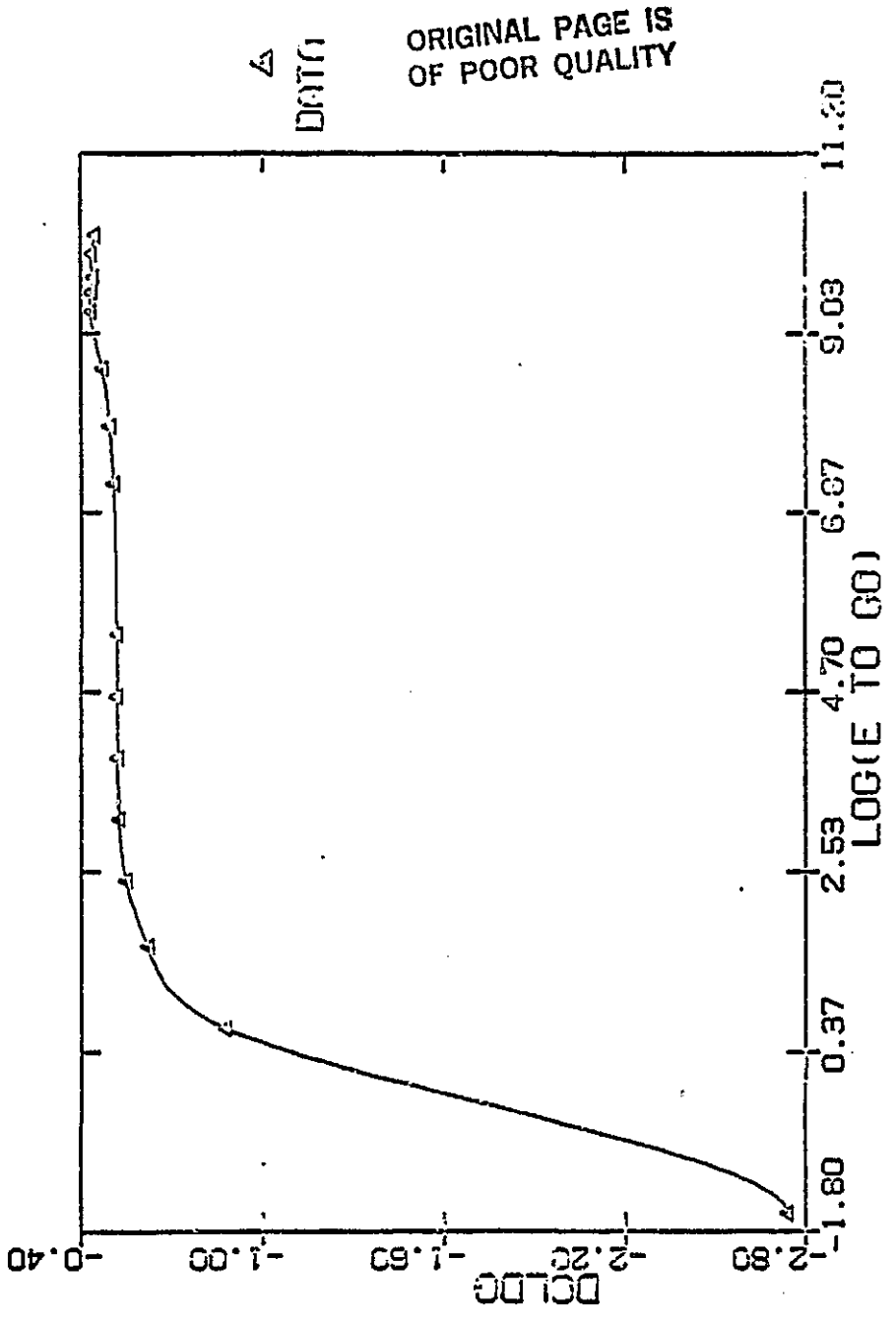

Fig 35.....Path-Angle Gain vs Log(E)

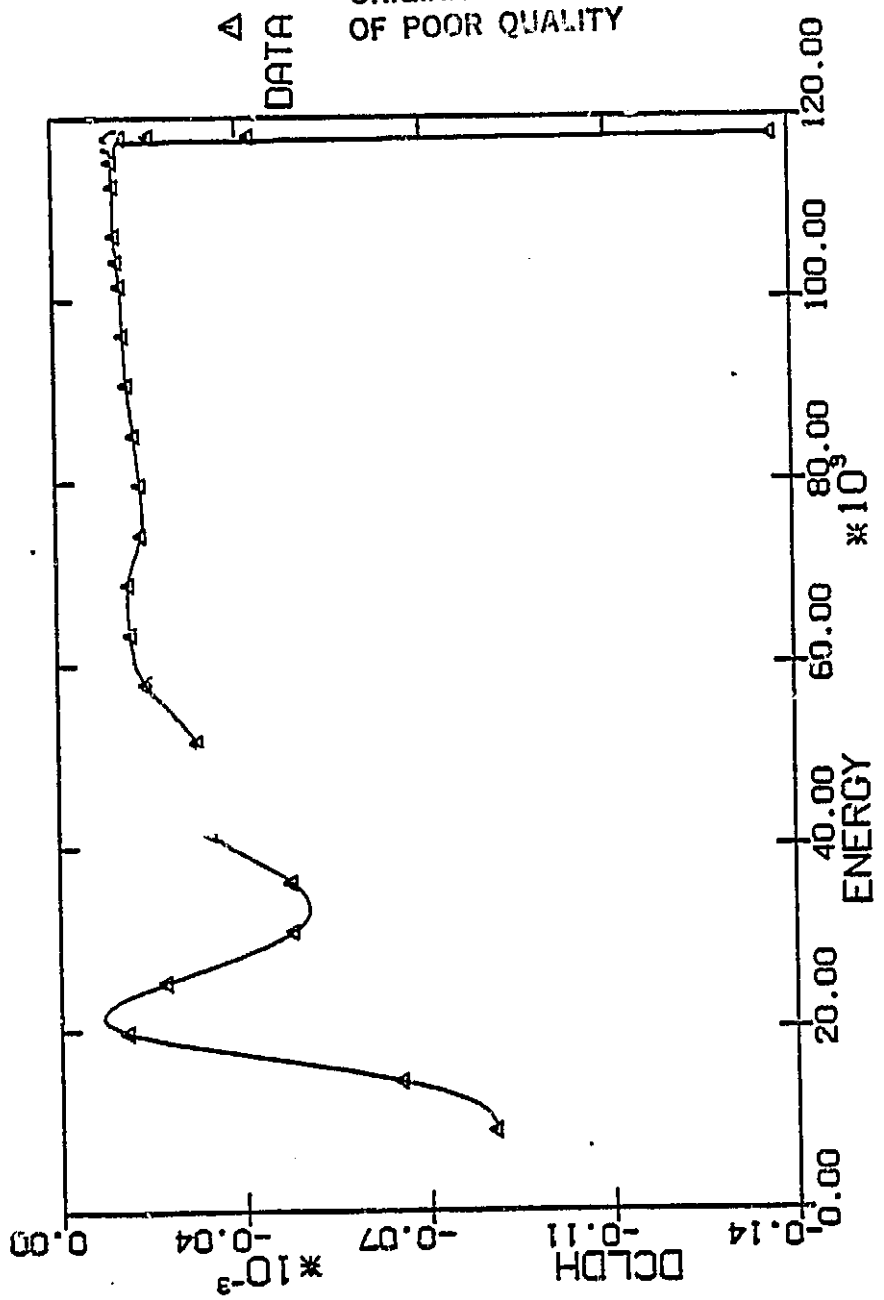

Fig 36.....Altitude Gain vs Energy

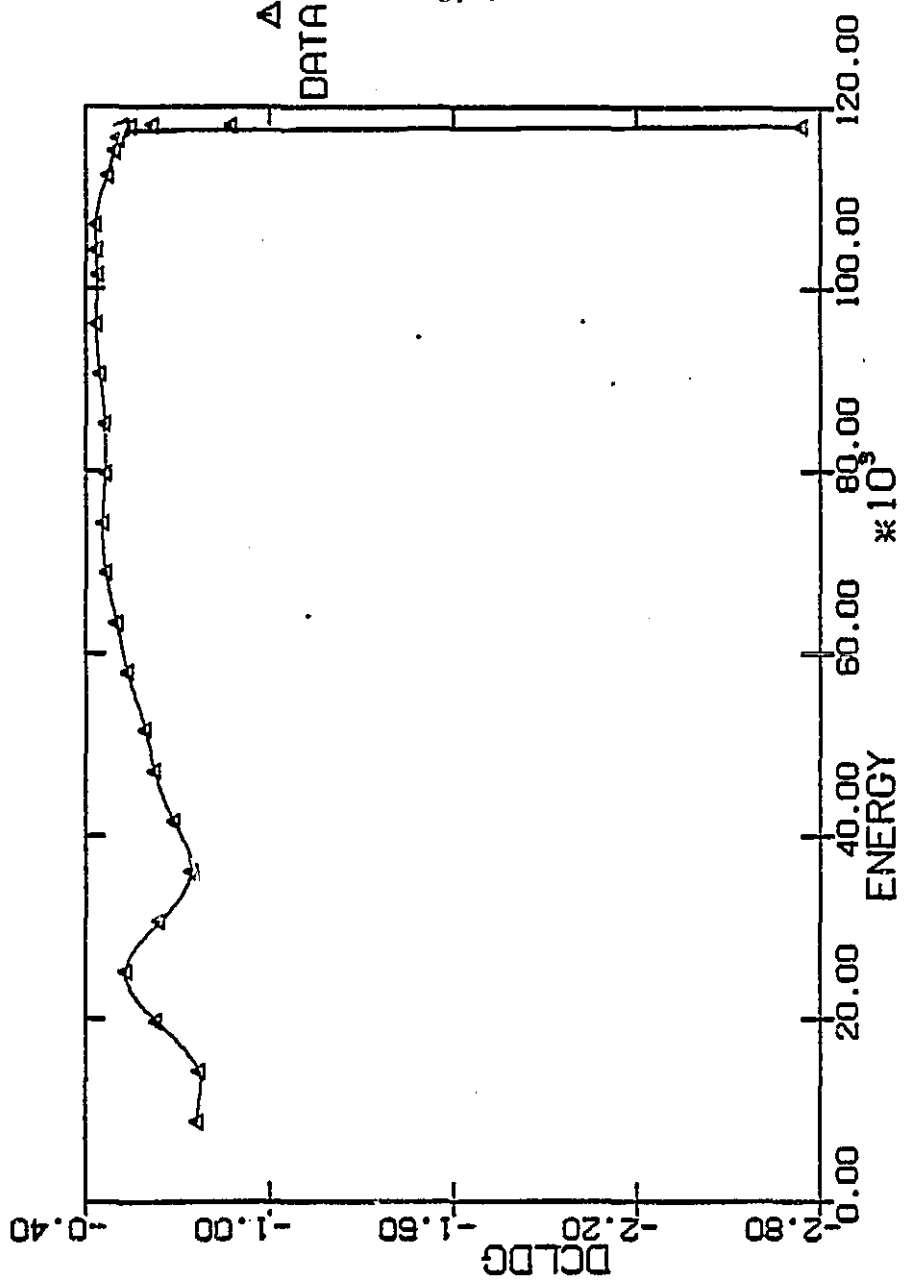

Fig 37.....Path-Angle vs Energy

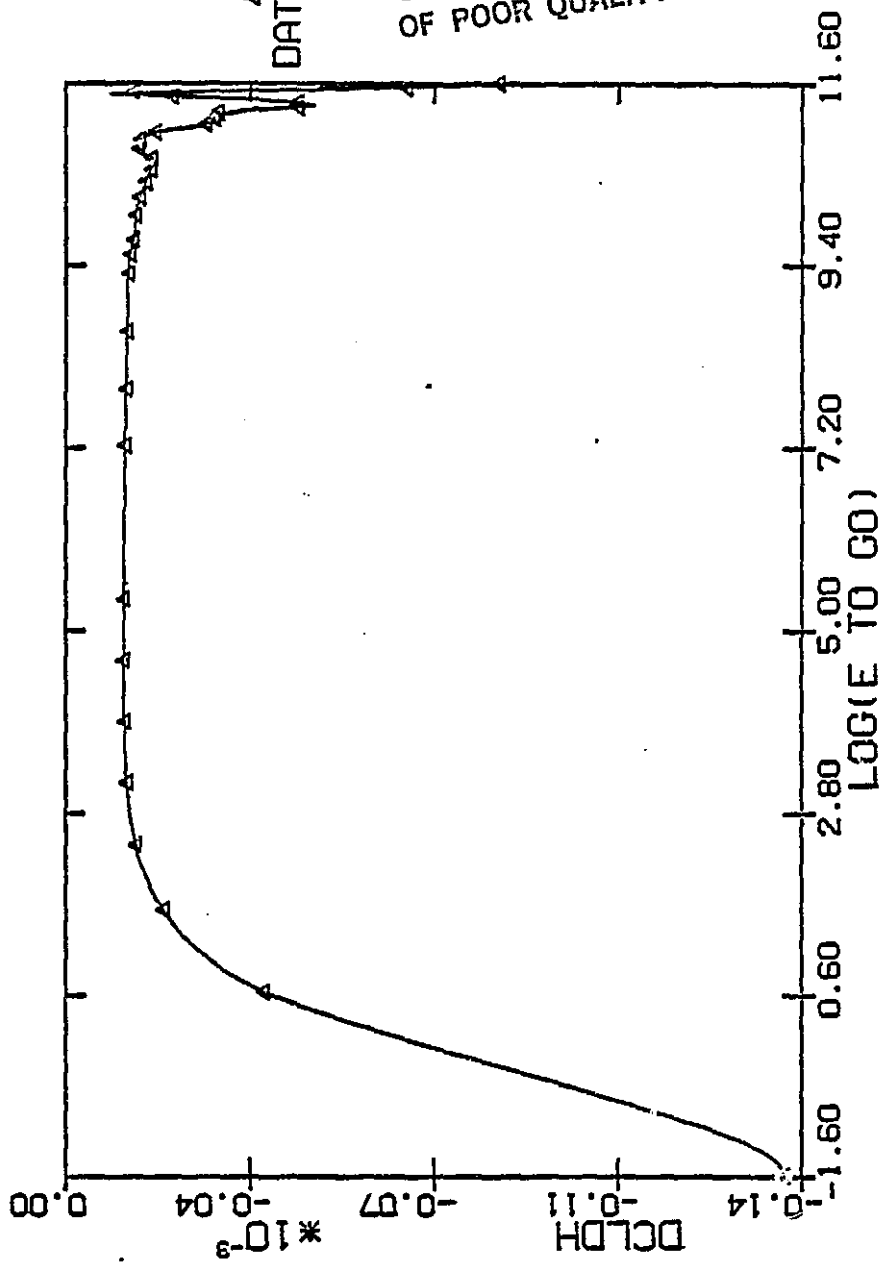

Fig 38.....Altitude Gain vs Log(E)

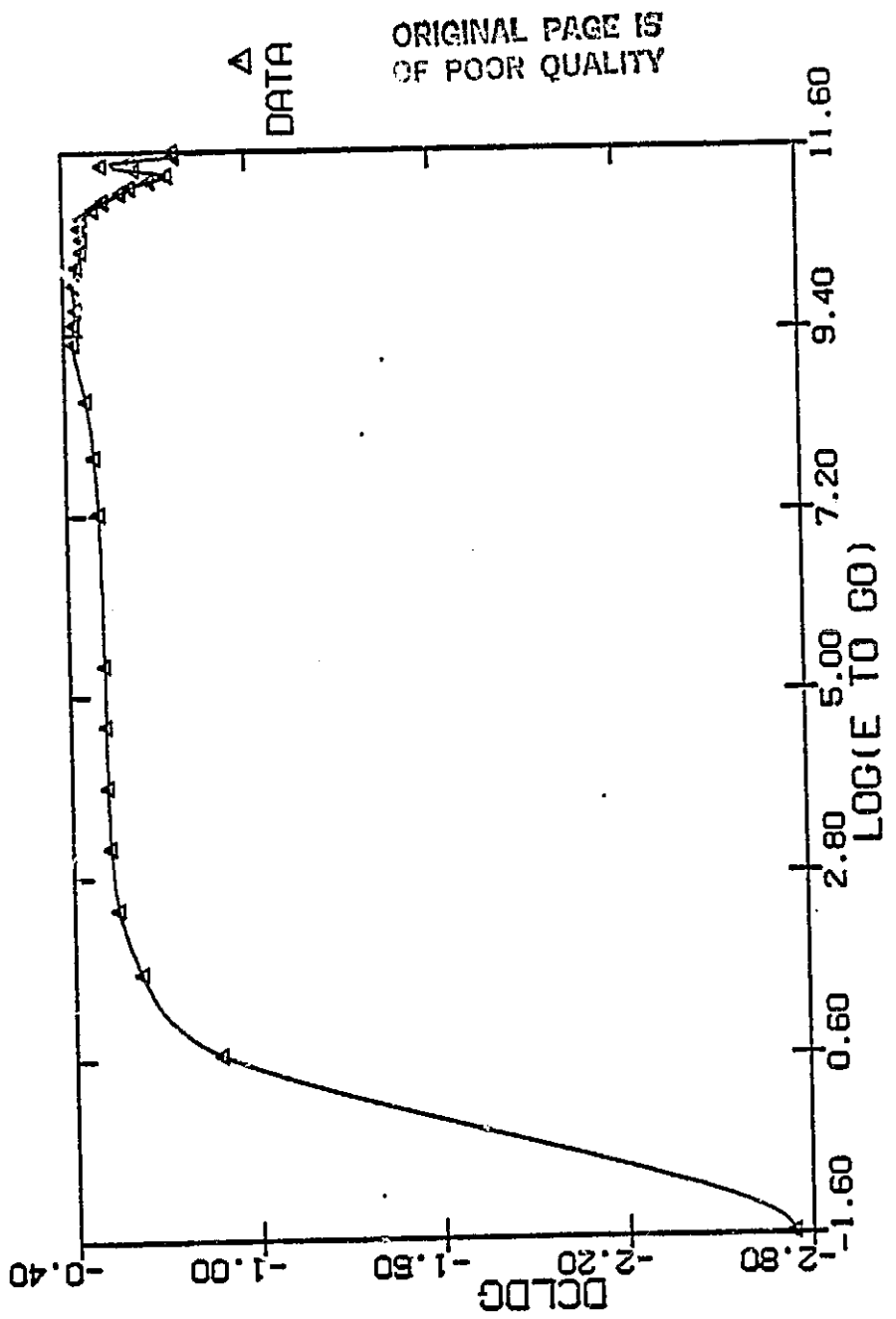

Fig 39.....Path-Angle Gain vs Log(E)

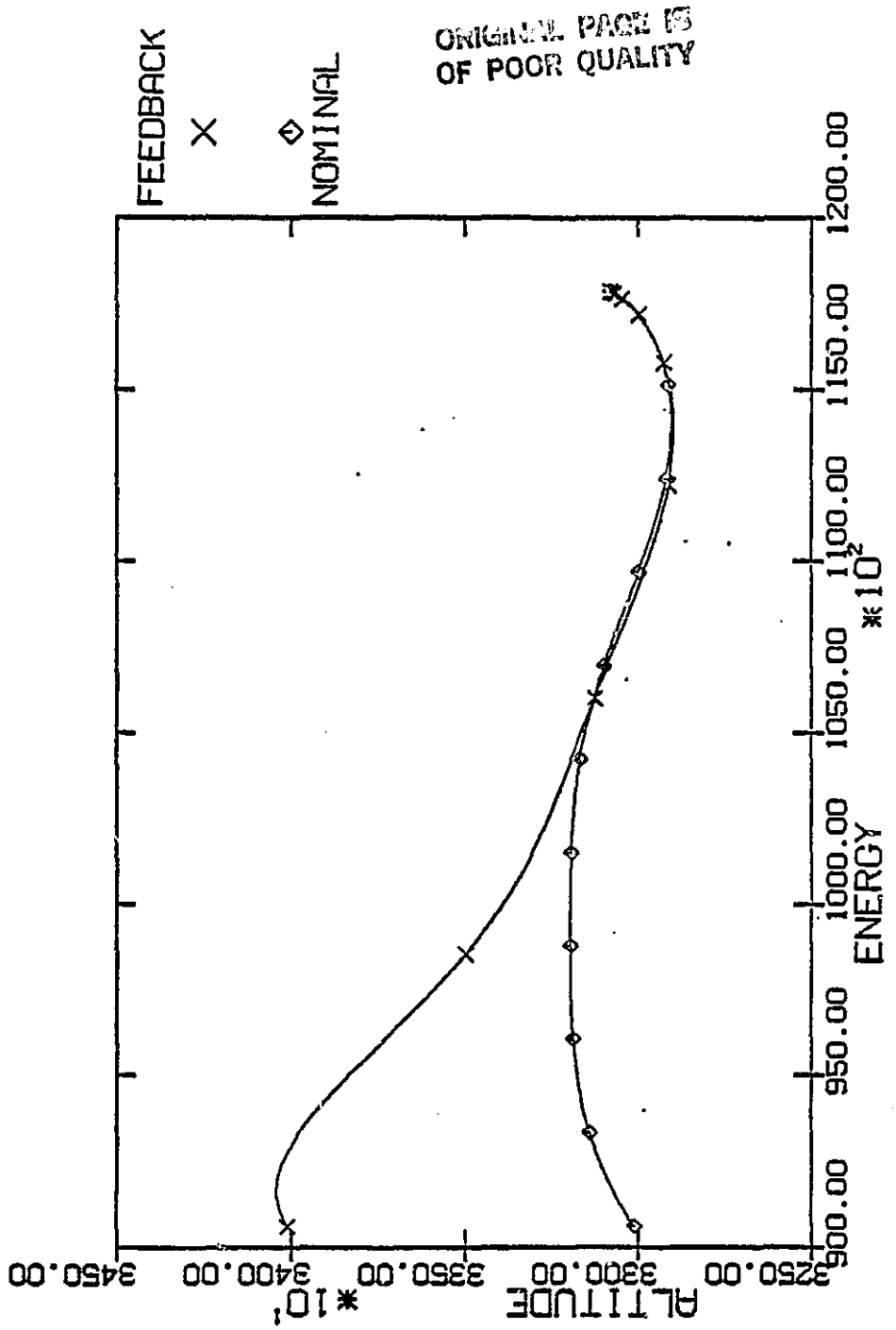

Fig 40.....Altitude vs Energy, 1000 ft above

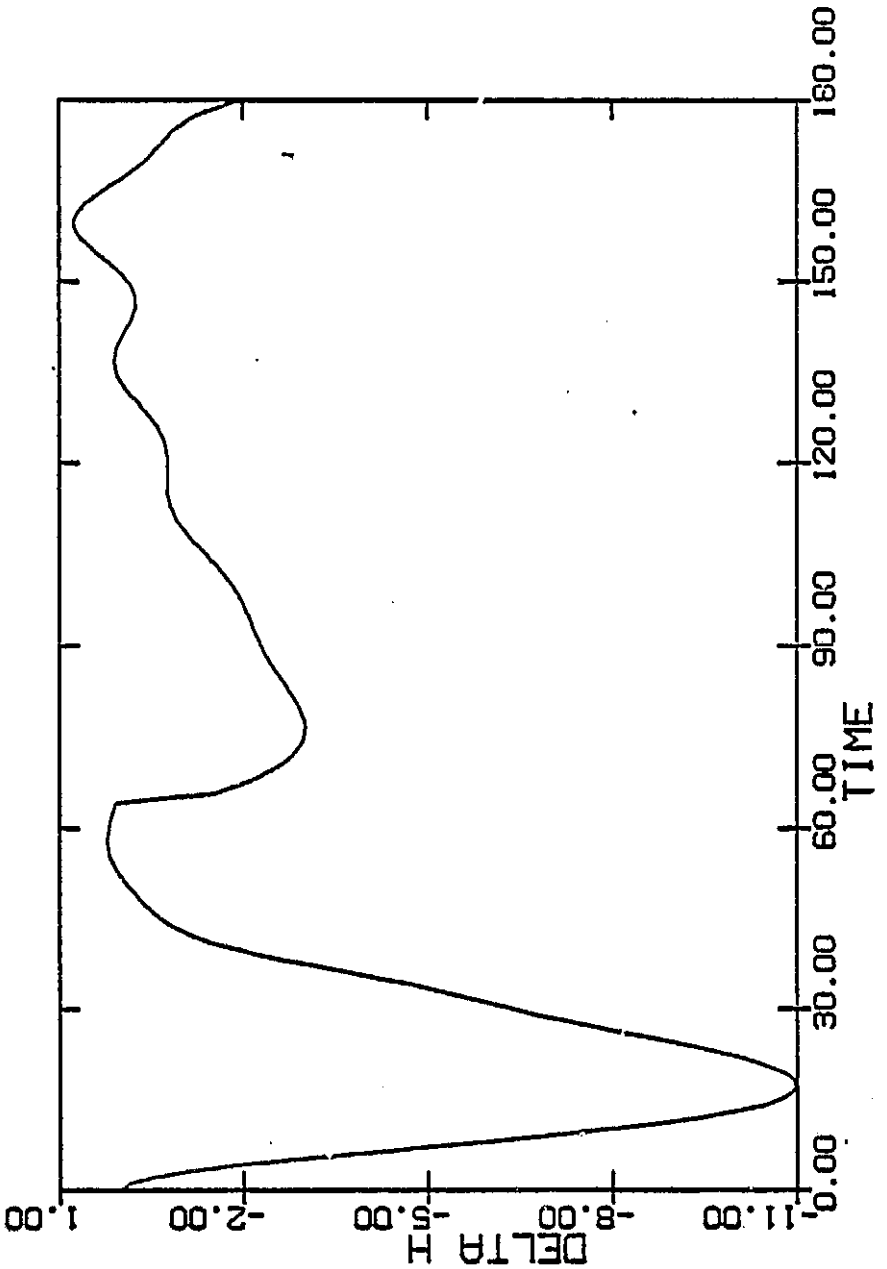

Fig 41.....Altitude Error vs Time

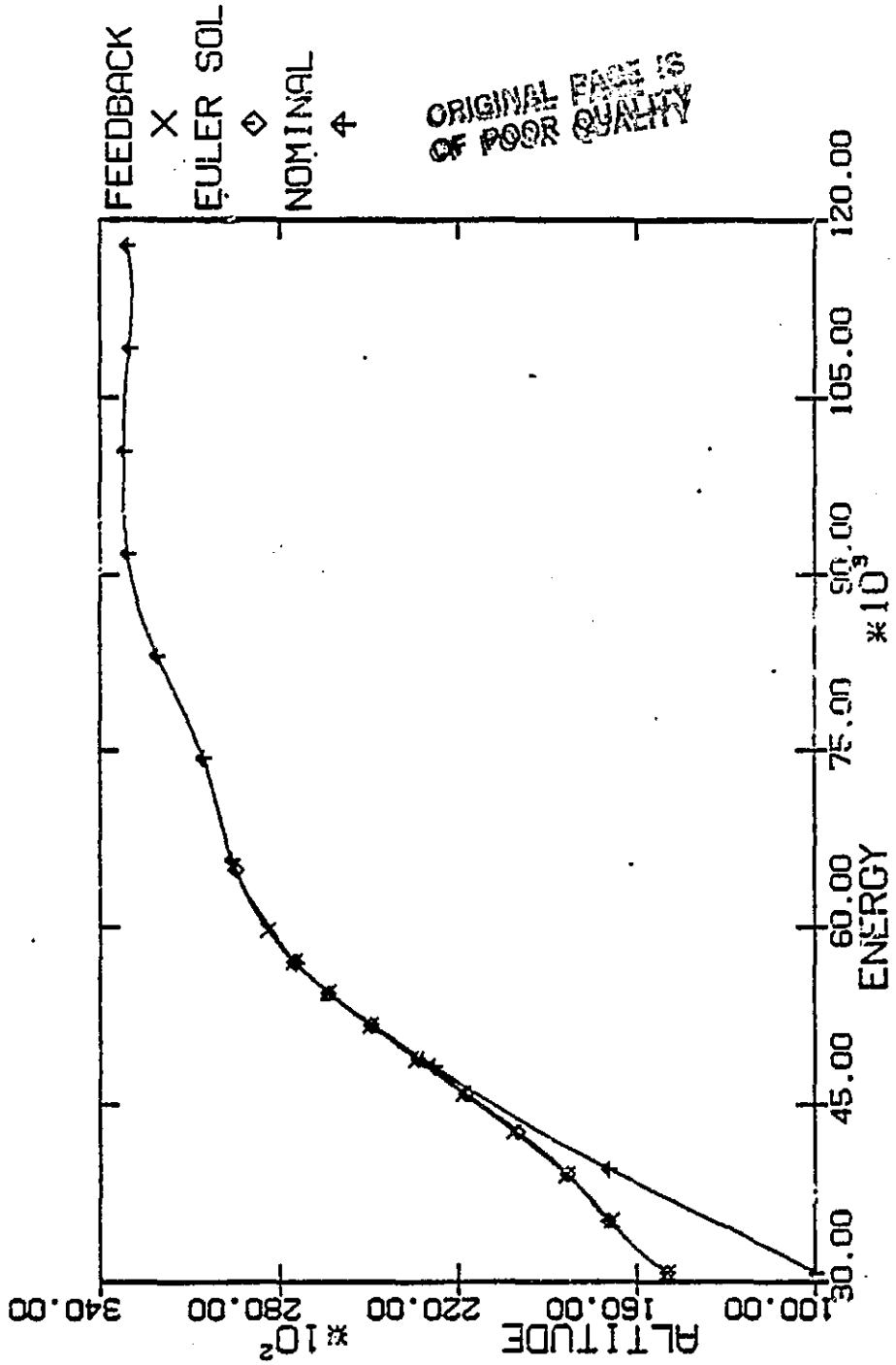

Fig 42.....Altitude vs Energy, 5000 ft above

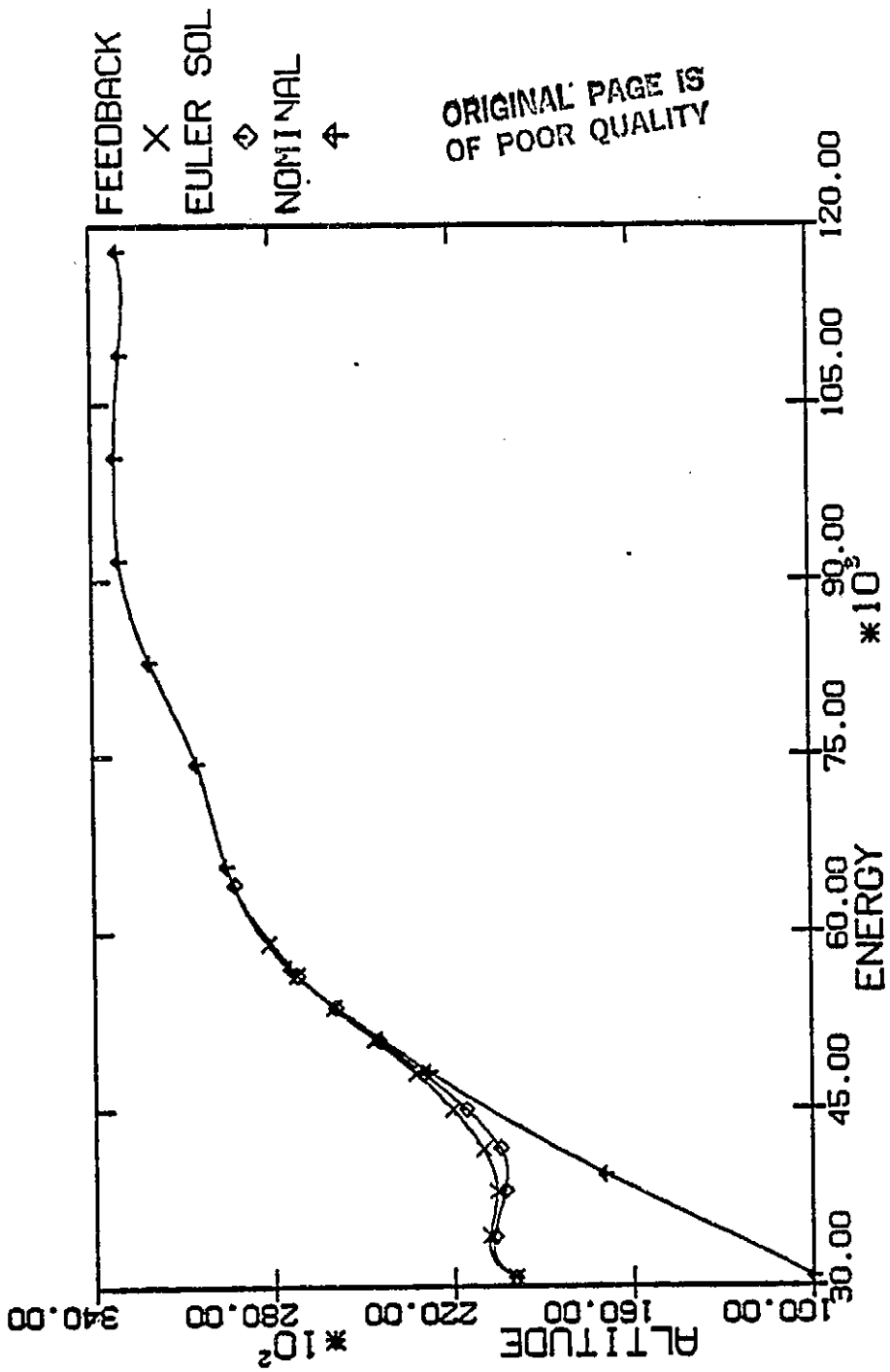

Fig 43.....Altitude vs Energy, 10000 ft above

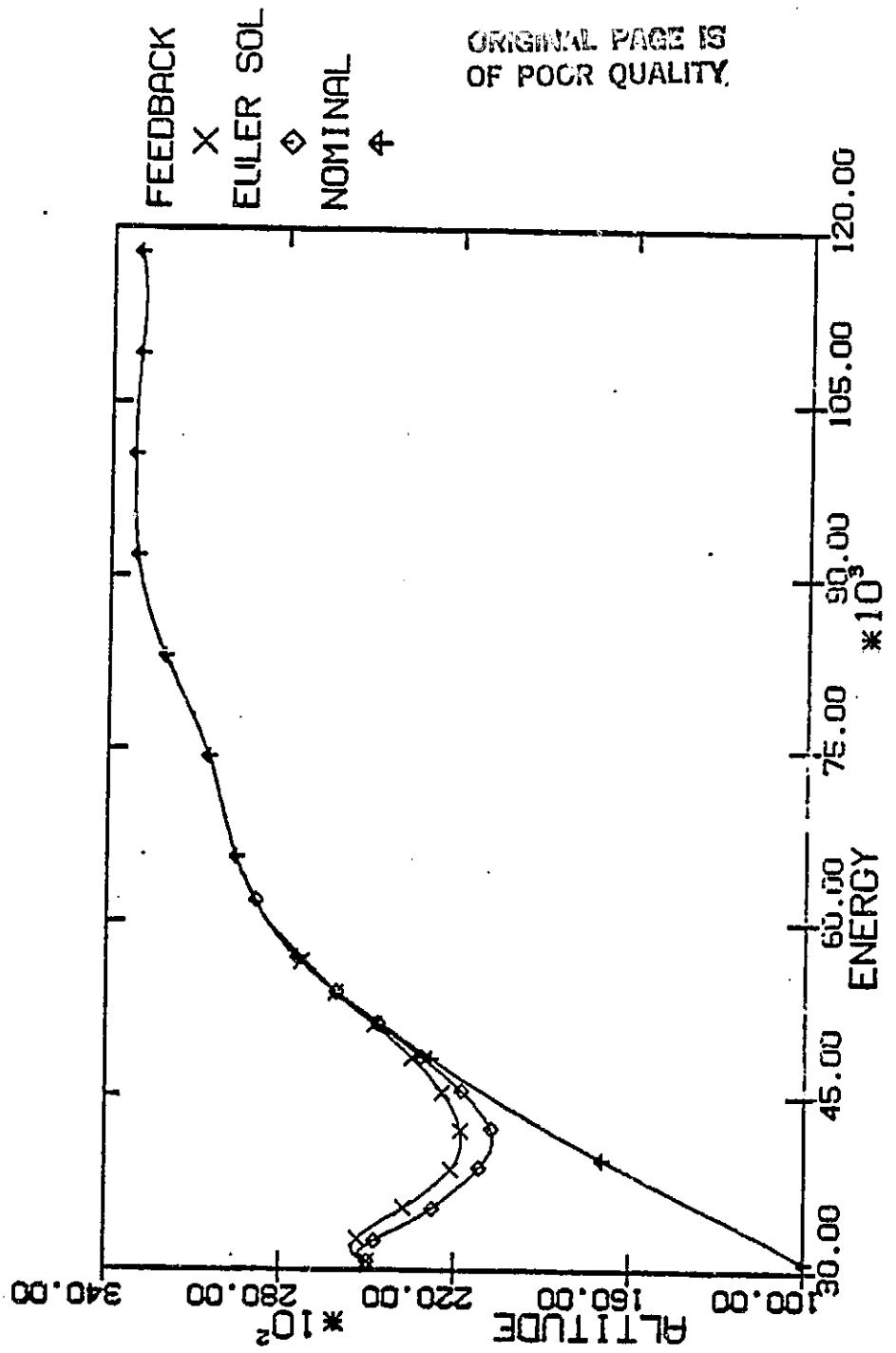

Fig 44.....Altitude vs Energy, 15000 ft above

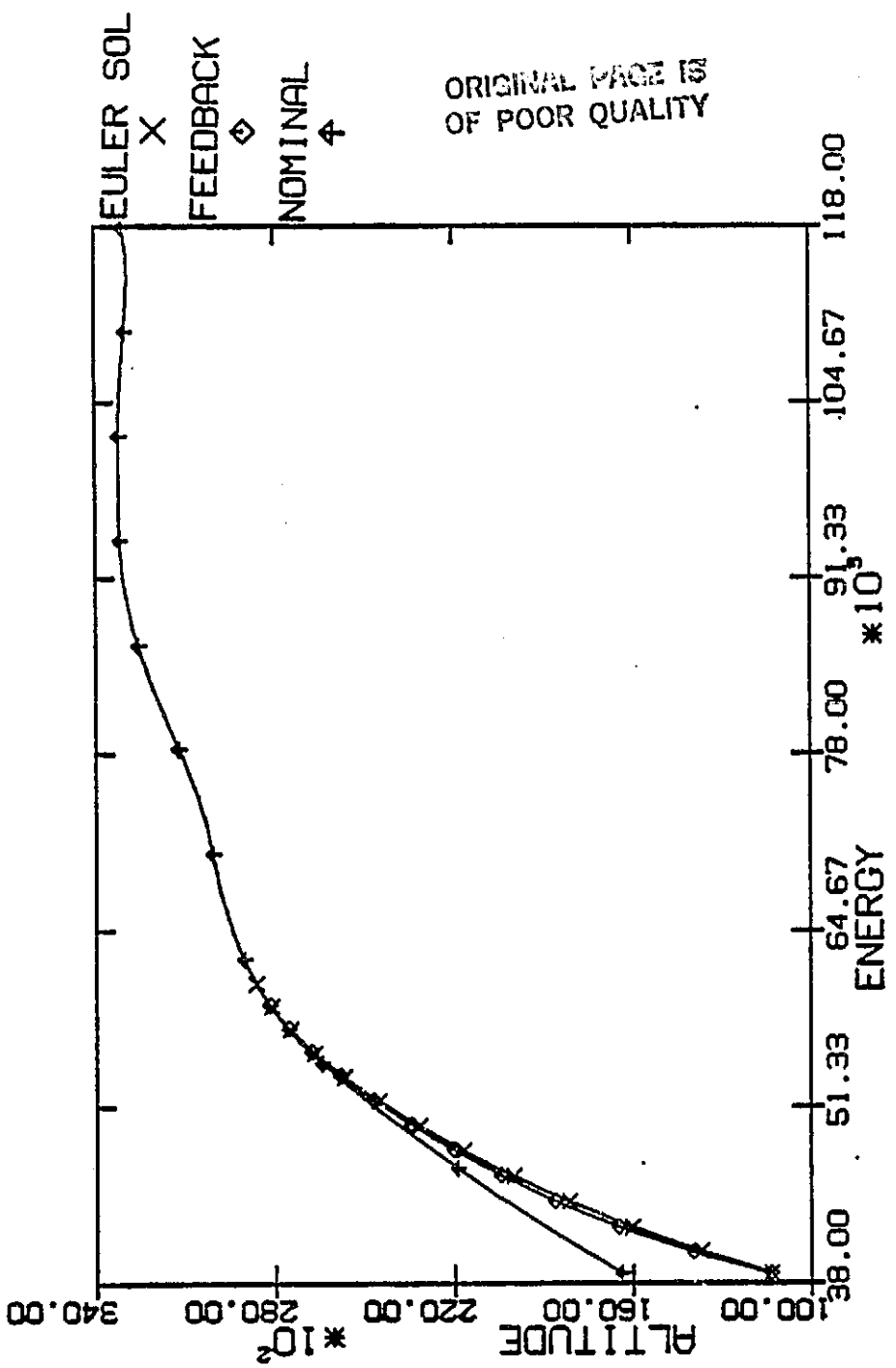

Fig 45.....Altitude vs Energy, 5000 ft below

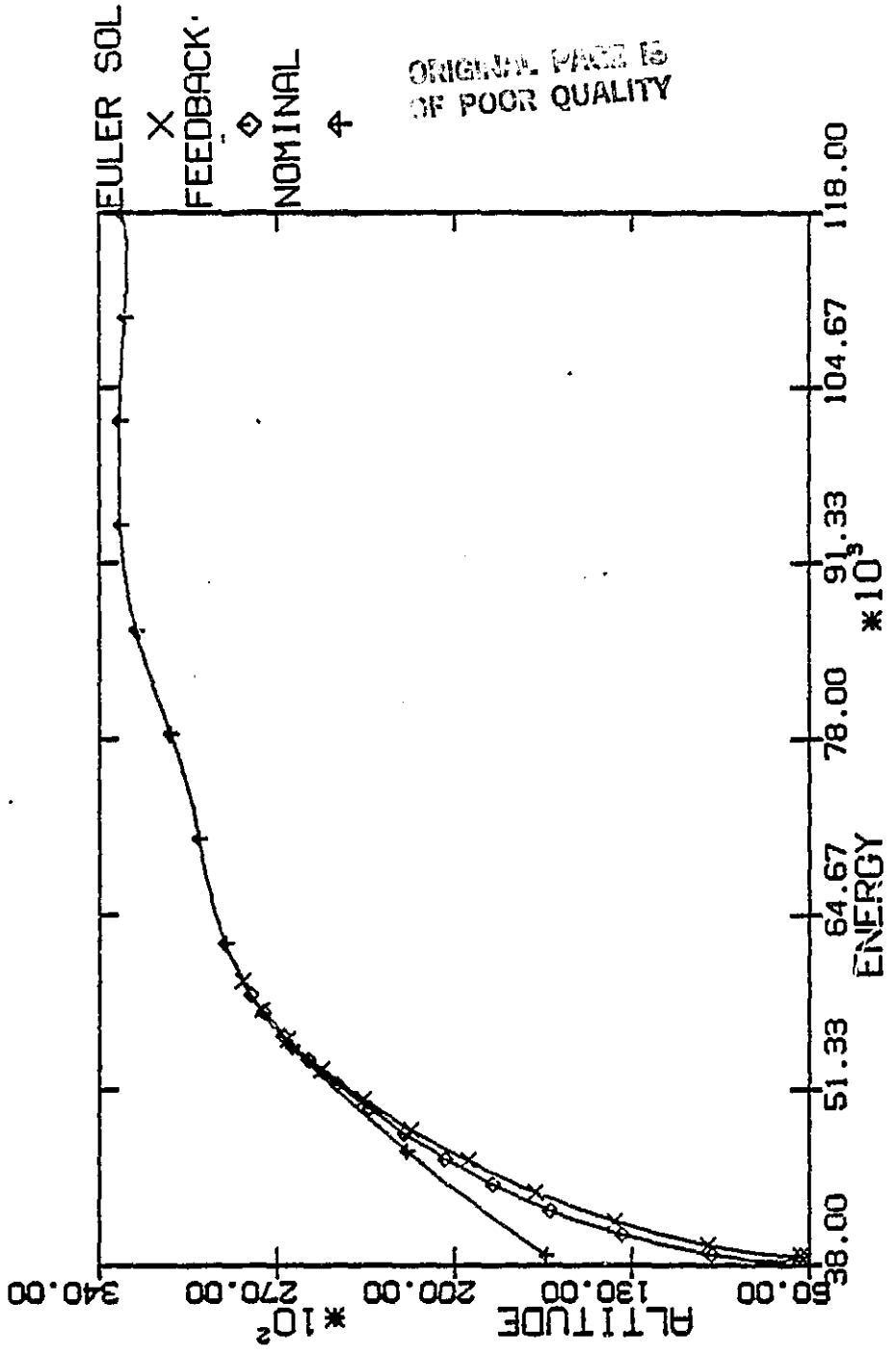

Fig 46.....Altitude vs Energy, 10000 ft below

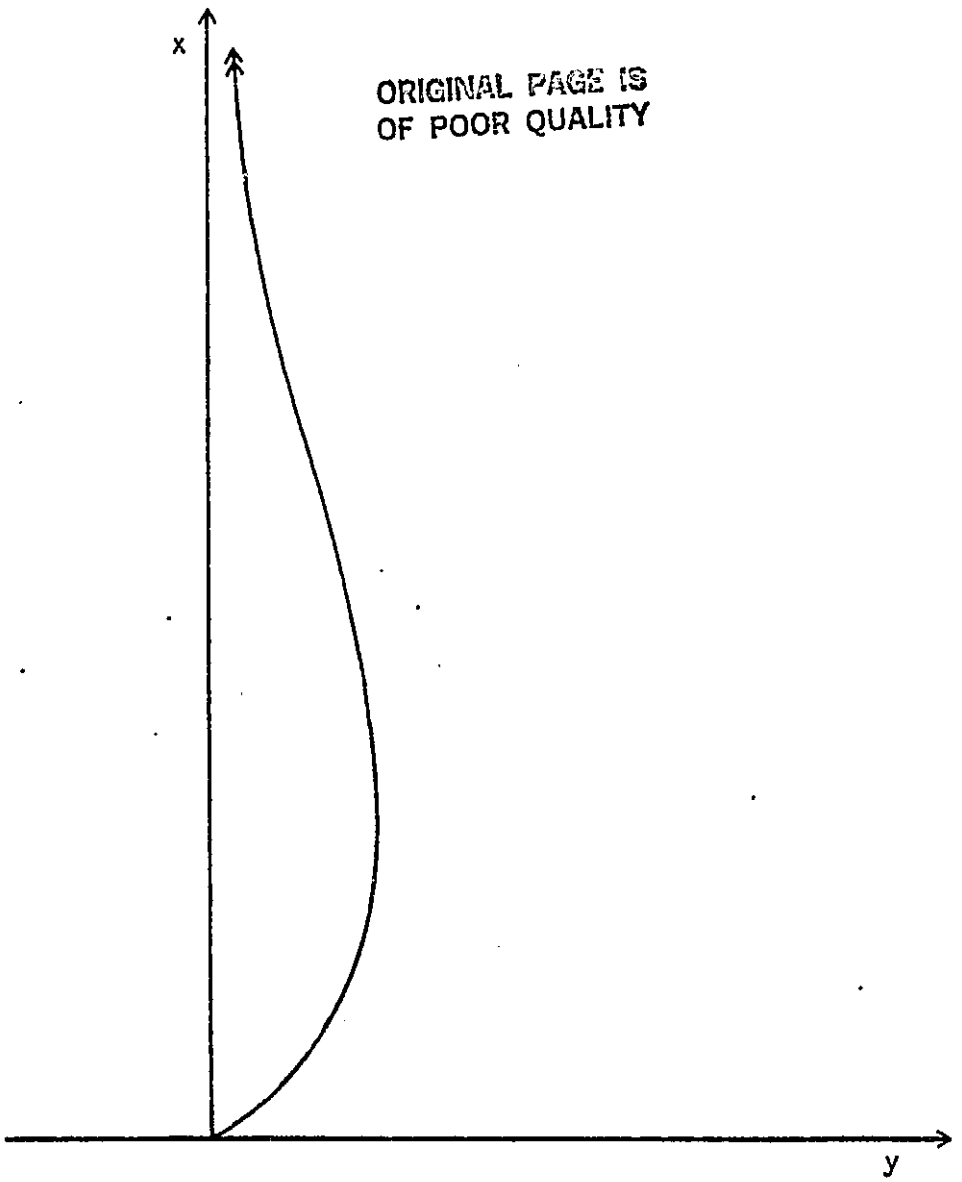

Fig 47 Interceptor Path with y as Running Variable

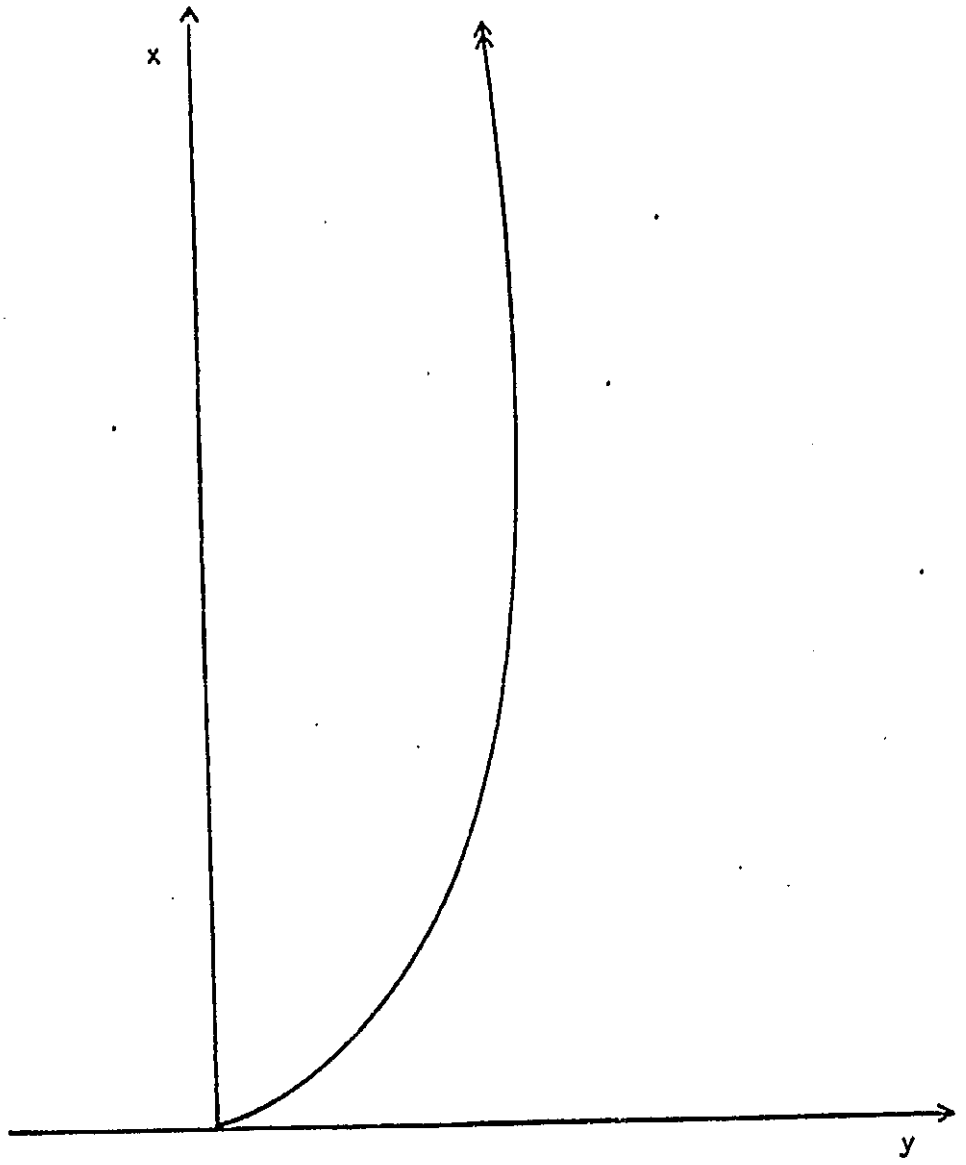

Fig 48 Interceptor Path without y as Running Variable

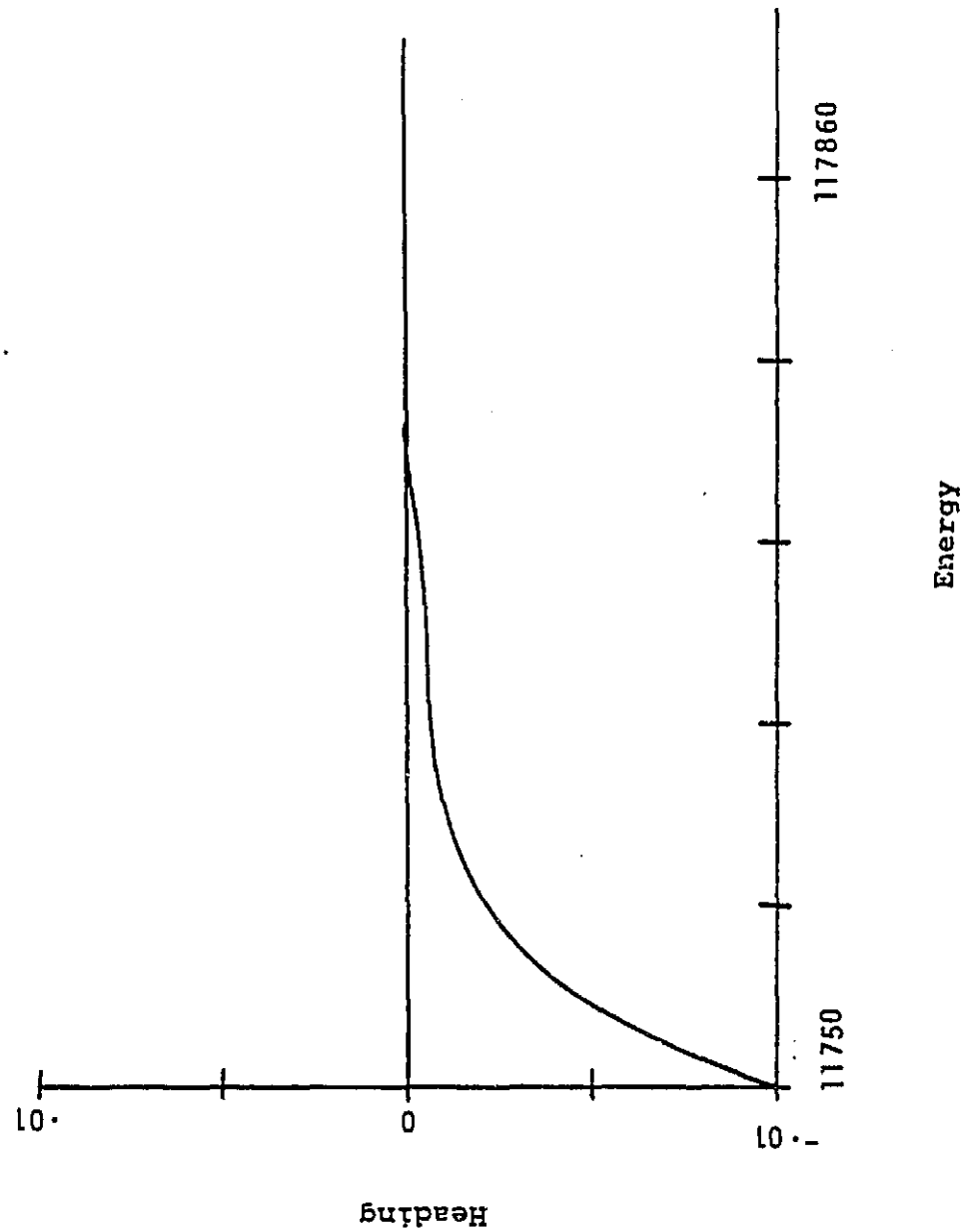

Fig 49 Heading vs Energy

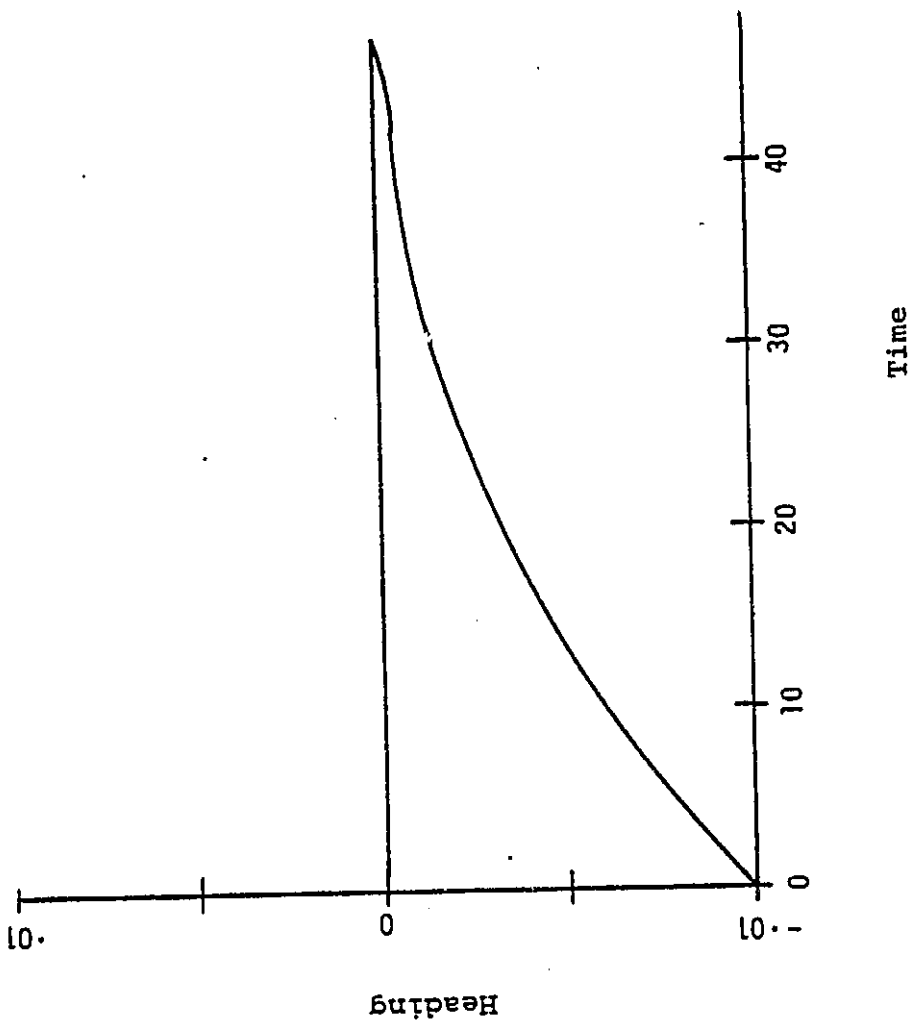

Fig 50 Heading vs Time